Nanoscale

ROYAL SOCIETY OF CHEMISTRY

REVIEW

View Article Online
View Journal

Cite this: DOI: 10.1039/d6nr00357e

# Emerging strategies for controllable mechanical exfoliation of crystalline thin films and nanomembranes

Ze-Wei Chen,†[a,b] Qi Chen,†[a,b] Rithwik Rayani,[a] Soo Ho Choi[a,b] and Hyunseok Kim *[a,b,c,d]

Received 26th January 2026,
Accepted 16th April 2026

DOI: 10.1039/d6nr00357e

rsc.li/nanoscale

Building crystalline heterostructures with arbitrary material combinations, which has been often referred to as "anything-on-anything" integration, has remained a central challenge in materials science and device platforms. Membrane-based technologies provide a viable pathway toward this goal by decoupling thin-film growth from the resulting heterostructures. By isolating high-quality single-crystal layers from their host substrates, lift-off techniques bypass the intrinsic constraints imposed by substrate properties and enable the production of freestanding films and nanomembranes as previously inaccessible material building blocks. Among various lift-off strategies, mechanical lift-off is particularly attractive due to its wide applicability to virtually any material systems. However, the difficulty in manipulating cracks during mechanical lift-off, which determines the properties of exfoliated membranes, has limited the widespread adoption of the technology. Here, we provide key insights into the fundamental mechanics governing mechanical lift-off and discuss how recent breakthroughs in interface design, epitaxy techniques, and crack-guiding principles have enabled highly controlled spalling with atomic precision, scalability, and throughput. We then highlight how such innovations in mechanical lift-off technology, along with other emerging lift-off methods, have advanced membrane-based technologies and have opened new application spaces. Finally, we discuss remaining challenges not only in the lift-off processes themselves but also across the full process flow, outlining pathways toward the broader adoption of lift-off technologies for both fundamental scientific studies and advanced device platforms.

Open Access Article. Published on 11 maio 2026. Downloaded on 27/05/2026 13:44:17.
This article is licensed under a Creative Commons Attribution-NonCommercial 3.0 Unported Licence.

## 1. Introduction

Thin-film heterostructures and interfaces constitute the backbone of virtually every advance in modern electronics and are central to exploring condensed-matter physics. Unlike amorphous or polycrystalline materials, single-crystal thin films and heterojunctions allow charge, phonons, excitons, and spins to propagate with minimal scattering, enabling high-performance electronics, photonics, quantum devices, and emergent interfacial phenomena. As a result, the ability to create high-quality crystalline layers and integrate them together with atomically precise interfaces is essential both for device engineering and for exploring new physical behavior.

Despite their importance, creating high-quality heterostructures across a broad range of material combinations remains difficult. Conventional epitaxy allows crystalline films to inherit the lattice order of the underlying substrate, but this process requires close lattice and thermal-expansion matching.[1–3] Few material pairs satisfy these conditions and attempts to epitaxially integrate mismatched systems typically lead to dislocations, strain, warpage, or cracking. Alternative approaches such as direct wafer bonding followed by thinning provide another route, yet they impose strict requirements on surface chemistry, thermal budgets, and bonding strength, and they often consume costly wafers in the process.[4] Furthermore, these constraints prevent the reliable integration of many promising materials and make it nearly impossible to interface crystalline films with other substrates or films that are textured, fragile, temperature-sensitive, or chemically inert. As a result, both the accessible material combinations and the achievable interface quality by these approaches remain limited.

[a]Department of Electrical and Computer Engineering, University of Illinois Urbana-Champaign, Urbana, Illinois 61801, USA. E-mail: hyunseok@illinois.edu
[b]Nick Holonyak, Jr. Micro and Nanotechnology Laboratory, University of Illinois Urbana-Champaign, Urbana, Illinois 61801, USA
[c]Department of Materials Science and Engineering, University of Illinois Urbana-Champaign, Urbana, Illinois 61801, USA
[d]Materials Research Laboratory, University of Illinois Urbana-Champaign, Urbana, Illinois 61801, USA

† These authors contributed equally.

Open Access Article. Published on 11 maio 2026. Downloaded on 27/05/2026 13:44:17.
This article is licensed under a Creative Commons Attribution-NonCommercial 3.0 Unported Licence.

A promising way to overcome these integration challenges is to decouple thin-film growth from the heterostructures or interfaces that are formed as a result. This can be achieved by growing a high-quality single-crystal layer on a suitable substrate, isolating it as a freestanding membrane, and then transferring it to any desired platform. This approach removes the constraints imposed by lattice and thermal matching in epitaxy, enabling arbitrary combinations of materials as long as grown layers can be released intact. Once separated from the thick and rigid growth wafer, the isolated ultrathin membrane becomes mechanically compliant, allowing integration onto substrates that are textured, flexible, curved, or otherwise incompatible with conventional epitaxy or bonding. Concepts based on such layer lift-off and transfer of single-crystal membranes date back to the 1980s,[5,6] beginning with chemical lift-off techniques and later expanding to mechanical and laser-based lift-off methods. These early demonstrations laid the foundation for today's membrane-based integration strategies.

Among the various lift-off strategies, mechanical lift-off is the most broadly applicable because it is not constrained by material-specific chemical reactions or optical absorption. In mechanical lift-off, tensile stress applied by various means initiates a crack at a predetermined depth, and the crack then propagates laterally to separate a thin membrane from the underlying substrate. Mechanical peeling can, in principle, be applied to virtually any crystalline film, if the applied stress can exceed the fracture toughness of the material to facilitate crack generation and propagation. On the other hand, other lift-off techniques cannot be applied universally to diverse material systems: chemical lift-off requires a sacrificial layer that can be selectively etched, and laser lift-off relies on an interfacial layer that efficiently absorbs incident light. The universality of mechanical lift-off makes this technique particularly attractive for both device engineering and fundamental scientific studies.

In recent years, the need to advance membrane-based integration technologies has grown rapidly. In electronics, continued scaling to keep up with Moore's law is constrained by short-channel effects, power limits, and escalating fabrication complexity.[7,8] To overcome these challenges and meet the computing demands of AI and data centers, the field increasingly depends on three-dimensional heterogeneous integration (3DHI): introducing new materials with superior electronic or photonic properties and stacking functional layers vertically to shorten interconnect lengths and expand system bandwidth. Beyond conventional electronics and photonics, many emerging device concepts, as well as platforms that exploit correlated or topological properties, require novel heterostructures and interfaces with precise control over layer quality and thickness.[9–11] Freestanding membranes offer a practical way to assemble such structures with far fewer restrictions than direct epitaxy or bonding. At the same time, emerging areas such as bioelectronic systems, soft robotics, and Internet-of-Things (IoT) devices require placing functional single-crystal films onto unconventional substrates that are flexible, curved, or mechanically incompatible with conventional approaches. These trends highlight the growing importance of methods that can release high-quality crystalline membranes and integrate them with virtually any target platform.

Driven by these expanding needs, membrane-based lift-off techniques have experienced a significant resurgence recently, with many important advances occurring in mechanical lift-off. Traditional mechanical exfoliation approaches offered limited control over the depth, uniformity, and quality of the released membrane. Recent breakthroughs in several areas—including epitaxial control of interfacial properties, engineered growth templates, post-growth interface modification, tailored crack-initiation schemes, and refined strategies for guiding crack propagation—now enable exfoliation with far greater controllability, approaching sub-nanometer control of membrane thickness, and across a much wider range of materials than were previously inaccessible. These advances are opening new opportunities for devices and unconventional integration platforms.

**Ze-Wei Chen**

*Ze-Wei Chen received his B.S. degree in Electrical Engineering, from National Taiwan University, and is currently a Ph. D. student in Electrical and Computer Engineering at the University of Illinois Urbana-Champaign. His research focuses on semiconductor device fabrication, hetero-integration, membrane transfer, and material growth, with particular interest in 2D-material-enabled epitaxy and thin-film integration.*

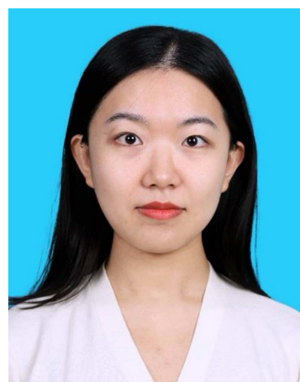

**Qi Chen**

*Dr. Qi Chen received her Ph.D. in Microelectronics and Solid-State Electronics from the Institute of Semiconductors, CAS. She is currently a postdoctoral researcher at the University of Illinois Urbana-Champaign. Her research focuses on the MOCVD growth of III-nitride materials, 2D/3D interface engineering, and integration strategies. She is interested in developing remote and van der Waals epitaxy of nitrides, as well as exploring heterogeneous integration through direct growth approaches.*


This journal is © The Royal Society of Chemistry 2026

Open Access Article. Published on 11 maio 2026. Downloaded on 27/05/2026 13:44:17.
This article is licensed under a Creative Commons Attribution-NonCommercial 3.0 Unported Licence.

The goal of this review is to present a comprehensive overview and perspective on mechanical lift-off approaches for producing freestanding thin films and nanomembranes and utilizing them for diverse applications (Fig. 1). Throughout this article, "lift-off" is used as a broad term for releasing a membrane from its growth substrate, regardless of the driving mechanism. "Exfoliation" is considered a subset of lift-off that involves a mechanical force or mechanism for release. In exfoliation, the crack plane may propagate either within the substrate or along a weak interface. "Spalling" is used more specifically to describe a stressor-driven form of exfoliation in which a crack propagates beneath and parallel to the surface, most often within the substrate. We begin by outlining the theoretical background and conventional mechanical lift-off methods that established the foundation of the field. We then discuss recent breakthroughs across the key areas described above, highlighting how these advances have transformed the precision, reliability, and accessible material space of mechanical exfoliation. For a balanced context and comparison, we also briefly summarize progress in other lift-off techniques. Finally, we introduce emerging applications that have become possible by these innovations, along with remaining challenges and potential solutions to enable the holy grail—enabling "anything-on-anything" platforms for condensed-matter research, post-Moore electronics, and new classes of device.

## 2. Mechanical lift-off: theory and methodology

Mechanical lift-off is one of the most direct and versatile ways to obtain freestanding crystalline membranes. Because crack formation and propagation depend only on mechanical fracture rather than on chemistry or optical absorption, nearly any material can be separated from its growth substrate if sufficient stress is applied. This simplicity has made mechanical peeling an attractive concept for decades, and it has been demonstrated across many semiconductors, oxides, and compound systems. However, its practical use has long been limited by difficulties in controlling the depth at which the crack propagates, maintaining interfacial smoothness across large areas, and directing propagation in materials that exhibit asymmetric fracture toughness across different crystallographic orientations. These challenges are especially critical when targeting ultrathin films, such as nanomembranes, where deviations of even a few nanometers can compromise the electronic properties and device performance. As a result, although mechanically induced lift-off is broadly feasible, achieving precise, reproducible exfoliation has required a more rigorous understanding of the underlying mechanics and interface physics.

In this section, we describe the theoretical and methodological foundations that historically enabled controlled mechanical lift-off. We first discuss the mechanics of spalling, including energy release rates, fracture modes, and how these principles extend from bulk fracture to the thin-film regime. We then introduce methodology for generating and sustaining the stresses required for crack initiation and propagation, ranging from deposited stressor layers to externally applied forces and engineered interfacial features. These fundamental concepts provide the basis of mechanical lift-off processes and context for the recent innovations presented in later sections.

### 2.1. Thin-film spalling theory

In a mechanical lift-off process, a membrane is separated from a bulk substrate or epitaxial stack through a cracking process known as spalling. For practical use, the crack must advance along a prescribed plane that is preferably parallel to the surface, which is referred to as controlled spalling. Controlled spalling of crystalline membranes is typically achieved by applying stress and enabling crack generation and propagation

**Rithwik Rayani**

*Rithwik Rayani is currently a Senior in Electrical Engineering at the University of Illinois Urbana-Champaign. He will be pursuing a Ph.D. focusing on materials and devices for semiconductors and quantum science.*

**Soo Ho Choi**

*Soo Ho Choi received his B.S., M.S., and Ph.D. degrees from the Department of Physics of Dongguk University. As a postdoctoral researcher in the Center for Integration Nanostructure Physics at Sungkyunkwan University, he focused on the epitaxial growth of 2D materials. He is currently a research professor at Sungkyunkwan University and a postdoc research associate at the University of Illinois Urbana-Champaign. His research interests include the fabrication of the 2D-based heterostructures and the exploration of their physical properties.*

Open Access Article. Published on 11 maio 2026. Downloaded on 27/05/2026 13:44:17.
This article is licensed under a Creative Commons Attribution-NonCommercial 3.0 Unported Licence.

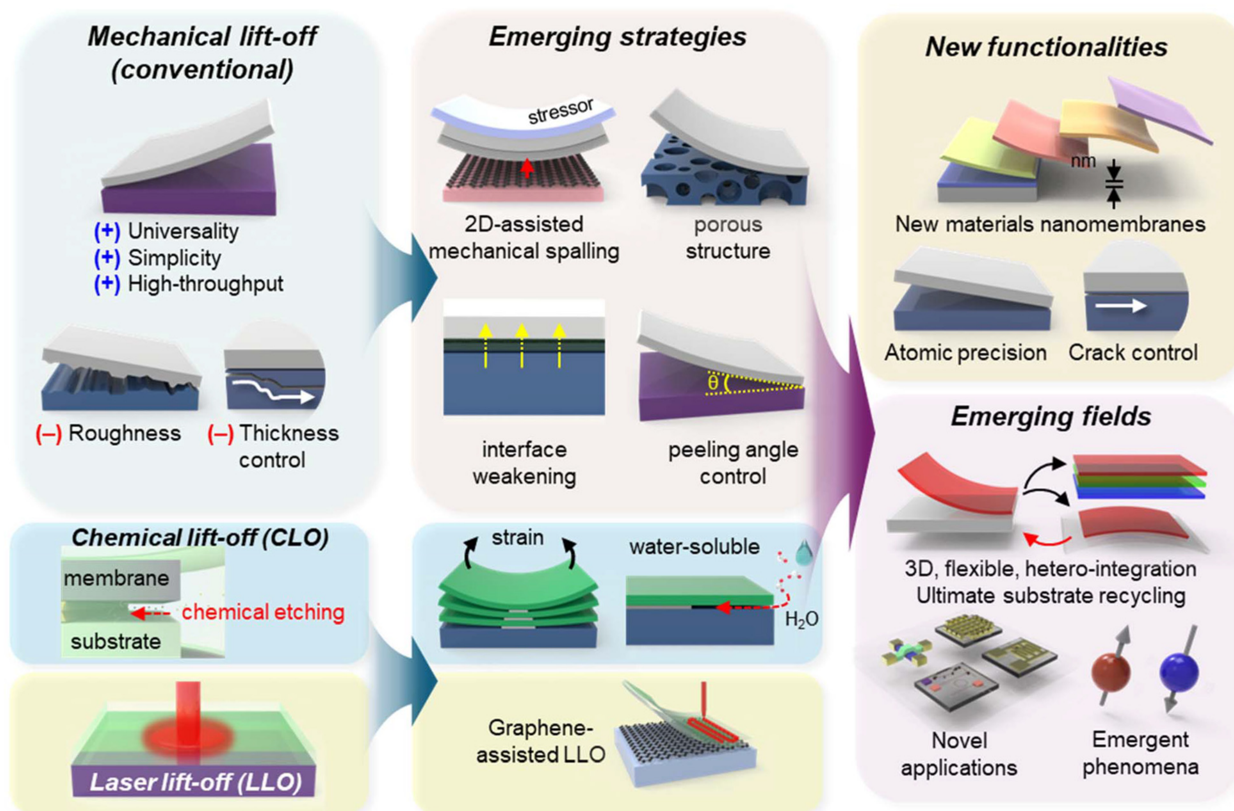


**Fig. 1** Schematic overview of the advantages and limitations of conventional lift-off techniques, emerging strategies to overcome these limitations, and the resulting new functionalities and emerging fields. Conventional lift-off, while offering universality and high throughput, faces challenges such as rough interfaces and poor thickness control. These challenges have been addressed through interface engineering approaches, including 2D-assisted mechanical spalling and the use of porous substrates, enabling improved control over crack propagation and interface quality. In parallel, other lift-off techniques have also advanced. Together, these developments enable the realization of nanometer-thick freestanding membranes from a wide range of materials, opening new opportunities for emergent phenomena and novel device applications.

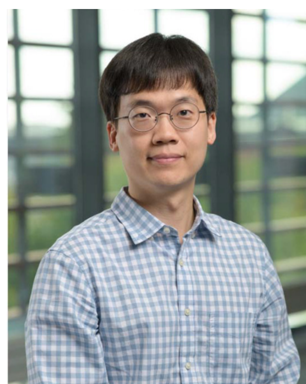

**Hyunseok Kim**

*Hyunseok Kim is an assistant professor at the University of Illinois Urbana-Champaign. His research interests include materials development of compound semiconductors and 2D materials, mixed-dimensional heterostructures for novel physical phenomena and coupling, and heterogeneous integration technologies for electronic, optoelectronic, and photonic device platforms. He received his B.S. and M.S. in EECS from Seoul National University, and Ph.D. in ECE from UCLA. After his Ph.D., he worked as a postdoctoral associate and a research scientist at MIT, until he joined UIUC in Spring 2024.*

either through an external trigger or by spontaneous initiation under the imposed stress field.

When the load applied to a medium is sufficient for the crack-driving force to exceed the fracture resistance of the material, crack initiation and subsequent propagation occur along a path dictated by the applied stress. Typically, crack propagation can be categorized into three modes: Mode I (opening/peel), Mode II (in-plane shear), and Mode III (out-of-plane shear) (Fig. 2a). Crack advance is governed by the strain energy-release rate $G$ at the crack front relative to the critical energy-release rate (often written as $G_C$ or $\Gamma$). For mechanical lift-off, Mode I is generally preferred because it promotes a stable and predictable path well-suited for producing membranes. With this fracture-mechanics basis, spalling theory quantifies how stressor parameters and substrate properties determine the depth of the spalling plane and the conditions for stable Mode-I propagation.

Spalling theory was initially developed by Thouless *et al.* in 1987.[12] However, the theory had appreciable discrepancies compared to experimental data since it assumed infinite substrate thickness. Drory *et al.* successfully resolved these discrepancies

 This journal is © The Royal Society of Chemistry 2026

Open Access Article. Published on 11 maio 2026. Downloaded on 27/05/2026 13:44:17.
This article is licensed under a Creative Commons Attribution-NonCommercial 3.0 Unported Licence.

**Fig. 2** Mechanics and procedures for mechanical lift-off. (a) The three canonical fracture modes at a crack front: mode I (opening), mode II (in-plane shear), and mode III (out-of-plane shear);[23] Copyright 2021, Elsevier. (b) Schematic illustrating tape-assisted peeling under an applied bending moment $M$ and edge force $P$, which generate stress-intensity factors $K_I$ and $K_{II}$ that drive crack initiation and guide the crack toward an energetically favorable spalling plane. (c) Example of crystallography-guided, non-planar crack propagation during spalling of (100) GaAs;[22] Copyright 2022, Elsevier. (d) Photograph of a released SiC membrane after controlled spalling;[30] Copyright 2024, American Chemical Society. (e) Representative crack-initiation methods, namely (e1) laser ablation, (e2) localized substrate etching, and (e3) a wedge spaller. (f) Single-roller (f1) and double-roller (f2) spallers that provide a controlled, steady peeling force during propagation;[23] Copyright 2021, Elsevier.

by considering a more realistic, finite thickness substrate using a finite element calculation method.[13,14] The formulation used by Drory *et al.* treats spalling as a traction-prescribed boundary-value problem in a bimaterial system. The elastic mismatch between the two constituents—the stressed stressor layer and the spalled substrate—is represented compactly by the Dundurs parameters $\alpha$ and $\beta$. This mismatch then enters indirectly through the nondimensional coefficients $U$, $V$, $\gamma$, $c_2$ and the phase $\omega$, each a function of $\alpha$ or $\beta$. Under force and moment equilibrium, the six external loads reduce to two independent parameters, edge force $P$ and bending moment $M$ (Fig. 2b). The corresponding energy-release rate is described as:

$$G = \frac{c_2}{16}\left[\frac{P^2}{Uh} + \frac{M^2}{Vh^3} + \frac{2PM}{\sqrt{UV}h^2}\sin\gamma\right]$$

To characterize the crack-tip fields, we introduce the Mode-I and Mode-II stress-intensity factors, denoted by $K_I$ and $K_{II}$. Using the mixed-mode linear elastic fracture mechanics identity $G = \frac{c_2}{8}(K_I{}^2 + K_{II}{}^2)$ and the expression above for $G$, we

Open Access Article. Published on 11 maio 2026. Downloaded on 27/05/2026 13:44:17.
This article is licensed under a Creative Commons Attribution-NonCommercial 3.0 Unported Licence.

obtain,

$$K_{\mathrm{I}} = \frac{P}{\sqrt{2Uh}}\cos(\omega) + \frac{M}{\sqrt{2Vh^3}}\sin(\omega+\gamma)$$

$$K_{\mathrm{II}} = \frac{P}{\sqrt{2Uh}}\sin(\omega) - \frac{M}{\sqrt{2Vh^3}}\cos(\omega+\gamma)$$

where $h$ is the stressor thickness.[14,15]

Given the stressor thickness $h$, the elastic constants and the Poisson's ratios of both the stressor and substrate, and the residual stress in the stressor layer (all experimentally measurable or independently obtainable material parameters), or equivalently the resulting edge force $P$ and bending moment $M$, the elastic-mismatch parameters $\alpha$ and $\beta$ can first be determined. These parameters are then used to determine $U$, $V$, $\gamma$, $c_2$, and $\omega$ in the Drory formulation, from which $G$, $K_{\mathrm{I}}$ and $K_{\mathrm{II}}$ can be calculated as functions of crack depth. Crack initiation requires that the mixed-mode stress intensity be sufficiently large to overcome the fracture toughness ($K_{\mathrm{IC}}$) of the material, *i.e.*, $K_{\mathrm{I}}^2 + K_{\mathrm{II}}^2 \geq K_{\mathrm{IC}}^2$. Thus, both $K_{\mathrm{I}}$ and $K_{\mathrm{II}}$ contribute to fracture initiation, and mixed-mode loading can drive crack deflection onto an inclined plane. Once initiated, the crack trajectory is governed by the relative contributions of $K_{\mathrm{I}}$ and $K_{\mathrm{II}}$, which vary with depth. A positive $K_{\mathrm{II}}$ drives the crack deeper (downward), whereas a negative $K_{\mathrm{II}}$ causes it to deviate toward the surface (Fig. 2b). Consequently, the crack propagates unstably until it converges onto a trajectory where $K_{\mathrm{II}} = 0$. This condition satisfies the principle of maximum energy release rate, establishing a steady-state propagation regime where the crack advances strictly parallel to the surface.

For elemental semiconductors such as Si and Ge, controlled spalling along planes parallel to the substrate surface is relatively straightforward, because the fracture toughness does not vary dramatically among the major crystallographic planes. Several studies have demonstrated micron-scale controlled spalling of Si(100)[16–18] and Ge(100),[19,20] yielding single-crystal membranes with planar interfaces. These exfoliated membranes can be transferred and fabricated into functional devices—such as complementary metal–oxide–semiconductor (CMOS) circuits and solar cells—while retaining mechanical flexibility. However, for polar materials such as GaAs, the controlled spalling along ⟨100⟩ is difficult. Since zinc-blende III–V crystals have polar {111} terminations, cleavage is favored on the non-polar {110} planes.[21] In other words, the fracture toughness of the {110} plane is lower than that of {100}, where the {110} plane is inclined at a 45-degree angle relative to the surface of a {100}-oriented wafer. In this case, the $K_{\mathrm{II}}$ component changes sign during the peeling process. As the crack kinks upward onto {110}, $K_{\mathrm{II}}$ can increase until it overcomes the toughness difference $K_{\mathrm{IC}\{-100\}} - K_{\mathrm{IC}\{100\}}$ after which the crack turns back downward. Repeating this process produces a zig-zagging crack (Fig. 2c).[22]

These formulations establish the mechanical criteria that determine when and how a stable spalling plane forms, as well as the resulting spall depth (*i.e.*, the thickness of the exfoliated membrane), for a given set of material properties. The theory and experimental results indicate that controlled, uniform-thickness peeling cannot be universally achieved across all crystalline materials, particularly when the fracture toughness along the intended membrane orientation is not the weakest. Moreover, even in favorable crystallographic orientations, achieving perfectly uniform thickness remains challenging, as any spatial fluctuation in stress can perturb the crack front and introduce local thickness variations. This implies that uniform control of the stressor over large areas is crucial for scalable membrane production, as we discuss next.

### 2.2. Stressor layers for controlled spalling

As described above, controlled spalling of crystalline membranes requires stress applied to the target substrate. Most reported controlled-spalling processes employ the stack configuration (Fig. 2b):[14,19,23] (1) a substrate containing the crystalline thin film to be exfoliated, (2) a stressor layer, typically a ductile metal with built-in stress, and (3) a handle layer, which provides mechanical support and allows for the exertion of an external force.

The stressor layer is a central component for mechanical lift-off as it can provide controllable and uniform stress throughout the entire substrate, where various material systems can serve as the stressor. An ideal stressor should possess sufficiently high, uniform, and tunable residual stress for accurately controlling and tuning the thickness of exfoliated membranes. The stressor layer should also exhibit strong adhesion to the underlying membrane, and be mechanically robust to avoid cracking or rupturing during peeling. Stressors must also be compatible with standard deposition methods, such as physical vapor deposition and electroplating, and be compatible with subsequent fabrication processes.

A wide range of stressor materials have been explored for mechanical spalling, spanning both metals and dielectrics. For instance, Dross *et al.* demonstrated stress-induced spalling using evaporated Al and Ag overlayers.[24] Beyond these examples, residual stress in other metals (*e.g.*, Au, Pd, In) has also been leveraged to drive exfoliation and applied to delaminate stacked 2D material layers.[25] Dielectric films such as $SiN_x$ and $SiO_2$ can likewise develop substantial intrinsic stress during deposition; however, their comparatively low fracture toughness and limited ductility often lead to cracking or self-delamination during growth, leading to constrained practical use as stressors.[26] Among many candidates, Ni has been proved to be the most powerful and convenient choice due to its low cost, high fracture toughness, good adhesion, and broad stress tunability.[19] Ni stressors can commonly be deposited by sputtering or electroplating, where the sputtered Ni can exhibit tensile stress up to 700 MPa,[27] whereas electroplated Ni offers a broader tunable stress window up to ∼2 GPa,[28,29] enabling the exfoliation of tough materials such as SiC (Fig. 2d).[30]

First, electroplating is one of the most straightforward routes to deposit stressed Ni films. The process typically begins with substrate degreasing followed by mild alkaline/

Open Access Article. Published on 11 maio 2026. Downloaded on 27/05/2026 13:44:17. This article is licensed under a Creative Commons Attribution-NonCommercial 3.0 Unported Licence.

acid treatments to remove surface contaminants and enhance wettability. The substrate is then electrically connected as the cathode and immersed in a $Ni^{2+}$-containing electrolyte (commonly based on nickel salts such as $NiSO_4$ and/or $NiCl_2$). Upon applying a DC bias between the cathode and an anode, $Ni^{2+}$ ions are reduced and deposited onto the cathodic surface —*i.e.*, the target substrate—forming a Ni stressor layer.[16] By tuning the electrolyte composition and electroplating current density, Crouse *et al.* demonstrated a wide range of Ni stress values, mapping to different spalled Ge thicknesses.[20] However, electroplated Ni stressors suffer from intrinsic limitations. The electroplating process is susceptible to co-depositing impurities like hydrogen and sulfur, resulting in poorly controlled residual stress. Furthermore, these films often exhibit significant thickness non-uniformity, being characteristically thicker at the wafer edge. This variation directly translates to an uneven stress distribution. Collectively, these challenges of impurity incorporation and poor uniformity severely limit obtaining high-quality, controllably spalled films *via* electroplating.[31]

Sputtered Ni provides more uniform stress/thickness distribution,[30] and offers higher tunability, and thus is the most commonly chosen way of stressor deposition in recent years. Several mechanisms contribute to the tensile residual stress in sputtered Ni—important when fine-tuning the stress for a spalling stressor. (i) Thermal-expansion mismatch: the coefficient of thermal expansion (CTE) of Ni is $\sim(12.9–17.0) \times 10^{-6}\ K^{-1}$ at 300–600 K,[32] *versus* $\sim2.5 \times 10^{-6}\ K^{-1}$ for Si as an example; heating during sputtering followed by cooling leaves the Ni film in tension. (ii) Grain coalescence and excess-atom incorporation: during deposition, polycrystalline grains coalesce (*e.g.*, *via* grain rotation), generating strain.[33] In the pre-coalescence stage, excess atoms can incorporate at grain boundaries or become trapped between surface ledges, also generating strain.[34–36] (iii) Atomic peening. Ion bombardment of the growing film densifies the near-surface and induces residual stress—analogous to hammer peening on metal. As the sputtering pressure increases beyond ~3 mTorr, the bombardment energy drops and the stress can transition from compressive to tensile.[37,38]

The wide tunability and versatility of Ni have made it an effective stressor layer for a broad range of material spalling processes and have enabled many applications leveraging controlled spalling. However, Ni presents intrinsic drawbacks, such as the compatibility with subsequent processes and the risk of chemical contamination during Ni removal. In addition, achieving precise and spatially uniform stress control over large areas is challenging with Ni, which complicates ultra-uniform membrane thickness control. It is also difficult to realize low or near-zero residual stress, which is required for more delicate processes such as exfoliation of 2D materials. More generally, achieving ultrathin nanomembranes is inherently difficult when relying solely on a stressor layer-driven spalling process. The stress required to initiate crack formation sets a lower bound on the achievable membrane thickness, corresponding to the depth at which the stress intensity factor satisfies the fracture criterion. This means that, regardless of stressor quality, an intrinsic limit exists on the minimum membrane thickness that can be produced. These limitations have motivated the development of emerging strategies that offer improved controllability, as discussed in the following sections.

### 2.3. Methodology for mechanical lift-off

Once a stressor layer is deposited (optionally with a handling layer), mechanical spalling can occur either spontaneously or *via* an external trigger. Spalling begins with the initiation of a crack, followed by its propagation.[23] Typically, spontaneous crack initiation due to the membrane or stressor's residual stress is not desirable, because cracks may nucleate at arbitrary locations and disrupt controllable, continuous crack propagation. This limits the ability to peel a uniform membrane over the entire substrate, as the crack can wander upward or downward until it settles on an energetically favorable cracking plane.

Therefore, various strategies have been explored to control the initiation of cracks and their propagation, which often involve applying external force. The mechanics in section 2.1 describes how a crack can spontaneously nucleate and propagate, yet it does not consider the role of such external force. Early studies paid limited attention to the controlled initiation of cracks, which often resulted in unpredictable thickness variations near the initial crack front. For example, a simple and widely used method employs adhesive tapes as a handle layer, which is applied to the stressor/membrane/substrate stack and then gently pulled upward manually.[19] Although this approach is straightforward to implement, it provides no control over where the crack is initiated. Once a crack is initiated arbitrarily, the crack may deviate upward or downward to seek an energetically favorable plane, leading to non-uniform film thicknesses. To address this limitation, various crack initialization methods have been developed, such as wedge spalling[39] laser ablation,[40] and substrate chemical etching (Fig. 2e).[41] In these approaches, a predefined notch or weakened region is formed at a predefined depth/plane, through a thin blade, localized laser ablation, or targeted etching, so that the crack initiates at this site and subsequently propagates along the intended path.

Even with controlled crack initiation strategies, non-uniformity in the applied force can still induce roughness and thickness variation. To address this, utilizing a single-roller spaller (a motor-driven cylinder) provides a steady, controllable, and reproducible peeling force and can greatly improve the thickness uniformity of the exfoliated membrane.[41] A two-roller spaller can enable control of the angle and tension of the handle layer, providing even more precise load control at the crack tip. By precisely calculating and controlling the load, the substrate can be spalled at the desired depth. This extra controllability of forces can affect the final spall depth.[42] Another advantage of such roller systems is high throughput; complete wafer-scale exfoliation can typically be achieved on the scale of seconds (Fig. 2f).[23] These attributes make roller-

Open Access Article. Published on 11 maio 2026. Downloaded on 27/05/2026 13:44:17.
This article is licensed under a Creative Commons Attribution-NonCommercial 3.0 Unported Licence.

based spalling particularly attractive for potential industrial translation. In practice, however, industrial adoption has so far been limited to specific applications, such as cost reduction of expensive single-crystal substrates (*e.g.*, GaAs or Ge) in III–V solar cell production.[23] Although exfoliation of various materials at a wafer scale (≥4 inch) has been demonstrated,[19,43] the key barrier to economical substrate reuse is the post-spall surface condition: spalling-induced roughness and morphological defects often necessitate chemical–mechanical polishing (CMP) before the wafer can be reused without compromising device performance. Mangum *et al.* systematically categorized spalling-induced defects and correlated them with performance degradation in III–V solar cells.[44] Consequently, to be able to minimize the requirement of CMP for substrate reuse, extreme precision in the interface of lift-off is required as discussed in the following section.

More broadly, mechanical splitting combined with wafer bonding has recently been commercialized to reduce the cost of high-quality SiC wafers. Specifically, a monocrystalline 4H-SiC wafer is bonded to a polycrystalline carrier and then split, yielding a 350–800 nm thick high-quality SiC film attached to a handle wafer.[45] This process is carried out at an industrial scale, enabling the production of 10 SmartSiC™ wafers from a single monocrystalline 4H-SiC wafer. A closely related ion-implantation-based splitting process (Smart Cut™) is widely used for silicon-on-insulator (SOI) wafers.[46]

To summarize, the framework of mechanical lift-off—including the theory of crack generation and propagation, the utilization of stressor layers to provide necessary forces, and the implementation of lift-off processes for controlling and guiding crack evolution—establish the foundation for producing high-quality crystalline membranes through controlled spalling. However, as discussed above, several limitations have constrained the broader adoption of conventional mechanical lift-off approaches, including thickness uniformity, surface roughness, crack deflection or zig-zag propagation, intrinsic lower bounds on achievable membrane thickness, and potential incompatibilities with process flows. Recent advances have now opened a new generation of mechanical lift-off strategies that leverage engineered interfaces and novel exfoliation schemes, enabling controlled crack propagation that results in atomically abrupt interfaces, nanoscale membrane thicknesses, broader material compatibility, enhanced reproducibility, and greater scalability. As discussed in the following sections, these developments substantially broaden the scope and applicability of mechanical lift-off.

## 3. Emerging technologies for ultimate controllability in mechanical lift-off

Mechanical lift-off technology has demonstrated broad applicability across various material systems. However, as emerging applications increasingly require ultrathin films, atomically smooth interfaces, and reproducible exfoliation over large areas, the limitations of conventional spalling methods become apparent. These challenges have motivated the redesign of the process in several distinct domains. One major direction focuses on interface modification—through substrate engineering, insertion of interlayers, epitaxial design, or structural modification—to define the spalling plane with far greater precision and controllability. Another direction focuses on post-growth manipulation strategies to govern how cracks are initiated and guided, enabling substantially improved uniformity, thickness control, repeatability, and throughput. As we describe below, these approaches have enabled producing crystalline films and nanomembranes with atomic-scale thickness precision, interface smoothness, wafer-scale uniformity, and excellent repeatability, thus positioning mechanical exfoliation techniques as truly versatile technology for membrane-based applications.

### 3.1. Interface engineering strategies

From the classical spalling theory, a crack in a stressed material propagates at a depth where the shear component of the stress intensity factor $K_{II} = 0$. While this criterion applies to homogeneous materials, the behavior can be different in heterogeneous material systems. In heterogeneous systems, the fracture toughness values of constituent layers, as well as the interfacial bonding strength, need to be collectively considered. Intuitively, the crack could follow the mechanically weakest path available, even if this path does not coincide with the depth that minimizes shear. For example, if the interfacial toughness ($K_{int}$) is significantly lower than the bulk material fracture toughness, the interface can act as a geometric constraint that forces the crack to propagate along the boundary. In this case, $K_{II}$ is not necessarily zero at the crack position, and the spalling criterion becomes $K_I^2 + K_{II}^2 > K_{int}^2$.

These considerations suggest a straightforward strategy for depth control: deliberately introducing a weak interface that defines the spalling plane. When such an interface is combined with an appropriately tuned stressor layer, the crack propagation can be guided along the heterointerface. Therefore, weakened interfaces provide a route to near-ultimate control of exfoliation, enabling atomically abrupt spalling interfaces and greatly expanded thickness tunability down to the nanoscale. Below we discuss notable interface tuning technologies that enabled controlled spalling.

**3.1.1. Mismatch-driven strategies.** Lattice and thermal expansion mismatches are commonly present in heteroepitaxial material systems and are known to generate internal strain and misfit dislocations. These strain fields and defects modify interfacial energies, creating opportunities to influence crack propagation and define the spalling plane.

For material systems with large mismatch, significant strain can accumulate at the heterointerface during growth and post-growth cooldown, which could promote spontaneous separation of the epilayer from the growth substrate. Voronenkov *et al.* studied the self-separation and cracking behavior in highly mismatched systems, revealing its strong dependence

Open Access Article. Published on 11 maio 2026. Downloaded on 27/05/2026 13:44:17.
This article is licensed under a Creative Commons Attribution-NonCommercial 3.0 Unported Licence.

on the film-to-substrate thickness ratio.[47] After exceeding a critical ratio, reproducible separation without cracking can be achieved. Taking GaN on sapphire as an example (~13.8% mismatch), controllable GaN separation on a standard 430 μm-thick 2-inch sapphire substrate could be achieved when the GaN thickness reaches 2800 μm, which is consistent with the report from Fujito *et al.*[48] Even in material systems with much smaller mismatches, mismatch-induced local strain and associated energy variations can still arise. These effects primarily originate from non-ideal interfaces and phase mixing caused by atomic interdiffusion or memory effects of precursors. By exploiting the localized misfit strain energy at the InP/$In_{0.53}Ga_{0.47}As$ heterointerface, Park *et al.* successfully reduced the surface energy of the (100) plane, which is parallel to the interface, to below that of the (110) plane.[49] As a result, the (100) plane becomes energetically favorable for layer release during spalling, providing a pathway for eliminating the zigzag fracture morphology commonly observed at the spalled interfaces in III–V materials. Consequently, the epitaxial structure can be separated at the heterointerface (Fig. 3a). The estimated exfoliation yield was about 78%. Moreover, thickness uniformity measurements over a 15 × 15 $mm^2$ sample showed uniform layer release over an area of >12 × 12 $mm^2$, highlighting the potential for producing atomically flat, uniform III–V membranes over large areas.

In addition to lattice-mismatch-induced strain, mismatch in the CTE between the epilayer and the substrate provides another useful pathway to generate the strain required for membrane release, which could spontaneously occur during cooldown after epitaxy, or be induced intentionally through post-growth annealing. First, in thin-film epitaxy, which is typically performed at elevated temperatures, films grown beyond the critical thickness often become partially or fully relaxed through dislocation formation. During subsequent cooldown, however, thermal stress builds up due to CTE mismatch between the epilayer and the substrate. Specifically, when the CTE of the epilayer is larger than that of the substrate, the epilayer tends to contract more than the substrate upon cooling. This differential contraction generates significant tensile stress within the film, which can be harnessed to drive spontaneous membrane release.[24,50]

Second, intentional post-annealing processes applied after heterostructure growth can be used to trigger spontaneous delamination. During such post-annealing processes, the strain evolution generally undergoes three sequential stages: the initial release of pre-stored residual strain, a temporary thermally strain-free state near the growth temperature, and finally, the induction of new thermal strain due to the CTE mismatch upon further temperature increase. This mode is particularly effective when the epilayer possesses a lower CTE than the substrate. In this case, while the film might be under compression after growth, the higher expansion rate of the substrate during post-annealing pulls the epilayer into a state of high tensile strain. When this newly generated thermal strain energy surpasses the interface bonding tolerance, spontaneous interfacial delamination can occur (Fig. 3b). Utilizing this phenomenon, Lu *et al.* demonstrated a spontaneously exfoliated $Ga_2O_3$ film from the AlN template by annealing as-grown $Ga_2O_3$/AlN/sapphire wafer in a furnace.[51] Interestingly, the intentional introduction of dopants, such as Si, enhanced interfacial thermal stability and promoted exfoliation along the desired interface before interdiffusion occurs. This increases the yield of successful spontaneous delamination and enables reuse of the host substrate.

These examples clearly illustrate that the mismatches in lattice and thermal properties provide an intrinsic driving force for film separation and offer opportunities for controllable mechanical exfoliation with atomic precision. Such strategies can, in principle, be extended to a wider range of material systems that can be grown epitaxially. However, lattice and thermal mismatches are often accompanied by dislocation formation, which can degrade film quality and thus the performance of devices fabricated using the membranes. Lattice and thermal mismatch can also be unevenly distributed over wafer-scale films, which is a challenge for industrial scaling. In addition, the thermal budget associated with high-temperature processes must be carefully considered when implementing mismatch-driven strategies for membrane production.

**3.1.2. Structural modification strategies.** Besides the strain-induced exfoliation, another effective strategy for achieving controlled film release is to artificially engineer the interface within the epitaxial structure. Instead of relying solely on lattice or thermal mismatch, this approach focuses on intentionally modifying the interfacial structure to lower its adhesion energy or fracture toughness, thus making a natural path for crack propagation during spalling. Various techniques have been proposed to achieve such interfaces, including nanopatterning-assisted strain localization, porous layer formation, and strain-induced phase transformation.

First, nanopattern-assisted strain localization strategies rely on patterned interlayers, where selectively exposed regions of the substrate govern the nucleation and epitaxial lateral overgrowth, while the masked area with weak interfacial bonding guides crack propagation. This approach allows the fracture to follow predefined, low-energy paths and enables precise control of exfoliation depth and location. McClelland *et al.* first reported the cleavage of lateral epitaxial film for transfer (CLEFT) technique for III–V material membrane production and substrate reuse.[52] The process involves lithography, carbonization of the photoresist, lateral overgrowth, and exfoliation of laterally overgrown epilayers. Since the adhesion between the mask (*i.e.*, carbonized photoresist) and the substrate is weak, the epilayer strongly adheres only to the unmasked area where the III–V epilayer and the substrate are directly bonded. This approach has enabled the exfoliation of GaAs film from a GaAs substrate without significant degradation. However, CLEFT is highly dependent on substrate orientation and is largely limited to (110) oriented substrates, making extension to (100) substrates challenging. As described above, {110} planes are the primary cleavage planes for zinc-blende III–V materials, and cracks generated on (100) substrates tend to deviate towards the inclined {110} facets during

Open Access Article. Published on 11 maio 2026. Downloaded on 27/05/2026 13:44:17.
This article is licensed under a Creative Commons Attribution-NonCommercial 3.0 Unported Licence.

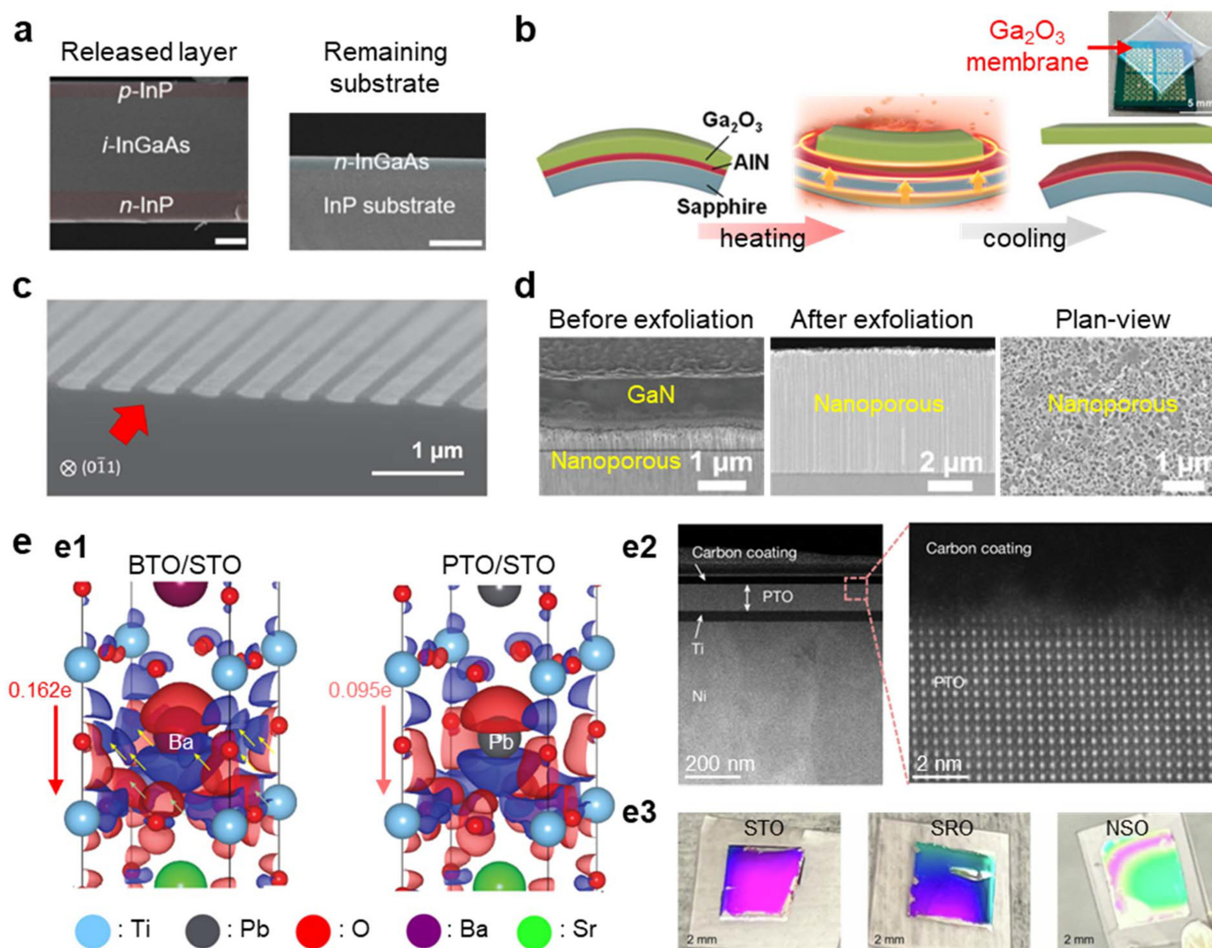


**Fig. 3** Advanced membrane release techniques: mismatch-driven and structural-modification approaches. (a) Cross-sectional scanning electron microscope (SEM) images of the released layer and the remaining substrate after InP/InGaAs/InP layer exfoliation;[49] Copyright 2022, American Association for the Advancement of Science. (b) Schematic of the exfoliation based on CTE mismatch and a photograph of the as-exfoliated $Ga_2O_3$ membrane;[51] Copyright 2023, Elsevier. (c) SEM image of a substrate after exfoliation, exhibiting patterned features and fracture traces;[22] Copyright 2022, Elsevier. (d) Cross-sectional FIB-SEM images of the GaN membrane on the nanoporous GaN layer before exfoliation (left) and the remaining nanoporous GaN layer after exfoliation (center), together with a plan-view SEM image of the nanoporous GaN layer after exfoliation (right);[61] Copyright 2023, Wiley-VCH GmbH. (e) Pb-induced weakening of the PTO/STO interface enables clean exfoliation. (e1) Charge transfer calculated at the interface of BTO/STO (left) and PTO/STO (right). (e2) Cross-sectional transmission electron microscopy image. (e3) Photographs of released oxide films after the ALO process and freestanding membrane production using PTO as an interlayer;[66] Copyright 2025, Springer Nature.

propagation. Micron-scale patterns employed in CLEFT induce such crack deflection, limiting the deployment of the process to (100) substrates.

On the other hand, reducing the opening sizes to the nanoscale provides a chance to enable spalling along the (100) planes of III–V materials. For example, nano-imprint lithography (NIL) patterned $SiO_2$ masks could effectively confine the crack within the engineered interfacial layer.[53] High-density nanoscale patterns act as periodic stress concentrators that force the crack to propagate laterally along the intended (100) interface before it has the opportunity to deflect into the natural {110} cleavage planes. Braun *et al.* studied the effects of the shape, dimension, and arrangement of the patterned buried layer on the spalling of the GaAs epilayer.[22] It was found that maintaining the pattern continuity along the spall direction is the most important for creating the favorable fracture path, besides a proper aspect ratio, high-fill factor, and void formation during the overgrowth further helping stabilize the crack propagation along the NIL interlayer rather than along facet-forming planes (Fig. 3c). Fine-tuning the patterns has enabled the controllable exfoliation of millimeter-scale (100) oriented GaAs with a smooth interface. These results highlight that nanopatterning-assisted strain localization approaches provide a controllable route for guiding crack propagation and acquiring membranes with smooth surfaces. However, these techniques require additional lithography and etching steps, which increase process complexity. Furthermore, lateral overgrowth often leads to defect formation at coalescence boundaries in both homoepitaxial and heteroepitaxial systems, which need to be addressed to obtain

 This journal is © The Royal Society of Chemistry 2026

Open Access Article. Published on 11 maio 2026. Downloaded on 27/05/2026 13:44:17.
This article is licensed under a Creative Commons Attribution-NonCommercial 3.0 Unported Licence.

high-quality membranes.[54,55] In addition, selective three-dimensional nucleation typically requires growth to a certain thickness to achieve film planarization, which imposes a lower bound on the achievable membrane thickness.

Utilizing porous interlayers can also enable the guidance of crack propagation along the interface for controlled film release. In this method, a porous layer, typically formed by electrochemical etching or oxidation of a sacrificial buffer layer, is introduced between the epitaxial film and the substrate, thereby locally reducing the mechanical strength and adhesion energy at the interface. This technique has been widely established for producing Si membranes, in which a sacrificial porous silicon layer is formed *via* electrochemical anodization and subsequently serves as a structurally compliant template for epitaxial growth of Si and mechanical separation.[56,57] A similar strategy has been extended to germanium, where porous Ge layers created by anodization or metal-assisted chemical etching can act as sacrificial or fracture layers.[58,59]

This approach could be employed even for materials with significantly higher fracture toughness and chemical stability, such as nitrides. Min *et al.* demonstrated the utilization of porous interlayers to decrease the high interfacial toughness of GaN for controllable exfoliation.[60] The process involves electro-chemical etching to form a porous GaN layer, which dictates the depth of membranes, followed by the regrowth of nitride layers. During this high-temperature regrowth, the porous layer transforms into cavities, further reducing the interface toughness and facilitating membrane separation. Finally, by depositing a stressor layer, the GaN epitaxial structure can be readily spalled at the pre-defined porous interlayer at the wafer scale and subsequently used for device fabrication. To enhance the precision of this method, Zhang *et al.* introduced a graded-porosity design and demonstrated that stacking layers with varying porosities enables tuning of the interfacial fracture toughness to selectively match the energy release rate of the external stressor (Fig. 3d).[61] Porous interlayer-based approaches have also been successfully applied to other compound semiconductors, such as GaAs and InP, demonstrating their general applicability for achieving controlled exfoliation and substrate reuse.[62–64] However, etching-induced surface damage and impurity contamination may degrade the regrown film quality, while the thick overlayer required to flatten the porous morphology increases process time and cost, limiting the practical applicability of this technique.

Another unique structural engineering strategy relies on strain-induced structural phase transformations. Certain materials act as 'phase-change switches', which remain in a stable phase under equilibrium but transform into other metastable phases under applied stress. Kim *et al.* exemplified this concept using a molybdenum (Mo) interlayer.[65] When a Mo film was initially deposited on a glass substrate, the strain-free condition stabilizes Mo in a body-centered cubic (BCC) phase. Upon deposition of a stressed layer, such as $SiO_2$, the Mo layer near the interface transforms to a face-centered cubic (FCC) phase because of its higher stability under strain. The BCC/FCC interface formed within Mo exhibits substantially lower adhesion energy than its bulk counterparts, creating a preferred pathway for crack propagation. This allows for the successful exfoliation of the ~1 μm thick inorganic membrane at a centimeter scale, supporting the large-scale transfer of the 32 × 32 memory array without mechanical degradation.

Direct modulation of chemical bonding provides another pathway, particularly in complex oxide systems. Zhang *et al.* demonstrated that chemical doping, specifically introducing Pb into the perovskite lattice, can substantially reduce interfacial bonding strength by suppressing electron transfer between cations and oxygen.[66] Based on this strategy, controllable exfoliation of various perovskite oxides, such as SRO, BTO, and STO, was achieved with atomic precision, reaching thicknesses of sub-10 nm (Fig. 3e). Notably, the yield of pyroelectric device arrays fabricated over an entire 80 nm-thick transferred membrane reached 100%. These breakthroughs highlight that phase and chemical engineering approaches enable the production of ultrathin freestanding membranes with pristine surfaces.

In summary, these structural modification strategies focus on artificially reducing interfacial bonding strength to guide crack propagation. While well-defined, atomically abrupt interfaces can be achieved in many cases, preserving crystallinity and structural integrity remains challenging, especially as the film area is scaled up. In addition, these strategies cannot be universally applied across entire material systems, as their effectiveness depends strongly on the specific etching chemistry, bonding chemistry, three-dimensional growth, phase diagram, and process compatibility, necessitating the development of more universal exfoliation approaches that combine precise control with broad materials compatibility.

**3.1.3. Insertion of 2D materials at the interface.** Unlike bulk materials, layered 2D materials possess surfaces free of dangling bonds, resulting in intrinsically low surface energy and weak interfacial adhesion. This unique feature provides ideal conditions for film exfoliation or layer transfer without the need for additional sacrificial layers or complex template preparation processes. Beyond its simplicity, the introduction of 2D interlayers offers unparalleled precision in defining the fracture plane. Because atomically thin 2D interfaces form weak van der Waals bonds, the exfoliation path is strictly confined to a single atomic layer, eliminating the deflection of cracks or roughening of surfaces commonly observed in bulk spalling or porous-layer-based approaches. Consequently, this approach removes the lower limit on the thickness of the produced layers, enabling the production of ultrathin, high-quality, and atomically smooth nanomembranes.

A prerequisite for 2D materials-assisted exfoliation is forming crystalline thin films on the substrates coated with 2D layers. As a notable example, Chung *et al.* established a 3D-on-2D growth and transfer platform, demonstrating that epitaxial films can be mechanically exfoliated and transferred onto arbitrary substrates while maintaining high crystalline quality and device performance.[67] This discovery has motivated extensive

Open Access Article. Published on 11 maio 2026. Downloaded on 27/05/2026 13:44:17.
This article is licensed under a Creative Commons Attribution-NonCommercial 3.0 Unported Licence.

research into developing novel epitaxial growth and lift-off techniques assisted by 2D materials. Representative techniques for growing epitaxial films on 2D surfaces include remote epitaxy, where the crystalline substrate underneath the 2D material governs the growth, and quasi van der Waals epitaxy, where the 2D material itself serves as the guiding template.[68–71] These 2D-material-assisted epitaxy mechanisms provide a solid foundation for further developing 2D materials-assisted lift-off techniques (2DLT). Building on these foundational studies, many groups have demonstrated successful membrane growth and exfoliation across various material systems (Fig. 4a), including nitrides, arsenides, and perovskites.[72–76] The choice of 2D interlayers is also diverse, covering graphene, hexagonal boron nitride (h-BN), and transition metal dichalcogenides (TMDCs).[77–82] Using graphene as an interlayer, Kim *et al.* demonstrated remote epitaxy of high-quality GaAs, InP, and GaP, followed by precise film release from the host substrate along the (100) plane.[68] Similarly, Yuan *et al.* reported strain-relaxed perovskite films that were successfully exfoliated and transferred through graphene-mediated lift-off.[83] Yin *et al.* demonstrated nitride exfoliation assisted by $WS_2$,[78] while Kobayashi *et al.* showed that h-BN is also applicable for nitride transfer.[84] More recently, with the maturation of 2D material synthesis techniques, Snure *et al.*

Fig. 4 2D materials-assisted lift-off techniques. (a) Overview of 2DLT with representative membranes and 2D interlayers;[68,72–75,78,80] Copyright 2017 and 2022, Springer Nature, Copyright 2020 and 2021, American Chemical Society, Copyright 2019, 2022, and 2024, Wiley-VCH GmbH. (b) Wafer-scale GaN exfoliation by a 2DLT technique combined with CTE mismatch method;[92] Copyright 2021, American Chemical Society. (c) 2-inch GaAs exfoliation assisted by nanopatterned graphene: (c1) schematic of the stack structure, (c2) photograph of the exfoliated GaAs membrane and the remaining Ge wafer, and (c3) SEM image of the Ge surface after exfoliation;[15] Copyright 2022, Springer Nature. (d) Layer-by-layer harvest process in the 2DLT technique;[93] Copyright 2023, Springer Nature.

Open Access Article. Published on 11 maio 2026. Downloaded on 27/05/2026 13:44:17.
This article is licensed under a Creative Commons Attribution-NonCommercial 3.0 Unported Licence.

achieved wafer-scale (4-inch) GaN membrane transfer using the 2DLT method.[85] Further progress toward scalable manufacturing was demonstrated by Vuong *et al.* They reported the metal–organic chemical vapor deposition (MOCVD) growth of h-BN and subsequent vdW epitaxy of blue GaN-based multiple quantum wells (MQWs) light-emitting diode (LED) heterostructures on full 6-inch h-BN/sapphire wafers, followed by full-wafer device fabrication, membrane lift-off, and transfer.[86] This demonstration is particularly impactful for industrial translation, as it brings 2DLT from earlier proof-of-concept demonstrations into a wafer-scale format compatible with established manufacturing platforms.

Besides enabling scalable membrane transfer, 2D-material-assisted epitaxy may also provide opportunities for defect engineering. This possibility is particularly attractive for nitride systems, where defect management remains a long-standing challenge. Unlike the conventional nitride/sapphire interface, Liu *et al.* found that no periodic array of misfit dislocations or strain core is observed at the nitrides/graphene/sapphire interface. This indicates that the nitrides epilayer tends to release the strain spontaneously, rather than forming dislocations at the interface.[87] Shi *et al.* further explained that the spontaneous lattice relaxation at the GaN/graphene/sapphire interface originates from the reduced interfacial slip potential barrier, which is responsible for the strain and misfit dislocation reduction.[88] By using a graphene buffer layer (GBL)-covered SiC substrate, Qiao *et al.* substantially enhanced the interaction between the GaN epilayer and the underlying substrate while maintaining the releasable nature of the film. As a result, they achieved a releasable GaN film with record crystalline quality. Moreover, the GBL was able to withstand multiple growth-release cycles and enabled a 100% release yield for the epilayer, as demonstrated by three rounds of substrate reuse without re-graphitizing or any polishing process.[89] More recently, Wen *et al.* showed that the graphene interlayer enabled high-quality nitride epitaxy at reduced film thickness, further highlighting the potential of 2D interlayers for defect management in thin nitride epilayers.[90] Although these findings were established for graphene, similar interfacial effects may also be relevant to other 2D interlayers such as h-BN.[80] 2DLT also shows capability for maintaining film quality after transfer. For example, Blanton *et al.* achieved GaN films and subsequent AlGaN/GaN high-electron-mobility transistor (HEMT) structures on h-BN-covered sapphire substrates and found that the transfer process had minimal influence on both the film quality and device performance.[91] Kobayashi *et al.* also reported GaN films and subsequent blue InGaN/GaN MQWs grown on h-BN-covered sapphire substrates, for which clear MQWs satellite peaks remained visible after transfer, suggesting that the structural quality was largely preserved.[84] These results highlight the potential of the 2DLT approach for rapid film transfer, defect control, and integration compatibility.

In addition to its intrinsic capability for membrane formation and transfer, the 2DLT approach is highly compatible with other lift-off strategies. Karrakchou *et al.* showed an example of combining CTE engineering and 2DLT for the controllable exfoliation of epilayers (Fig. 4b).[92] The GaN-based LED structure is first grown on the h-BN covered sapphire substrate, and then a 30 μm thick copper layer is deposited on the top *via* electroplating. Upon annealing at a moderate temperature of 100 °C, far below the nitride growth temperature, the entire LED membrane detached spontaneously due to the shear stress induced by the CTE mismatch between the copper layer and the sapphire. As a result, crack-free membranes were obtained, and all 400 tested LEDs remained emissive, corresponding to a 100% crack-free transfer yield. Compared with approaches that rely solely on CTE mismatch-induced stress, this method is more compatible with back-end-of-line (BEOL) processes owing to its low thermal budget.

Besides CTE engineering, the 2DLT strategy is also compatible with nanopattern-assisted membrane exfoliation. Kim *et al.* reported a method to produce freestanding single-crystalline membranes based on nanopatterned graphene and developed the corresponding mechanics theory to precisely guide the cracks through the graphene layer (Fig. 4c).[15] The process includes graphene formation, patterning, and selective-area epitaxy of epilayers, which is analogous to the nanopattern-assisted membrane exfoliation described above. Owing to the weak bonding strength at graphene-covered regions, the epitaxial interface can be efficiently weakened, facilitating epilayer release. By appropriately matching the stressor thickness, epilayer thickness, and graphene coverage, wafer-scale controllable exfoliation has been achieved across a range of materials, from elemental semiconductors to III–V compounds. The resulting separation surfaces exhibit good spatial control, remaining flat over graphene-covered regions while showing height fluctuations in the exposed openings.

It is also worth mentioning that the 2DLT technique can be combined with chemical lift-off processes. Recently, Gao *et al.* demonstrated that integrating 2DLT with chemical lift-off provides an effective route for preserving the structural integrity of released thin films in liquid etchants, enabling lossless, wafer-scale stripping of GaN-based LED structures. These examples show the compatibility of 2D materials-based interface engineering strategies with various epitaxy and lift-off techniques, highlighting the versatility of 2D materials for membrane production with atomic precision.

Another appealing feature of 2DLT technique is that it provides a high-throughput pathway to produce freestanding single-crystalline membranes, which greatly compensate for the drawbacks of the conventional layer transfer process. Moving beyond high-crystalline quality 2D materials like graphene or h-BN, Kim *et al.* explored the use of thin amorphous carbon (TAC) and BN as interlayers.[93] These materials can be deposited at significantly lower temperatures than their crystalline counterparts while still allowing the underlying substrate to guide epitaxy. This enables the formation of multiple alternating layers of 2D materials and epilayers in a single growth run. Consequently, each epilayer can be harvested layer-by-layer, providing a pathway to produce multiple freestanding membranes from a single wafer (Fig. 4d). Moreover, atomic-

Open Access Article. Published on 11 maio 2026. Downloaded on 27/05/2026 13:44:17.
This article is licensed under a Creative Commons Attribution-NonCommercial 3.0 Unported Licence.

precision exfoliation at the 2D interface allows the reuse of the host wafer for subsequent membrane production without requiring a complicated refurbishing process, which is beneficial for reducing cost and processing time.

Placing 2D materials as cleavage planes provides a clean, versatile, and highly compatible strategy for producing free-standing single-crystalline membranes with well-defined thickness at the atomic scale. One of the key challenges in implementing 2DLT lies in controlling the film thickness and crystallinity, due to the nucleation difficulty on the inert 2D material surface and the possible interface contamination if 2D materials are prepared by transfer. The difficulty in forming pristine and uniform 2D materials as templates, as well as preserving them under harsh epitaxy environments, also remains a challenge—especially when considered for use at wafer-scale for high-volume manufacturing.[94,95] Fortunately, various strategies are being developed to address these challenges, which can be found in other reviews.[96,97] These advances establish a strong foundation for the future development of 2D materials-based lift-off technology.

### 3.2. Advanced lift-off techniques

In addition to engineering the interface, which we discussed above, achieving fully controllable exfoliation also requires precise management of crack initiation. If a crack nucleates randomly, instead of at a predetermined location and depth, this leads to variations in spalling depth and thus nonuniform film thickness and reduced yield. Once a crack is initiated, its subsequent propagation must also be regulated to maintain a consistent spall depth, avoid film cracking, and prevent deviations from the intended release plane. Therefore, precise exfoliation requires control over both the initiation of the crack and its subsequent propagation, which are particularly crucial for emerging applications requiring nanoscale thickness control. Here, we describe lift-off techniques that can be employed "after" growth to address these two aspects—establishing reliable initiation sites and regulating the applied peeling forces—and achieve reproducible and uniform membrane release.

First, deterministic control of the crack initiation position is a prerequisite for precise exfoliation, since it ensures that fracture begins at a designed depth before propagating through the substrate. A common approach is cutting the wafer edge or using a wedge fixed on a wall to create a crack, as described in section 2.2. For materials with higher fracture toughness, however, such mechanical initiation may be insufficient. In these cases, introducing localized damage such as a shallow trench at the substrate edge can further reduce the energy threshold for crack initiation. Using this approach, Horn *et al.* demonstrated the controllable exfoliation of 4H-SiC membranes with a Ni stressor (Fig. 5a).[30] For applications requiring higher precision in spalling positioning, applying an

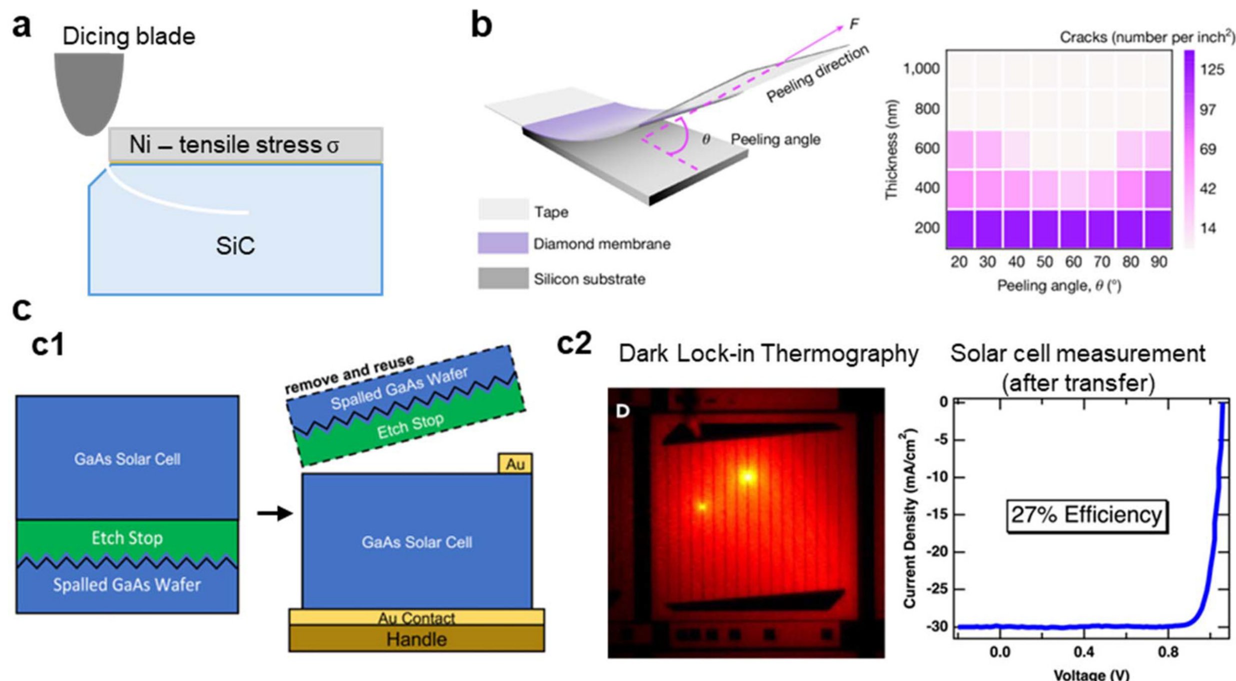


Fig. 5 Emerging lift-off techniques for controlled membrane exfoliation. (a) Schematic of the spalling geometry for crack initiation and propagation;[30] Copyright 2024, American Chemical Society. (b) Schematic and experimental statistics of microcrack density and crack-propagation probability for an exfoliated diamond membrane under different peeling angles;[98] Copyright 2024, Springer Nature. (c) Acoustic spalling for GaAs wafer reuse: (c1) process schematic; (c2) (left) a dark lock-in thermography image of the as-grown GaAs solar cell device on a spalled GaAs wafer, revealing localized non-linear shunt hot spots associated with the rough spalled surface; (right) *J*–*V* characteristics of a GaAs solar cell after transfer onto a Au layer, achieving ~27% efficiency with suppressed shunting;[103] Copyright 2023, Cell Press.

Open Access Article. Published on 11 maio 2026. Downloaded on 27/05/2026 13:44:17.
This article is licensed under a Creative Commons Attribution-NonCommercial 3.0 Unported Licence.

adhesion demoter or laser becomes an effective method to initialize cracks. The demoter is a material (such as ink or powder) that reduces the adhesion between the stressor layer and the substrate. By localized adhesion reduction, it ensures clean fracture propagation within the substrate center and prevents uncontrolled cracking at the wafer edge after stressor deposition. Laser-assisted crack initiation is a technique where a laser is used to create well-defined notches at the substrate edge, providing controlled starting points for fracture. This approach allows precise definition of the crack initiation site, improving reproducibility and uniformity in exfoliation, and thus has been widely applied to Si membrane exfoliation and substrate reuse.

Second, once a crack is initiated, subsequent crack propagation also needs to be carefully managed to achieve a uniform exfoliation. Consequently, various methods have been developed to regulate the applied stress and crack dynamics during peeling, ensuring controllable propagation and improved film quality. One primary cause of non-uniformity in exfoliated film was the uneven stress induced by the Ni stressor, which stems from thickness variation during deposition. To address this, Ward *et al.* designed a spalling tool integrating a laser displacement sensor and an active tension control system.[42] This closed-loop system compensates for local stress variations during peeling, improving Si film thickness uniformity by 53% and surface roughness by 67% compared to conventional tools without thickness compensation.

In addition to controlling the uniformity of stress distribution, how to apply a peeling force plays a significant role in governing crack propagation and membrane integrity. Jing *et al.* systematically studied the effect of peeling angle on diamond membranes and revealed that the optimal peeling angle strongly depends on the film thickness.[98] For thick membranes (800–1000 nm), successful exfoliation can be achieved over a wide range of angles, while thin membranes (~600 nm) require a narrower angle range of 40°–70° to avoid cracks (Fig. 5b). By utilizing an appropriate peeling angle, diamond membranes are successfully exfoliated at the wafer scale with minimal damage. As another approach, Li *et al.* mitigated the stick–slip instability commonly encountered in tape-based peeling, arising from the stretching and abrupt failure of adhesive fibrils, by replacing conventional tape with a hot-pressed thin thermoplastic polyurethane (TPU) handle layer.[99] This approach isolates adhesive fibrillation from other influencing factors, yielding more reproducible results.

Ultrasonic and other externally assisted methods can further facilitate controlled crack propagation, enabling uniform membrane separation in otherwise challenging material systems. To utilize ultrasonic vibration for controlled spalling, Bertoni *et al.* pre-stressed substrates to just below the fracture threshold and then applied controlled ultrasonic waves, which transiently increased the total stress beyond the material's fracture toughness.[100] This approach enabled gradual crack propagation and subsequent membrane separation, which could be applied to Si, sapphire, and glass systems. Sacchitella *et al.* applied this technique to reuse GaAs substrates—they grew the same cells by MOCVD on a fresh substrate, a substrate that had been spalled once, and a substrate that had been spalled twice.[101] They noted that the best devices from each wafer were very similar, but the reused substrates had more variability in their devices. Similarly, Coll *et al.* demonstrated substrate reuse in SiC, successfully harvesting membranes from wafers with thicknesses of 68.1 ± 7.6 μm and 22.3 ± 3.2 μm, respectively, highlighting the effectiveness of acoustic-assisted spalling in enabling the exfoliation of high-fracture-toughness materials.[102] For 50 mm SiC wafers, the lift-off area reached approximately 80%–90% of the wafer. Although these approaches enable controllable exfoliation, acoustic-assisted spalling faces challenges in maintaining surface uniformity and minimizing roughness, which are critical for subsequent epitaxial growth. Schulte *et al.* explored mitigating the issue *via* growth design; by incorporating wet etching, thick-layer growth, and planarizing regrowth steps, defects in the GaAs epitaxial structure could be mitigated.[103] As a result, solar cells with 26.9% photovoltaic conversion efficiency were obtained, which are comparable to devices fabricated by conventional methods (Fig. 5c).

Overall, the emerging strategies reviewed here demonstrate significant progress in improving the controllability of mechanical lift-off. Interface engineering, structural modification, 2D interlayers, and more advanced lift-off techniques have together provided new ways to control crack initiation and propagation, making it possible to obtain crystalline membranes with improved thickness uniformity, smoother interfaces, and better reproducibility over large areas. These developments suggest strong potential for reducing manufacturing costs, improving device performance, and expanding the application space of membrane-based technologies. Nevertheless, several limitations remain to be addressed. Most approaches introduce additional complexity, such as narrow process windows, extra process steps, or material-specific mechanisms, which restrict their wider applicability. In addition, achieving precise exfoliation without compromising film quality is still challenging in many systems. Further advances will therefore require more universal strategies that integrate multiple aspects, including broad materials compatibility, interface-driven structure design, simplified processing, and robust exfoliation control, rather than relying on any single approach. Progress along multiple fronts will be essential for translating these techniques into scalable manufacturing technologies.

## 4. Emerging non-mechanical lift-off techniques

Mechanical exfoliation is often regarded as a simple and low-cost approach for producing freestanding membranes. Nevertheless, even with the advanced strategies described above, mechanical exfoliation still faces limitations in terms of the final membrane thickness, uniformity, and crystallinity. To address these constraints, alternative lift-off methods—such as

Open Access Article. Published on 11 maio 2026. Downloaded on 27/05/2026 13:44:17.
This article is licensed under a Creative Commons Attribution-NonCommercial 3.0 Unported Licence.

chemical lift-off or laser lift-off—have played an important historical role in membrane release. Chemical lift-off offers deterministic control of exfoliation depth by using sacrificial layers engineered to dissolve with high selectivity, enabling ultrathin films independent of fracture mechanics. In material systems where lattice-matched sacrificial layers are available, this approach can also preserve the crystalline quality of the resulting membranes. Laser lift-off relies on localized energy absorption to melt or break interfacial bonds, allowing large-area separation of materials that lack suitable sacrificial layers. As with mechanical lift-off, these methods have seen important recent innovations that expand their applicability, precision, and scalability. For a balanced perspective, we introduce these techniques here and discuss their advantages, limitations, and integration considerations.

### 4.1. Chemical lift-off

Chemical lift-off (CLO) is a release technique that utilizes a chemical etchant to selectively remove an interlayer, separating an originally stacked structure from its host substrate. Typically, the sacrificial layer is intentionally introduced so that the release occurs at the designed interface, allowing the target film to be detached as a thin membrane. If both the target layer and the sacrificial layer are epitaxially grown, this process is often referred to as epitaxial lift-off (ELO). CLO is a broader term as CLO does not necessarily require the layers to be epitaxially formed. For example, for a SOI wafer composed of a $Si/SiO_2/Si$ structure made by wafer bonding, CLO can be used to obtain a thin Si membrane by selectively removing the buried $SiO_2$ layer. Compared with mechanical lift-off, this method provides two distinct advantages: it can produce a sharp surface, and it offers good control of membrane thickness. This is because the final thickness is defined by the epitaxial growth (for ELO) or by the bonding/interface geometry (for bonded stacks), rather than by a mechanical fracture. Consequently, CLO has received increasing attention as a reliable approach for producing high-quality nanomembranes.

**4.1.1. Principles and conventional material systems for chemical lift-off.** CLO is broadly applicable in material systems where a selectively removable sacrificial layer can be inserted between the growth substrate and the target epitaxial device layer. A generalized CLO workflow typically consists of: (i) integrating a sacrificial layer beneath the device layer, (ii) laminating or depositing a temporary handle/carrier layer (*e.g.*, black wax, polymer carriers, or thermal release tape) to provide mechanical support during and after release, (iii) exposing the sacrificial layer through edge opening or patterned access windows, (iv) selectively etching the sacrificial layer to laterally undercut and release the device membrane, and (v) transferring and bonding the freestanding single-crystal membrane onto a foreign host substrate through van der Waals bonding or an adhesive interlayer (*e.g.*, spin-on glass (SOG),[104] polyimide (PI),[105] or benzocyclobutene (BCB)[106]) (Fig. 6a).

A representative example of a "ready-to-use" CLO template is the SOI wafer, consisting of a Si handle wafer, a buried oxide (BOX), and a device Si layer. After attaching a temporary handle layer on the top Si device layer, the BOX can be selectively removed in hydrofluoric acid (HF), yielding a freestanding single-crystal Si nanomembrane supported by the handle. The BOX dissolution is commonly written as,[107]

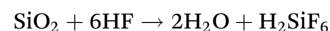

$$SiO_2 + 6HF \rightarrow 2H_2O + H_2SiF_6$$

The released Si nanomembrane can then be transferred and integrated onto arbitrary rigid or flexible substrates, enabling diverse device implementations such as metal oxide semiconductor field effect transistors (MOSFETs)[108,109] and solar cells.[110] Because silicon remains the backbone of modern microelectronics, silicon-based membranes provide a powerful pathway toward monolithic 3D integration, allowing high-performance Si device layers to be stacked up for both more Moore and More-than-Moore applications.

In many III–V material systems, high-quality sacrificial layers can be epitaxially grown together with the device stack; therefore, CLO is most often implemented in the form of ELO. For III–V ELO processes, the most widely adopted sacrificial layer is AlAs (or high-Al-content AlGaAs), which can be etched with extremely high selectivity relative to GaAs-based device layers. Pioneering studies by Yablonovitch *et al.* established the feasibility of lifting off high-quality epitaxial films by selectively dissolving an AlAs release layer in HF, provided that the structure is designed to ensure efficient etchant transport and byproduct removal at the advancing etch front.[5,111] This extreme selectivity between GaAs and AlAs is later elucidated by Voncken *et al.* The etching reaction of AlAs in the process can be written by

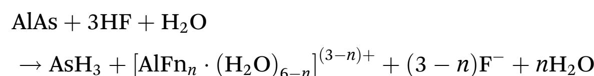

$$\begin{aligned} & AlAs + 3HF + H_2O \\ & \rightarrow AsH_3 + [AlFn_n \cdot (H_2O)_{6-n}]^{(3-n)+} + (3-n)F^- + nH_2O \end{aligned}$$

with $n$ = 0, 1, 2 or 3.[112] The etching reaction demonstrates the safety concerns of the process, due to the usage of HF as well as the production of arsine gas, which is highly toxic. The process also imposes limitations for recycling substrates. For substrate reuse, the remaining substrate surface should remain epi-ready; however, post-release residues and surface roughening can require additional repolishing (*e.g.*, a polishing etch and, in some cases, CMP), adding cost and potentially limiting the number of reuse cycles. These issues have motivated the search for alternative sacrificial-layer/etchant pairs that avoid toxicity and reduce residues.[113,114]

As an example, Cich *et al.* have demonstrated using InGaP as a sacrificial layer which can be selectively etched by HCl.[115] Leveraging the high selectivity between epitaxially grown GaAs and the InGaP layer, they achieved sharp undercuts, demonstrating its viability as a sacrificial layer. However, this material combination suffers from a slow etch rate, reported to be 0.9 $\mu m\ min^{-1}$, which is approximately 16 times slower than the conventional HF/AlAs (1 $mm\ h^{-1}$) pair.[5] To address this limitation, Ansbæk *et al.* demonstrated that using InAlP with HCl provides both high selectivity and an etch rate approximately 10 times faster than InGaP.[116] Furthermore, they found

Open Access Article. Published on 11 maio 2026. Downloaded on 27/05/2026 13:44:17.
This article is licensed under a Creative Commons Attribution-NonCommercial 3.0 Unported Licence.

Fig. 6 Conventional and advanced approaches for chemical lift-off. (a) Generic CLO process flow: a target film on a sacrificial layer is supported by a handle, selectively released, and then transferred/bonded to a foreign substrate. (b) Anisotropic etching of InAlP in HCl, producing suspended cantilevers through lateral undercutting of the sacrificial layer;[116] Copyright 2013, AIP Publishing. (c) Schematic of bandgap-selective PEC ELO, where the lower-bandgap InGaN absorbs photons and dissolves in KOH, while the GaN remains intact. (d) Wafer-scale lift-off of a micrometer-thick GaN film using an InGaN release layer and bandgap-selective PEC;[122] Copyright 2017, Wiley-VCH GmbH. (e) NPAs as the sacrificial layer, enabling fast release of an α-$Ga_2O_3$ membrane;[128] Copyright 2025, American Chemical Society. (f) Strain-assisted ELO, where multiple films are released simultaneously together with the strained layers, greatly increasing throughput;[129] Copyright 2023, American Chemical Society. (g) Released $Al_2O_3$ film using an SAO sacrificial layer, along with a scanning transmission electron microscopy (STEM) image of the STO/SAO epitaxial structure;[142] Copyright 2021, Wiley-VCH GmbH.

the etch rate to be highly anisotropic, with the ⟨100⟩ direction etching ten times faster than the ⟨110⟩ directions. This crystallographic dependence makes InAlP a promising candidate for the sacrificial release of high-aspect-ratio structures. This is achieved by aligning the long axis of the structure with the fast-etching direction, ⟨100⟩ in this case (Fig. 6b).

Although alternative sacrificial-layer/etchant pairs have been successfully demonstrated in GaAs-based systems, extending purely chemical ELO to GaN-based devices is intrinsically challenging. III–nitrides are chemically robust, and nitride layers that are closely lattice-matched to GaN and suitable as growth templates (*e.g.*, AlN) are only modestly more reactive than GaN itself in typical alkaline solutions.[117] As a result, reported AlN-based sacrificial schemes for GaN release exhibit limited selectivity and slow, poorly controlled lateral undercut.[118] Nevertheless, Horng *et al.* reported removal yield-rates of approximately 70% and 90% for GaN employing patterned $SiO_2$ and AlN/patterned-$SiO_2$ intermediate sacrificial layers, respectively, suggesting that proper intermediate-layer design can partially mitigate these limitations and improve CLO performance and template reusability.[119] Still, these results suggest that chemistry alone is often insufficient for GaN ELO and have motivated the development of mechanism-engineered strategies, in which additional driving forces are

Open Access Article. Published on 11 maio 2026. Downloaded on 27/05/2026 13:44:17.
This article is licensed under a Creative Commons Attribution-NonCommercial 3.0 Unported Licence.

introduced to expand the usable space of sacrificial-layer/etchant systems, as discussed below.

**4.1.2. Emerging strategies for chemical lift-off.** Chemical lift-off processes are attractive when a suitable sacrificial-layer/etchant pair exists: high selectivity enables precise control of membrane thickness and the process is fundamentally non-destructive, unlike substrate grinding[111] or membrane spalling. However, its applicability is restricted by the requirement for a highly selective, lattice-compatible sacrificial layer. Furthermore, CLO processes that rely on lateral undercut are often slow (even taking days), particularly for large-area substrates, and typically depend on hazardous chemistries such as HF.

To extend the usable space of sacrificial-layer/etchant pairs to nitrides, photon-enhanced (photoelectrochemical, PEC) etching has been widely adopted. In this method, illumination with photon energies exceeding the bandgap of the sacrificial layer generates holes that drive oxidation and subsequent dissolution (Fig. 6c).[120] In this scheme, InGaN is commonly chosen as the sacrificial layer, because it is closely lattice-matched to GaN to support high-quality epitaxial growth, and its narrower bandgap compared to GaN creates a spectral window where optical absorption exclusively occurs in the InGaN layer. The PEC process can be summarized as follows: (i) the GaN/InGaN stack is connected to the anode in a KOH electrolyte. (ii) The sample is illuminated with photons with their energy $h\nu$ satisfying $E_g(\text{InGaN}) < h\nu < E_g(\text{GaN})$, so that electron–hole pairs are generated predominantly in the InGaN release layer. (iii) Holes drift or diffuse to the semiconductor–electrolyte interface, where they oxidize the InGaN; the resulting oxides/hydroxides then dissolve in KOH. (iv) The excess electrons flow through the external circuit to the cathode, where they reduce water or dissolved oxygen. Several groups have demonstrated that this bandgap-selective PEC process enables the reliable lift-off and transfer of epitaxially grown GaN layers onto arbitrary host substrates,[121,122] and can be integrated into the fabrication of functional GaN-based devices.[123,124] As a representative example, Youtsey *et al.* demonstrated wafer-scale lift-off of a micrometer-thick GaN film using an InGaN release layer by PEC etching in KOH (Fig. 6d).[122] They further showed that the prefabricated GaN Schottky barrier diode characteristics are preserved after transfer, with reverse-bias leakage reduced for most devices. Because PEC does not require substantial modification of conventional chemical lift-off processes—beyond the addition of optical excitation—it represents a versatile and broadly applicable strategy for enabling selective release in material systems where purely chemical approaches are otherwise ineffective.

In addition to utilizing photon energy to enable selective etching, exploiting conductivity differences in an electrochemical process provides an alternative pathway. In conductivity-selective electrochemical etching, a heavily doped $n^+/n^{++}$-GaN layer embedded in the stack serves as the sacrificial layer. Under anodic bias in an electrolyte such as oxalic acid (often with auxiliary UV illumination), the current concentrates in this highly conductive layer. Similar to PEC, holes generated at the semiconductor–electrolyte interface drive oxidation and dissolution of the sacrificial layer, while the adjacent semi-insulating GaN remains largely unaffected. Zhang *et al.* first systematized this behavior in $n^+$-GaN;[125] Chang *et al.* adopted the process to selectively remove an $n^{++}$-GaN layer and release AlGaN/GaN nanomembranes for HEMT;[126] and Huang *et al.* exploited the mechanism to form nanoporous/air-gap GaN beneath LEDs, enhancing light extraction rather than achieving full lift-off.[127]

In parallel, substantial efforts have been devoted to mitigating the intrinsically slow lateral undercut. For instance, to accelerate the etching process, Li *et al.* engineered a novel structure by growing a $\alpha$-$Ga_2O_3$ thin film on $\alpha$-$Fe_2O_3$/$\alpha$-$Ga_2O_3$ nanopillar arrays (NPAs).[128] Here, $\alpha$-$Fe_2O_3$ serves as the sacrificial layer and can be selectively removed in HCl, while the nanopillar geometry provides open channels for etchant transport, facilitating rapid dissolution and byproduct removal (Fig. 6e). This architecture reduced the total etching process to the scale of minutes, a significant improvement over the several hours required by conventional planar etching. This process provides an additional merit: as the film laterally overgrows on top of the pillars, strain can relax laterally without forming dislocations. Consequently, the authors found that the edge dislocation density in the resulting film was decreased compared to films grown directly on a planar sapphire substrate, leading to improved film quality. As another approach to accelerate the release speed, Haggren *et al.* demonstrated a strain-engineered multilayer ELO process based on an epitaxially grown multilayer heterostructure.[129] They inserted an extra strained InGaAs layer between each device/sacrificial (GaAs/AlInP) stack. Due to its larger lattice constant, this strained layer exerts a tensile force. Once the sacrificial layer starts to dissolve by the etchant, the internal tensile force causes the released portion to bend upward. This action opens a wider channel for the etchant to flow, dramatically accelerating the etching process. By engineering the tensile stress in each layer, they demonstrated the ability to etch multiple films simultaneously, which greatly enhances release efficiency and lowers cost (Fig. 6f). When implemented for III–V solar cells, this advantage translated into a substantial reduction in cost per watt: 55% for a three-layer strain-engineered multilayer ELO process and 74% for a ten-layer process relative to a reference single-junction ELO cell.

These emerging strategies represent a significant advance in CLO processes, expanding the range of material systems that can be accessed, enhancing the effective selectivity achievable within these systems, and substantially improving process throughput. Although CLO has long been pursued as a precise route for single-crystal membrane production and as a means to reduce cost through reuse of substrates (such as III–V wafers, which are orders of magnitude more expensive than Si), its broader adoption has been limited by challenges associated with slow release kinetics, low yield, and the need for extensive substrate refurbishment. Recent breakthroughs that integrate new release mechanisms, structural designs, and stress engineering tactics offer a potential pathway toward

overcoming these limitations, positioning CLO as a more viable platform not only for precise thickness control in nanomembranes but also for scalable manufacturing and cost-effective heterogeneous integration.

**4.1.3. Water-soluble sacrificial layers: oxides and fluorides.** Despite the excellent selectivity and thickness control offered by CLO processes, their practical deployment is often constrained by reliance on hazardous chemicals such as HF for removing sacrificial layers. These limitations have motivated considerable efforts to develop alternative sacrificial-layer/etchant pairs that enable safer and more benign release chemistries. To circumvent the use of strong and toxic acids traditionally required to lift off GaAs epilayers from AlAs-based sacrificial layers, Sharma *et al.* engineered a water-soluble fluoride sacrificial heterostructure, a Ge/(Ca, Sr)$F_2$/$BaF_2$/(Ca, $Sr_2$).[130] In this design, the central $BaF_2$ layer readily dissolves in deionized water at room temperature and serves as the actual release layer, while the surrounding (Ca, Sr)$F_2$ layers provide lattice matching to both Ge and $BaF_2$. This strategy also avoids the expensive post-release CMP process typically required for conventional lift-off, which can cost about 25% of a pristine 6-inch GaAs substrate. The top Ge layer offers a more favorable surface for subsequent GaAs nucleation and growth compared with direct growth on fluoride buffers, leading to improved epitaxial quality and enhanced performance of the resulting GaAs solar cells. At the same time, the process retains the practical advantage of a clean, water-soluble sacrificial layer for release. Although water-soluble sacrificial spacers had previously been explored mainly in complex-oxide systems as we discuss below, this study extends the same concept to GaAs release and enables a broader use of water-soluble sacrificial layers.

Complex oxides have recently emerged as a compelling class of materials for CLO. Their appeal is twofold: they can function as clean, water-soluble sacrificial layers, and they intrinsically possess rich functionalities and intriguing new physics. These oxides exhibit numerous phenomena such as superconductivity,[131] colossal magnetoresistance,[132] piezoelectricity,[133] ferroelectricity,[134] multiferroicity,[135] magnetism,[136] catalytic activity,[137] and high mobility two-dimensional electron gas (2DEG) at the interface with the insulator.[137–140] Although tremendous progress has been made in synthesizing high-quality complex-oxide films, engineering sophisticated structures to meet advanced technological demands remains challenging. CLO, by removing the target layer from the constraints of its growth substrate, provides a crucial solution. This freedom allows researchers to handle, stack, and strain the film post-growth, enabling the construction of vertically stacked heterostructures and superlattices that are inaccessible by conventional epitaxy alone.

Among various oxide materials, the $Sr_3Al_2O_6$ (SAO) family has become the most widely used platform. SAO is a water-soluble perovskite-derived oxide with a pseudocubic lattice parameter (~3.96 Å) close to that of $SrTiO_3$ (STO), making it epitaxially compatible with many perovskite oxides commonly grown on STO (Fig. 6g).[141,142] However, a practical complication is that SAO surfaces can partially amorphize during overgrowth, degrading the crystalline quality of the subsequent functional layer. To address this, Salles *et al.* introduced Ca-substituted $Sr_{3-x}Ca_xAl_2O_6$ ($SC_xAO$) as the sacrificial layer for $La_{0.7}Sr_{0.3}MnO_3$ (LSMO) membranes.[143] A brief vacuum anneal was sufficient to recrystallize the $SC_xAO$, sharpen the RHEED streaks, and significantly improve the structural quality of the overgrown LSMO. In parallel, other aluminate variants such as $(Ca,Ba)_3Al_2O_6$,[144,145] as well as simpler binary oxides such as BaO and SrO,[146,147] have also been developed as water-soluble sacrificial layers. This broader choice of sacrificial oxides provides flexibility to select lattice constants that best match the epitaxial growth requirements of the functional film of interest. Beyond their benign dissolution chemistry, these complex oxides can be deposited using a range of well-established thin-film techniques—including pulsed laser deposition (PLD), molecular beam epitaxy (MBE), and sputtering—further lowering the barrier to integrating sacrificial layers into complex-oxide heterostructure designs. Collectively, these advantages have positioned complex-oxide sacrificial layers as a key enabler for advanced studies of freestanding complex-oxide membranes and heterostructures.

The ability to create freestanding complex-oxide membranes has opened a broad range of experimental and technological opportunities. Once released from their substrates, these films can be elastically strained, bent, or stacked in ways that are inaccessible in substrate-clamped architectures, enabling systematic control of polarization, electronic structure, and interfacial coupling.[148–150] At the same time, transferable membranes provide a straightforward route to integrate functional oxides with conventional semiconductor and photonic platforms,[151,152] so that water-soluble sacrificial oxides serve not only as a tool for membrane exfoliation but also as a practical bridge between complex-oxide functionalities and existing device technologies.

### 4.2. Laser lift-off

Along with other lift-off techniques, laser lift-off (LLO) has been widely explored to achieve membrane separation along a deliberately engineered sacrificial interface. LLO is arguably the most commercially successful lift-off technology to date. In contrast to CLO, which relies on wet chemical reactions to dissolve a sacrificial layer, LLO uses laser irradiation through a transparent substrate onto an absorbing epilayer to induce localized decomposition or ablation at the interface. This method offers several distinct advantages: the separation depth is well-defined at the substrate/epilayer interface, the method supports high-throughput, wafer-scale processing, and it is a purely dry process that avoids chemical etchants. These features make LLO particularly attractive for large-scale manufacturing of ultra-thin electronics that are incompatible with aggressive chemicals or prolonged high-temperature processing.

**4.2.1. Principles of laser lift-off.** The primary requirement for LLO is that the carrier substrate is transparent to the wavelength of laser light used, whereas the separation layer strongly

Open Access Article. Published on 11 maio 2026. Downloaded on 27/05/2026 13:44:17.
This article is licensed under a Creative Commons Attribution-NonCommercial 3.0 Unported Licence.

Open Access Article. Published on 11 maio 2026. Downloaded on 27/05/2026 13:44:17.
This article is licensed under a Creative Commons Attribution-NonCommercial 3.0 Unported Licence.

absorbs the laser to decompose through localized heating. Once these criteria are met and a laser is shone upon the sample of interest, there are three primary mechanisms by which film separation can occur (Fig. 7a):[153,154]

1. Photothermal ablation: long laser pulses, on the scale of nanoseconds, can lead to significant heating of the absorbent layer, raising the temperature up to melting or vaporization. While the melting contributes to the delamination of the film,

**Fig. 7** Mechanisms and strategies of laser lift-off. (a) Schematic illustration of three primary mechanisms associated with LLO. (b) Map of laser–matter interaction regimes, showing the different breakdown mechanisms triggered as a function of the interaction between time and light intensity;[153] Copyright 2022, Wiley-VCH GmbH. (c) Representative LLO outcomes across the process window, highlighting failure modes at excessive laser fluence;[154] Copyright 2020, Elsevier. (d) Comparison of graphene-enabled LLO (GLLO) and conventional LLO, showing that GLLO provides a wider process window over a broader fluence range;[156] Copyright 2024, Springer Nature.

Open Access Article. Published on 11 maio 2026. Downloaded on 27/05/2026 13:44:17.
This article is licensed under a Creative Commons Attribution-NonCommercial 3.0 Unported Licence.

the heat-affected zone can extend hundreds of nanometers into the device layer, potentially causing thermal damage.

2. Photomechanical spalling: when a short-wavelength laser irradiates the substrate–film interface, the above-bandgap ultraviolet photons are strongly absorbed and rapidly heat the material, generating gaseous or plasma byproducts at the interface. The resulting rapid expansion launches shock waves that propagate through the film and mechanically spall it from the substrate. Because crack propagation can extend beyond the directly illuminated region, exfoliation is not strictly confined to the laser spot, allowing a lower pulse density to be used. However, the same shock waves can also induce uncontrolled cracks, wrinkles, and other damage in thin films.

3. Photochemical bond cleavage: high-energy picosecond and femtosecond lasers can lead to film separation *via* two-photon or multiphoton absorption/ionization (MPA/MPI), which directly breaks chemical bonds at the interface of interest. Sun *et al.* reported that such processes can achieve lift-off with a lower total energy input than nanosecond lasers, while also significantly reducing thermal damage.[155] Because of the reduced heat load, this mechanism has been referred to as "cold" LLO. The high cost and complexity of ultrafast lasers have limited the widespread adoption of cold LLO methods.

These mechanisms can be organized in the parameter space of pulse duration and laser fluence (Fig. 7b). Nanosecond pulses fall in the photothermal/photomechanical spalling regimes, where energy diffusion and shock waves dominate interface decomposition. Picosecond–femtosecond pulses access a photochemical bond cleavage regime, where multiphoton processes drive bond breaking at lower fluence with a much smaller heat-affected zone.

Laser fluence is a critical parameter that defines the boundaries between residual adhesion, successful lift-off, and violent wrinkling and rupture of the film (Fig. 7c).[154] Excessive laser fluence leads to excess ablated material which results in the formation of a gas bubble and the buildup of tensile strain along the bubble perimeter. In contrast, laser fluence below the ablation threshold results in incomplete separation, degrading the process yield. Optimal lift-off is achieved at a fluence just above the ablation threshold, allowing clean separation of the device film without inducing wrinkles or gas-induced damage. As reported by Kang *et al.*, the optimal fluence for retaining good film quality is narrow: to lift-off a 2.9 μm PI-on-glass film, a fluence of 111 mJ $cm^{-2}$ led to good separation, whereas a 15% decrease led to under-exfoliation and a 15% increase caused destructive separation accompanied by wrinkling.[156] These multiple LLO mechanisms, along with the strong influence of pulse width and fluence, emphasize the need for rigorous process design to ensure uniform, scalable, and low-damage lift-off.

**4.2.2. Material systems for laser lift-off.** LLO is advantageous for thin-film production because the released films typically exhibit low residual stress, the process does not require the deposition of additional materials on the film surface, and it avoids the use of potentially hazardous chemicals. The first demonstration of LLO was reported in 1997, when Kelly *et al.* showed that ablating an interface between GaN and sapphire by the incidence of laser light from the sapphire side would lead to delamination of the GaN.[157] A year later, in 1998, Wong *et al.* demonstrated the successful lift-off and transfer of 2.5–3 μm thick 3 × 4 mm GaN flakes from sapphire, establishing GaN-on-sapphire as the prototypical LLO system.[158]

Subsequent work has clarified that key requirements for successful LLO include a suitable combination of the laser-responsive layer and excitation wavelength: the carrier substrate must be nearly transparent at the laser wavelength, while the film or an interfacial "release" layer is strongly absorbing the laser light. For III–N semiconductors, this design rule leads naturally to single-crystal GaN, InGaN, or AlGaN films grown on sapphire or amorphous layers deposited on glass, processed with deep-UV excimer sources such as 248 nm (KrF) or 308 nm (XeCl), where the nitride layer absorbs and decomposes while the carrier remains essentially transparent.[157–159] Another example includes oxide thin films on transparent substrates. ZnO, $PbZr_{1-x}Ti_xO_3$ (PLZT) and related oxide films grown on sapphire (for crystalline layers) or deposited on glass (for polycrystalline or amorphous layers) can be detached using similar excimer wavelengths (~248–308 nm), again exploiting the strong absorption in the oxide layer *versus* the wide bandgap of the carrier.[160–162] In Si-based stacks on glass, amorphous or poly-Si and a-Si:H absorber layers are lifted off from glass using 248–355 nm sources, with the glass acting as the transparent entrance window.[163,164] Finally, a large group of systems use polyimide or adhesive layers on glass or silicon as the laser-responsive layer: here, commercial PI or debonding films absorb 308–355 nm (or, in some cases, 1064 nm IR) radiation, enabling the debonding of device layers or redistribution structures from rigid carriers without directly exposing the active films to strong absorption.[153,165]

Overall, the applicability of LLO is defined less by a specific material system than by the optical compatibility between the laser and the film/substrate stack: a transparent carrier, an absorbing and responsive separation layer, and a laser wavelength and fluence chosen to localize energy deposition at the desired interface. In practice, this requirement imposes an intrinsic constraint that the carrier substrate must possess a wider bandgap than the epilayer to ensure optical transparency. In addition, despite its scalability, LLO can introduce localized thermal or photochemical damage to the released film and the remaining substrate. Despite these constraints, LLO has shown many applications for decoupling thin films from transparent carriers across packaging, display, energy, and sensing platforms.[153,166–170]

**4.2.3. Emerging strategies for laser lift-off.** Although LLO has been demonstrated on a wide range of material systems, several practical constraints limit its broader adoption. The light-absorbing (inter)layer must be compatible with the transparent substrate and epitaxial growth, and minimizing the degradation of films during LLO is challenging. As a result, thicker sacrificial layers are often employed to maintain the intactness of device layers.

Open Access Article. Published on 11 maio 2026. Downloaded on 27/05/2026 13:44:17.
This article is licensed under a Creative Commons Attribution-NonCommercial 3.0 Unported Licence.

An effective strategy to mitigate chemical and mechanical damage during release is to introduce an intermediate layer that either (i) enhances optical absorption to lower the laser threshold or (ii) improves thermal transport to reduce peak temperature. As an example, Long *et al.* showed that inserting a carbon-nanotube (CNT) layer between GaN and sapphire can reduce the LLO energy threshold.[171] Because CNTs strongly absorb the incident laser light, the temperature elevates more efficiently within the CNTs and conducts heat to the surrounding GaN, accelerating the local decomposition of GaN. Raman and photoluminescence measurements further indicated reduced residual stress in the GaN after CNT-assisted LLO due to reduced mechanical damage. Extending the same idea to atomically thin absorbers, Kang *et al.* incorporated a monolayer graphene interlayer.[156] With graphene placed at the glass–PI interface, the laser energy is preferentially absorbed in the graphene, while its high in-plane thermal conductivity spreads heat laterally and suppresses localized overheating, thereby enabling successful lift-off over a broader laser fluence window (Fig. 7d). Moreover, graphene's weak out-of-plane adhesion helps redistribute interfacial stresses, which reduces wrinkling and damage in the PI film. As a result, the graphene interlayer not only lowers the effective release threshold but also enables cleaner PI detachment with fewer residues and less film damage.

An alternative route to better control exfoliation is utilizing a low-fluence multiscanning technique, which was first employed by Bian *et al.* Instead of relying on a single laser pulse above the ablation threshold, this method employs multiple scanning laser passes at sub-threshold fluence. Each scan incrementally decomposes the sacrificial layer, generating less thermal damage and fewer shock waves, thus avoiding cracks and surface roughening. This significantly widens the effective process window, reduces overall thermal loading, and yields smoother surfaces, making it especially suited to thin membranes.[172] These innovations in interlayer engineering and laser application have substantially improved the controllability of LLO while reducing process-induced damage.

In summary, CLO and LLO techniques represent powerful and increasingly mature pathways for diverse material systems and device applications, as they offer deterministic thickness control, selectivity, and compatibility with wafer-scale processing. As a result, both approaches have progressed beyond laboratory demonstrations and have been implemented in industry for application-specific manufacturing. CLO is most established in high-efficiency, lightweight, thin-film solar cells such as MicroLink Devices' GaAs-based cells for unmanned aerial vehicles (UAVs), space solar cells, and concentrated photovoltaics.[173,174] CLO is also a prominent technique for III–V substrate reuse.[175,176] LLO, on the other hand, is widely used for flexible and foldable OLED and μLED display panels[166,177–179] and shows good promise for use in thin-film electronics such as photovoltaics and sensors[154,169,170,180–184] due to its process simplicity and high throughput. Recent innovations ranging from epitaxial and structural engineering to lift-off strategies have significantly expanded the precision, throughput, and materials choices. Despite these advances, however, both chemical and LLO fundamentally rely on specific material requirements, such as the availability of selectively etchable sacrificial layers or optically transparent substrates with compatible absorption layers. As a result, these techniques are not universally applicable but instead operate complementarily with mechanical lift-off, with the optimal release strategy determined by material choice, structural design, and manufacturing context. By leveraging the complementary strengths of mechanical lift-off, CLO, and LLO, and strategically selecting or combining these approaches according to the material system and application requirements, along with the emerging technologies described above (Fig. 8), a broader and previously inaccessible design space for thin-film integration can be accessed, as discussed in the following section.

## 5. Applications

The development of controllable exfoliation and lift-off techniques has enabled the fabrication of freestanding membranes that can be released from their native substrates and transferred onto arbitrary platforms (Table 1). These transferable membranes combine high crystalline quality with mechanical flexibility, opening new design spaces for next-generation electronic, photonic, and energy devices. By decoupling the growth and functional substrates, freestanding membranes not only preserve intrinsic material properties but also introduce opportunities for structural reconfiguration, functional stacking, and large-area integration that are difficult to realize in conventional substrate-bound systems. Furthermore, recent advances in mechanical, chemical, and LLO techniques have introduced unprecedented control over membrane thickness, uniformity, strain state, and quality that were previously inaccessible. In this section, we highlight how these lift-off approaches have enabled new application spaces across five broad categories: (i) flexible device platforms, (ii) improved manufacturing economy through wafer recycling and enhanced throughput, (iii) 3D heterogeneous integration architectures, (iv) record-breaking device performances *via* new operating regimes in electronic and photonic devices, and (v) the exploration of emergent phenomena arising from freestanding membranes and their heterostructures. These examples illustrate how advances in lift-off science are directly translating into new device concepts and system-level functionalities.

### 5.1. Flexible, compliant, and wearable devices

In the ultrathin membrane form, even traditionally rigid thin films can become extremely flexible and mechanically compliant. The growing demand for wearable and flexible electronics has therefore driven the development of ultrathin, bendable, and stretchable devices capable of conforming to complex surfaces such as the human body. These devices span a wide range of materials, including silicon, III–V materials, and complex oxides, and have applications in health monitoring,

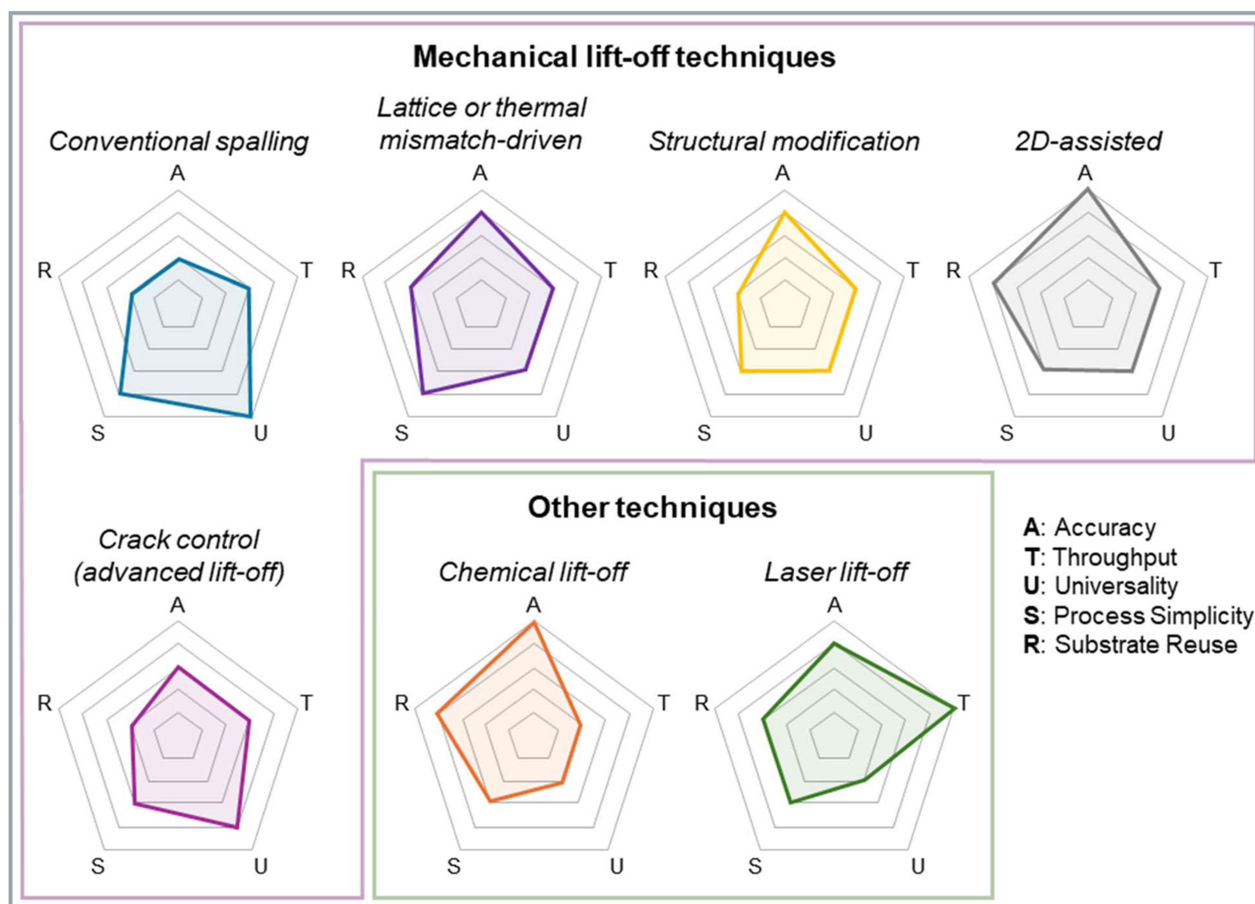


Fig. 8 Radar-chart comparison of representative lift-off and exfoliation strategies in terms of key practical metrics, namely accuracy (A), throughput (T), universality (U), process simplicity (S), and substrate reuse (R). This qualitative overview highlights the distinct strengths and trade-offs of each strategy, illustrating how recent innovations in interface design and release engineering are expanding the performance space of membrane fabrication technologies toward higher precision and greater substrate reusability, while preserving throughput and process simplicity.

Open Access Article. Published on 11 maio 2026. Downloaded on 27/05/2026 13:44:17.
This article is licensed under a Creative Commons Attribution-NonCommercial 3.0 Unported Licence.

flexible displays, energy harvesting, and integrated sensors. A key challenge is realizing high-performance electronic components that are not only integrated on mechanically flexible substrates but are made ultrathin without degrading their electrical or optical properties. In this domain, controllable lift-off techniques provide an effective approach to address such challenges.

The initial breakthrough in flexible high-performance electronics was achieved by stress-controlled mechanical spalling directly to fully fabricated wafers. This "post-fabrication" approach relies on the deposition of a high-stressor layer to induce a fracture parallel to the surface at a depth governed by fracture mechanics. A key validation of this technique is that the resulting mechanical fracture does not compromise the structural or electrical integrity of the nanoscale active devices. For instance, Zhai *et al.* demonstrated that integrated circuits (ICs) fabricated on bulk Si substrates could be exfoliated into thin membranes with thicknesses precisely controlled at tens of micrometers, while the transport characteristics of the resulting MOSFET remained unchanged.[185] Building on this promise, Shahrjerdi *et al.* established a robust approach for fabricating flexible ultrathin Si CMOS circuits by electroplating a thick nickel stressor (10–100 μm) onto a prefabricated ultrathin body silicon on insulator (UTB-SOI) wafer, which demonstrated full compatibility with standard BEOL thermal budgets and successfully produced the top 10–15 μm of the substrate containing the active devices (Fig. 9a).[186] Furthermore, after repeated bending up to 200 cycles, no noticeable change was observed in device metrics (*e.g.*, $V_{th}$ and $G_m$), highlighting the robustness of the spalled membrane. However, in the mechanical exfoliation method, the exfoliated thickness typically falls within the bulk regime and the fracture surface typically exhibits roughness reaching hundreds of nanometers, which thus requires subsequent CMP or wet etching to achieve the submicron thicknesses and ultra-flat surface needed for extreme flexibility. Furthermore, excessive residual stress and uneven thickness in the spalled layer remains another problem. As reported by Park *et al.*, the thicker device layers experienced more pronounced performance degradation, including threshold voltage shifts, mobility reduction, and gain variation, with differing impacts on n- and p-MOSFET, highlighting the need for precise process control in this approach.[17]

Table 1 Comparison of representative film exfoliation methods and the resulting film characteristics

| Exfoliation technique | Material system | Membrane thickness (μm) | Demonstration scale | Ref. |
|---|---|---|---|---|
| Conventional mechanical spalling | Si | 20–70 | 150 × 150 $mm^2$ | 16 |
| | | 2–15 | N/A | 17 |
| | | 5–38 | 1 inch | 18 |
| | Ga(In)As | 4 | 4 inch | 19 |
| | Ge | 10–60 | 4 inch | |
| | | 0.32–75.6 | 20 × 20 $mm^2$ | 20 |
| | 4H-SiC | 10–50 | 29 × 29 $mm^2$ | 30 |
| Mismatch-assisted exfoliation | GaN | 2800 | 2 inch | 47 |
| | InP/InGaAs | 3.3–28 | 15 × 15 $mm^2$ | 49 |
| | β-$Ga_2O_3$ | ~3.8 | 1 × 1 $cm^2$ | 51 |
| Pattern-assisted exfoliation | GaAs | 5–10 | ~4 $cm^2$ | 52 |
| Porous-interlayer-assisted exfoliation | Si | 10–24.5 | 10 × 10 $cm^2$ | 56 |
| | | 0.72 | 3 × 3 $cm^2$ | 57 |
| | GaN | ~3.4 | 2 inch | 60 |
| | | ~0.45–1.85 | 2 inch | 61 |
| | InP | N/A | 1 × 1 $cm^2$ | 63 |
| | | 2 | 2 $cm^2$ | 64 |
| Pb-mediated interface weakening | Perovskite | 0.01–0.2 | 1 × 1 $cm^2$ | 66 |
| 2D materials-assisted exfoliation | Perovskite | 0.01 | N/A | 72 |
| | | 0.14 | 4 $cm^2$ | 83 |
| | ZnO | ~7.5[a] | N/A | 73 |
| | GaN | ~2.5 | N/A | 67 |
| | | ~2 | N/A | 74 |
| | | ~2 | N/A | 76 |
| | | ~11[a] | 5 × 5 $mm^2$ | 77 |
| | | N/A | 1 × 1 $cm^2$ | 78 |
| | | ~1.2 | N/A | 79 |
| | | ~2 | 2 inch | 80 |
| | | ~1.3 | ~5 × 5 $mm^2$ | 82 |
| | | ~3.4 | 5 × 5 $mm^2$ | 84 |
| | | 1.9 | 4 inch | 85 |
| | | ~0.9 | 6 inch | 86 |
| | | ~0.9 | 4 × 3 $cm^2$ | 92 |
| | | 0.5 | 2 inch | 93 |
| | GaAs | 3 | 2 inch | |
| | | 1 | 2 inch | 15 |
| Leveraging peeling angle | Diamond | 0.2–1 | 2 inch | 98 |
| Acoustic spalling | GaAs | ~7.8 | 2 inch | 101 |
| | SiC | ~68.1 | 2 inch | 102 |
| | GaN | ~22.3 | 2 inch | |
| | GaAs | ~6.5 | 2 inch | 103 |
| Chemical lift-off | GaAs | 1–3 | 2 inch | 113 |
| | | ~4.15 | N/A | 114 |
| | | ~0.5 | N/A | 115 |
| | GaN | ~6.8 | 2 inch | 118 |
| | | ~5.3 | 2 inch | 119 |
| | | ~5 | 4 inch | 122 |
| | | ~5 | Quarter of 2-inch | 123 |
| | | ~14.74 | 2 inch | 124 |
| | AlGaN | ~0.3 | 0.5 × 0.5 $cm^2$ | 126 |
| | α-$Ga_2O_3$ | ~3 | N/A | 128 |
| | GaAs | ~3 | 2 inch | 129 |
| Water-based lift-off | GaAs | ~3.76 | N/A | 130 |
| | Perovskite | 0.06 | 5 × 5 $mm^2$ | 143 |
| | | 0.02 | Millimeter-scale | 144 |
| | | 0.06 | 5 × 5 $mm^2$ | 145 |
| | | 0.011–0.422 | 0.5 × 0.5 $mm^2$ | 146 |
| | | 0.2 | 4 × 10 $mm^2$ | 147 |
| Laser lift-off | GaN | 2.5–3 | 3 × 4 $mm^2$ | 158 |
| | | 5 | 2 inch | 159 |
| | ZnO | 2.6 | Millimeter-scale | 160 |
| | Perovskite | 2 | 3.5 × 3.5 $cm^2$ | 161 |
| | | 2 | N/A | 162 |
| | GaAs | 2.25 | 2 × 3.4 $mm^2$ | 163 |
| | IZO | ~4 | N/A | 164 |
| | GaN | 6 | 2 × 2 $cm^2$ | 171 |

[a] Nanorod structure.

Open Access Article. Published on 11 maio 2026. Downloaded on 27/05/2026 13:44:17.
This article is licensed under a Creative Commons Attribution-NonCommercial 3.0 Unported Licence.

Open Access Article. Published on 11 maio 2026. Downloaded on 27/05/2026 13:44:17.
This article is licensed under a Creative Commons Attribution-NonCommercial 3.0 Unported Licence.

**Fig. 9** Flexible devices (top panel) and scalable, low-cost manufacturing (bottom panel) enabled by membrane transfer and substrate reuse. (a) Schematic and photograph of a 100 mm UTB-SOI circuit transferred to a flexible substrate enabled by the controlled spalling;[186] Copyright 2013, American Chemical Society. (b) Schematic and SEM images of as-fabricated MESFET devices enabled by a multi-stack ELO approach;[187] Copyright 2010, Springer Nature. (c) Photographs of electroluminescence (EL) from an LED under bending, an LED array deformed into different shapes, and LED-adhered LEGO® minifigures in different postures;[189] Copyright 2020, American Association for the Advancement of Science. (d1) Transferred 2-inch AlGaAs LED on a Si wafer and the corresponding optical image of light emission. (d2) $J$–$V$ and EQE characteristics of GaAs single-junction solar cells grown and fabricated on new (green) and reused (blue) substrates;[113] Copyright 2013, Springer Nature. (e) Schematic of the GBL substrate and a photograph of the three-times-reused GBL substrate with exfoliated GaN epilayers;[89] Copyright 2021, American Chemical Society. (f) Schematic of successive membrane production by remote epitaxy, 2DLT and wafer recycling and the as-obtained crystalline membranes and reused substrates;[93] Copyright 2023, Springer Nature.

Alternatively, the advanced membrane exfoliation techniques with a predefined weak boundary, whether chemically sacrificial or mechanically distinct, offer hope for fabricating flexible devices with superior precision and throughput. For instance, utilizing the ELO approach, Yoon *et al.* fabricated seven-layer GaAs MESFET stacks in a single MOCVD run, which were subsequently released *via* HF etching of an AlAs sacrificial layer, and transferred the layers onto PI-coated glass (Fig. 9b). The as-obtained devices maintained a high on/off ratio (>$10^6$) and multi-GHz operation ($f_T$ ~ 2 GHz, $f_{max}$ ~ 6 GHz), demonstrating the viability of batch fabrication for high-performance flexible electronics.[187] Extending this precision to

Open Access Article. Published on 11 maio 2026. Downloaded on 27/05/2026 13:44:17.
This article is licensed under a Creative Commons Attribution-NonCommercial 3.0 Unported Licence.

wide-bandgap materials, Zhang *et al.* utilized GaN-on-insulator structures to define the release interface for flexible AlGaN/GaN HEMT. The as-transferred GaN-based HEMT responded differently to the applied tensile and compressive stress. Moreover, this strain response remained nearly unchanged after up to 50 bending cycles, supporting potential applications as thin-film, high-density strain sensors.[188]

In addition to these conventional lift-off techniques for III–V and nitride-based electronics, emerging 2DLT methods have also gained attention as a promising route for various applications. For instance, Jeong *et al.* achieved GaN-based LED array transfer to a flexible substrate based on the 2DLT strategy.[189] After transfer, the obtained 5 × 5 $mm^2$ panel still showed bright cyan/blue emission while it was able to withstand crumpling, twisting, and bending at up to 10 mm radius at over 1000 fatigue cycles with minimal degradation in turn-on voltage or peak electro-luminous intensity (Fig. 9c). In addition, the use of a graphene interlayer enabled clean separation and substrate reuse, further improving process sustainability. Beyond LEDs, the 2DLT strategy has been extensively extended to a variety of flexible and wearable electronics, including HEMT, UV photodetectors, solar cells, photocatalysts, and resistive random-access memory (ReRAM) arrays.[76,190–195] These devices maintain their high-quality single-crystalline performance even after being decoupled from rigid growth substrates, demonstrating the great potential of 2DLT for multi-functional flexible platforms.

These studies demonstrate that controllable exfoliation offers a universal route to realize high-performance and mechanically compliant electronic and optoelectronic systems. By decoupling the growth and functional substrates, this technique preserves intrinsic material quality while imparting flexibility, enabling applications ranging from stretchable integrated circuits to bendable optoelectronics devices.

### 5.2. Sustainable, cost-effective, and high-volume manufacturing

Beyond flexible electronics and heterogeneous integration, lift-off techniques offer a route toward economical, sustainable, and high-throughput manufacturing by enabling the reuse of donor substrates. By reducing the consumption of wafers, substrate reuse directly lowers material costs and improves the overall sustainability. Importantly, repeated layer-release and reuse of donor substrates can substantially increase effective wafer and device throughput, enabling higher-volume production. Below we introduce how different lift-off strategies facilitate donor substrate recycling and improve throughput for cost-effective and sustainable manufacturing.

One pathway lies in stress-controlled bulk mechanical spalling, which has been utilized across photoelectrochemical, photovoltaic, and light-emitting applications. Lee *et al.* showed that spalled Si and GaAs membranes could serve as efficient photocathodes, allowing donor-wafer reuse with minimal material loss.[196] Their spalled Si films decorated with Pt nanoparticles exhibited a hydrogen evolution reaction onset potential of 332 mV and a photocurrent density of −20.1 mA $cm^{-2}$ at 0 V, outperforming thin Si films prepared by conventional wet etching. Similarly, spalled GaAs films achieved performance comparable to 350 μm bulk GaAs controls. Similarly, Lee *et al.* fabricated spalled thin-Si photoelectrodes for PEC water splitting, intentionally texturing the Si (111) surface by KOH etching to enhance light trapping.[197] Incorporating a nickel oxide catalyst and a rear $pn^+$ junction, the devices achieved a photocurrent density of 23.43 mA $cm^{-2}$, demonstrating that spalled films can support high-efficiency PEC architectures.

This approach also shows potential in addressing cost and flexibility challenges in high-efficiency III–V solar cells, where expensive single-crystal substrates limit widespread adoption. For example, Shahrjerdi *et al.* fabricated flexible InGaP/(In)GaAs tandem solar cells on plastic substrates using controlled spalling for layer transfer.[198] The flexible tandems achieved ≥28% efficiency, a specific power >1995 W $kg^{-1}$, and stable operation under bending (up to 1000 cycles at a 10 mm radius). Device performance matched that of a chemically de-substrated control device, indicating that the spalling/transfer step maintained the layer quality. The substrate reuse enabled by controlled mechanical spalling has also been applied to LEDs. Bedell *et al.* spalled an InGaN/GaN MQWs structure from a sapphire wafer using a Ni stressor layer, removing ∼3 μm of the LED stack with the fracture occurring in the n-GaN layer.[199] The process provided immediate access to the n-contact, preserved the MQWs' integrity, and allowed reuse of the sapphire substrate and buffer. Electroluminescence measurements confirmed that device operation was not compromised by spalling.

However, a fundamental trade-off exists in mechanical bulk spalling-enabled substrate reuse; *i.e.*, the fracture surface typically exhibits roughness, necessitating CMP or wet etching to restore the epi-ready condition. This additional processing step not only increases cost but also gradually consumes the finite thickness of the donor wafer, limiting the number of reuse cycles. In the case of III–V solar cells for example, Horowitz *et al.* note that the Ge substrate used for triple-junction cells and the GaAs substrate with CMP for single-junction and dual-junction cells makes up the largest fraction of costs, of the order of 40–55% of the total manufacturing cost.[200] They show that reducing or eliminating the polishing costs for wafer reuse combined with a modest increase in the number of reuses would make substrate reuse much more cost-effective. Recently, Mangum *et al.* reported that epitaxial regrowth is possible directly on spalled surfaces without CMP.[44] By growing InGaAs single-junction solar cells on spalled Ge substrates, they were able to study the relationship between the various morphological defects and the efficiency of the devices grown on these regions. They showed that regions with no spalling defects had an efficiency of 23.4%, which is within 2% relative to the same cells grown on pristine epi-ready Ge substrates. This indicates the difficulty of achieving uniform wafer-scale yield solely through bulk fracture control, as three different types of defect were observed which could reduce efficiency. To bypass the need for surface refinishing and achieve theoretically infinite reuse, advanced exfo-

 This journal is © The Royal Society of Chemistry 2026

Open Access Article. Published on 11 maio 2026. Downloaded on 27/05/2026 13:44:17.
This article is licensed under a Creative Commons Attribution-NonCommercial 3.0 Unported Licence.

liation techniques with a precisely defined separation interface have been applied to achieving damage-free separation and substrate reuse. Cheng *et al.* replaced the conventional AlAs-based sacrificial layer and HF-based etchant with phosphide-based materials and HCl for a III–V materials ELO process.[113] This attempt minimized the post-etching residues and maintained the atomic smoothness, which enabled the direct reuse of GaAs substrates for high-performance devices without the safety hazards and surface degradation associated with traditional methods (Fig. 9d).

Unlike bulk spalling which relies on crack propagation through the crystal lattice, or CLO which is limited by specific etch selectivity, the 2DLT strategy exploits the intrinsically weak van der Waals layer to define the separation plane, which offers two distinct advantages. First, it guarantees an atomically precise exfoliation interface, thereby eliminating surface roughness and the need for post-process polishing. Second, its universal applicability allows it to be implemented across diverse material systems, from elemental semiconductors to complex wide-bandgap oxides, where traditional sacrificial layers may be unavailable. As an example, Qiao *et al.* chose the GBL on SiC as the growth and exfoliation platform for wide bandgap semiconductors, such as GaN and ZnO.[89] Unlike epitaxial graphene which interacts weakly with the substrate, the GBL is covalently bonded to the SiC, making it robust enough to withstand high-temperature growth while presenting a quasi-2D surface for release. Based on this platform, they achieved a GaN remote epilayer with record crystalline quality, high-yield membrane release (Fig. 9e). The 2DLT technique also offers a chance to support batch manufacturing and substrate reuse at the same time. Kim *et al.* developed a technique to grow multiple alternating layers of 2D materials and III–V or III–N epilayers in a single growth run.[93] Each epilayer in this multi-stack structure can be harvested *via* layer-by-layer exfoliation. The atomic-precision release interface enabled three cycles of wafer reuse without intermediate polishing steps and with nearly no degradation. This offers a pathway to dramatically reduce the cost of non-silicon technologies (Fig. 9f).

These studies highlight controllable exfoliation as a versatile platform for sustainability. By evolving from bulk fracture to exfoliation guided by well-defined interfaces, the field is moving toward a "growth–transfer–reuse" cycle that eliminates material waste and refinishing costs, making high-performance inorganic devices economically viable for large-scale deployment.

### 5.3. 3D and heterogeneous integration

As electronic and photonic systems continue to evolve toward higher levels of performance and functionality, integration technologies have become more important for device innovation. Beyond simple planar scaling, 3D integration and heterogeneous integration offer effective routes to increase performance and introduce new functionalities.[201] Membrane exfoliation provides the foundation to meet those requirements, initially through stress-controlled bulk mechanical spalling strategies. For example, exfoliation of thin Si membranes offers a rapid and cost-effective alternative to conventional wafer thinning methods for 3D integration. This approach is a critical enabler for vertical IC stacking, which addresses the growing demand for higher transistor densities. By stacking layers in this manner, interconnect paths are significantly shortened, reducing signal delays and power consumption, while simultaneously allowing the integration of diverse components, such as logic, memory, and sensors, into a single compact system.[172] Extending this strategy to photonic platforms, Thureja *et al.* demonstrated that single-crystalline barium titanate (BTO) films could be mechanically spalled using a Ni stressor. The resulting films exhibited electro-optic coefficients approaching those of bulk crystals, while the Ni stressor simultaneously served as a reflective contact, simplifying the subsequent high-speed modulator processing.[202]

While stress-controlled mechanical spalling is effective for homojunctions or robust bulk materials, it lacks the material selectivity and atomically smooth cleavage surfaces required for integrating dissimilar material systems with fragile interfaces. To address these limitations, advanced exfoliation techniques have been adopted to enable the damage-free assembly of complex heterogeneous architectures. A notable example is integrating exfoliated III–V layers, such as GaAs and InGaAs, onto Si substrates to combine high electron mobility with CMOS-compatible platforms. Geum *et al.* demonstrated high-performance GaAs HEMT transferred onto Si, achieving a subthreshold swing (SS) of 83 mV $dec^{-1}$ by employing pre-patterned mesas and HF-assisted lift-off, which greatly improved process efficiency, reducing the release time from over 30 hours to less than 20 minutes (Fig. 10a).[203] To further enhance scalability, Lee *et al.* realized the wafer-scale fabrication of InGaAs HEMT by growing device structures on large-area Si donor wafers and subsequently transferring them to target substrates *via* an ELO process.[204] The resulting devices exhibited electron mobilities 1.3 times higher than standard Si MOSFET due to the elimination of defective buffer layers. Beyond enhancing single-device performance, this precision enables the construction of multifunctional vertically stacked architectures. Geum *et al.* demonstrated a vertically stacked photodetector system, integrating a visible-light GaAs detector atop a near-IR InGaAs detector.[203] This precisely aligned, three-terminal structure allowed the simultaneous and independent detection of multiple wavelengths, illustrating the potential of exfoliation-based integration for compact, multifunctional optoelectronic systems. Pursuing higher integration density for advanced displays, Shin *et al.* utilized the 2DLT technique to realize vertically stacked full-color μLEDs, where ultrathin RGB membranes are epitaxially grown, released, and reassembled into compact multilayer architectures with the assistance of 2D materials. The resulting devices exhibit record pixel densities over 5000 PPI and ultrathin overall thickness, thereby providing a scalable pathway toward high-resolution AR/VR displays and three-dimensional optoelectronic integration (Fig. 10b).[205]

These cases exhibit the potential of controllable exfoliation to unify diverse materials and device functionalities, paving

Open Access Article. Published on 11 maio 2026. Downloaded on 27/05/2026 13:44:17.
This article is licensed under a Creative Commons Attribution-NonCommercial 3.0 Unported Licence.

**Fig. 10** Heterogeneous integration (top panel), device performance enhancement (middle panel), and emergent phenomena in thin crystalline film (bottom panel) enabled by membrane transfer. (a) Cross-sectional TEM of GaAs-OI on Si showing the GaAs HEMT stack, *J*–*V* of GaAs solar cells on Si *vs.* GaAs (control) (inset: top-view SEM), and IC-VCE (dark/photo) of an InGaP/GaAs heterojunction phototransistor (HPT) on Si;[203] Copyright 2016, Springer Nature. (b) Optical micrographs and a cross-sectional SEM image of vertical μLED pixels;[205] Copyright 2023, Springer Nature. (c) Photograph of an ELO-LED transferred to a Cu substrate and the corresponding peak emission wavelength at an injection current of 350 mA;[206] Copyright 2015, Optica Publishing Group. (d) Thermal performance of AlGaN/GaN HEMT with vdW bonding and polymer adhesive layers;[76] Copyright 2020, American Chemical Society. (e) Comparison of the bulk photovoltaic effect between strained and freestanding BFO films along the *x* (left) and *y* (right) axis;[150] Copyright 2025, Wiley-VCH GmbH. (f) Pyroelectric current density of the device with a thickness ranging from 10 nm to 200 nm compared with the laser modulation frequency ranging from 100 Hz to 760 Hz;[66] Copyright 2025, Springer Nature.

the way for compact, multifunctional electronic and photonic systems. However, such membrane-based 3D and heterogeneous integration faces several outstanding challenges. Thermal and stress management becomes increasingly critical as membrane-based device layers are stacked up, and full compatibility with CMOS BEOL processes has not been resolved to date. Addressing these challenges will require integrated solutions involving the co-design of materials, interfaces, and processes.

### 5.4. Device performance enhancement

Exfoliation and transfer techniques serve as powerful tools for enhancing device performance by transferring fully processed optoelectronic and electronic devices onto optimized sub-

 This journal is © The Royal Society of Chemistry 2026

Open Access Article. Published on 11 maio 2026. Downloaded on 27/05/2026 13:44:17.
This article is licensed under a Creative Commons Attribution-NonCommercial 3.0 Unported Licence.

strates. By decoupling the device layer from its native growth substrate, these methods enable improvements in thermal management, optical efficiency, and mechanical flexibility, while also allowing for novel device architectures, all enabled by integrating the exfoliated device layers onto adequate foreign platforms. However, when fully processed devices are released, precise control of the resulting interfaces becomes a critical consideration. The stochastic nature of fracture can introduce surface roughness or subsurface damage, which, if not properly managed, may lead to interfacial voids during subsequent bonding and degrade thermal, optical, or mechanical properties. These challenges underscore the importance of controlled exfoliation to fully realize the performance benefits of exfoliation-based device transfer.

Various advanced exfoliation techniques have been explored to circumvent these issues and enable precise controllability in interface separation. Wu *et al.* employed the ELO method to transfer vertical AlGaInP LEDs from GaAs onto high-thermal-conductivity Cu substrates (Fig. 10c).[206] Thermal simulations guided the design of a patterned Cu receiver that confined mechanical stress during release, producing crack-free LEDs with thermal and optical performance comparable to non-released reference devices. A similar process has been applied in high-efficiency thin-film III–V solar cells. Bauhuis *et al.* demonstrated a record 26.1% single-junction GaAs cell by combining lift-off with optimized low-temperature front contacts and a backside metal mirror for photon recycling.[207] Trying to solve the lattice-mismatch at the sacrificial interface induced dislocation generation in III–V materials, Chancerel *et al.* developed a strained AlAs/InAlAs superlattice sacrificial layer to lift off InGaAs solar cells from InP substrates, enabling high-quality membrane release while suppressing defect propagation.[208]

While chemical interface engineering has proved highly effective, it remains constrained by the stringent requirement for lattice-matched sacrificial layers and the complexity of wet etching processes. The 2DLT technique offers a new insight to overcome these crystallographic constraints and introduce novel physical functionalities. Addressing thermal limitations in high-power electronics without relying on chemical etchants, Motala *et al.* demonstrated the deterministic exfoliation of fully processed GaN HEMT onto various substrates using a monolayer h-BN as a weak interface (Fig. 10d).[76] This approach preserved device integrity, minimized strain-induced damage, and allowed direct bonding to high-thermal-conductivity substrates such as SiC or diamond. Burzynski *et al.* further enhanced flexibility and thermal performance by incorporating graphene nanoplatelets into PDMS, which reduced device self-heating during operation and preserved device performance (no observed reduction in the saturation current) after 100 bending cycles.[209]

These examples illustrate that transfer-based techniques offer reliable pathways to enhance thermal, optical, and mechanical performance across LEDs, solar cells, and HEMT, while enabling integration onto diverse substrates and supporting advanced device designs.

### 5.5. Emergent phenomena and new functionality

While the previous section discussed how transfer techniques optimize device performance through structure lift-off and transfer, such as superior heat sinking or optical management, this section focuses on a more fundamental aspect: the emergence of novel physical properties when materials transition from substrate-clamped bulk forms to freestanding membranes. The ability to produce freestanding thin films nanomembranes *via* lift-off techniques has opened avenues for exploring and exploiting novel physical phenomena arising from their new form factors. By freeing the material from its rigid support, intrinsic properties can be revealed or tuned, while the ultrathin nature of these films allows additional control through flexing, straining, or integration onto unconventional platforms. As a result, freestanding nanomembranes and their heterostructures provide a unique platform for accessing emergent properties that can be systematically engineered and harnessed.

Initially, stress-controlled mechanical bulk spalling was utilized to leverage the morphological features of the fracture surface for energy applications. Lee *et al.* demonstrated wafer-scale, 20 μm GaAs membranes as photocathodes for hydrogen production.[196] After minor surface treatment and Pt nanoparticle deposition, these membranes achieved a hydrogen evolution reaction onset potential of −136 mV (*vs.* RHE) and a saturation photocurrent density of 22.4 mA cm$^{-2}$, comparable to bulk GaAs controls. The spalling-induced sawtooth {110} facet structure further increased light absorption by ∼3%, illustrating that mechanical exfoliation can intrinsically enhance photonic and catalytic performance. Similar strategies were applied to silicon thin films with additional surface texturing,[197] highlighting the versatility of thin-film transfer for energy applications.

However, while the surface roughness inherent to bulk spalling benefits light trapping, it poses a significant obstacle for applications requiring high structural integrity and pristine interfaces. To access the intrinsic physics of the crystal lattice, such as ferroelectric relaxation or elastic strain limits, advanced exfoliation techniques are more favored due to their ability in producing atomically smooth, defect-free membranes. Utilizing this precision, researchers have unlocked material properties previously inaccessible in clamped films. For example, Lin *et al.* employed a water-soluble complex oxide sacrificial layer ($Sr_3Al_2O_6$) to exfoliate $BiFeO_3$ (BFO) membranes.[150] Once released, the films underwent structural relaxation, inducing larger non-central ion displacements and enhancing the bulk photovoltaic effect (BPVE) by approximately 200% compared to the original strained film (Fig. 10e). Beyond fundamental physics, this approach also enables practical heterogeneous integration. Takahashi *et al.* used BaO as a water-soluble sacrificial layer to release single-crystal BTO membranes, which were then transferred onto flexible PET substrates to create functional piezoelectric energy harvesters.[147] Pushing the boundaries of oxide exfoliation further, Zhang *et al.* achieved high-yield production of large-scale

Open Access Article. Published on 11 maio 2026. Downloaded on 27/05/2026 13:44:17.
This article is licensed under a Creative Commons Attribution-NonCommercial 3.0 Unported Licence.

membranes with thicknesses down to 10 nm based on a release-layer-free atomic lift-off technique.[66] In this ultrathin, freestanding regime, the removal of substrate clamping unlocked a pronounced dimensionality effect, resulting in a record-high pyroelectric coefficient of $1.76 \times 10^{-2}$ C $m^{-2}$ $K^{-1}$, which was nearly two orders of magnitude higher than conventional thin films (Fig. 10f). This breakthrough paves the way for cooling-free far-infrared (FIR) imaging systems capable of covering the full spectrum, outperforming state-of-the-art cooled HgCdTe detectors. Furthermore, the pristine surface quality of interface-defined membranes provides a route to extreme strain engineering. Jing *et al.* applied 1.2% tensile strain to ultrathin (1 μm) diamond membranes, reducing the bandgap from 5.31 eV to 5.06 eV and thereby enhancing UV responsivity. They further noted that, within a 2% strain window, the membrane can withstand >10 000 bending cycles without introducing cracks or surface damage.[210]

These examples demonstrate that freestanding thin films, enabled by lift-off techniques, unlock an unprecedented degree of freedom in mixing and matching materials, enabling electrical, mechanical, thermal, optical, and interfacial properties not attainable on growth substrates. At the same time, the current literature suggests that the transferred crystalline membrane can already retain promising mechanical robustness and stable electrical performance under moderate repeated deformation, with several studies reporting minimal degradation in key device metrics after bending. Some reports have also shown compatibility with practical processing constraints, such as BEOL thermal budgets, and have explored substrate or packaging designs to mitigate self-heating during operation. However, realizing these advantages at the system level requires continued advances. For freestanding membranes to serve as reliable platforms for fundamental scientific studies demands rigorous control over thickness uniformity, crystallinity, strain state, and defect properties, to ensure reproducibility and unambiguous interpretation of emergent physical phenomena. At the same time, advancing proof-of-concept membrane devices from lab to fab requires such rigorous control, and in addition, process compatibility, yield, and integration with existing workflows. Moreover, systematic studies of long-term reliability under extended electrical, thermal, and mechanical loading remain limited, and thus future study should move beyond proof-of-concept cycling tests toward standardized evaluations of bias stress, thermal aging, and coupled thermo-mechanical fatigue. Addressing these challenges through innovations in material growth, lift-off, and integration processes will be essential for the broader adoption of freestanding membrane concepts into device technologies.

## 6. Conclusion and outlook

Freestanding single-crystal membranes are fundamentally different from epitaxial thin films bound to their growth substrates in how they can be manipulated, tuned, stacked, and integrated. Lift-off techniques, when combined with epitaxial growth strategies, provide a route to decouple high-quality single-crystal films from their growth substrates and convert them into freestanding films and nanomembranes without sacrificing crystalline integrity. This capability substantially expands the accessible design space for heterostructures, interfaces, and device platforms. It has already led to recent demonstrations of emergent physical phenomena and unconventional device architectures that cannot be realized by conventional heterogeneous integration approaches alone. These advances position lift-off technologies not simply as alternative fabrication routes, but as a uniquely powerful tool for rethinking how crystalline materials are assembled, combined, and functionally exploited.

In this review, we discussed theoretical foundations, practical implementations, and recent innovations of lift-off techniques for producing freestanding crystalline membranes, as well as the emerging application spaces enabled by lift-off techniques, with a particular emphasis on mechanical lift-off. Mechanical exfoliation is intrinsically universal, as it does not rely on material-specific chemistry or optical absorption; however, its broader adoption was historically limited by poor control over crack initiation and propagation, which are critical for controlling membrane thickness and uniformity. Recent innovations in interface engineering, stressor design, crack initiation and manipulation schemes, and hybrid approaches that combine multiple physical effects, now allow exfoliation to be guided with far greater precision. These developments enable uniform membrane release with atomically precise thickness control, broader controllability of membrane thicknesses down to the nanometer scale, improved scalability, and access to material systems that were previously difficult or impractical to exfoliate, significantly expanding the scope and reliability of mechanical lift-off as a membrane-fabrication strategy. For a balanced perspective, we also introduced other lift-off techniques and their recent innovations, and discussed application spaces enabled by these complementary approaches.

Although a wide range of novel heterostructures have been enabled by lift-off techniques at the laboratory scale, fully commercialized devices that directly leverage these approaches remain limited. Among the various methods, LLO has achieved the greatest commercial success and is now widely used in applications such as chip packaging and display technologies, where its throughput, process maturity, and compatibility with large-area manufacturing are well established. In contrast, mechanical and CLO techniques have been extensively investigated for commercialization in areas such as III–V photovoltaics, wafer reuse, lightweight and flexible electronics, and high-performance optoelectronic devices, but they have not yet reached broad industrial adoption. While multiple startups and pilot efforts have pursued these approaches over the past decades, sustained commercial success is yet to be seen. The efforts to leverage lift-off techniques for emerging applications, such as 3D heterogeneous integration and bio-integrated systems, also largely remain at the early prototype stage.

 This journal is © The Royal Society of Chemistry 2026

Open Access Article. Published on 11 maio 2026. Downloaded on 27/05/2026 13:44:17.
This article is licensed under a Creative Commons Attribution-NonCommercial 3.0 Unported Licence.

In the near term, the most urgent challenge is to close the gap between proof-of-concept membrane release and reproducible device integration. First, the lift-off process itself must offer tighter control over exfoliation depth, interface roughness, thickness uniformity, and wafer-scale yield, all of which are essential for manufacturability, reproducibility, and device performance. In many applications, it is not sufficient to simply release a membrane; the released film must also retain the desired crystalline quality and thickness with high uniformity. This requirement becomes even more stringent for ultrathin membranes with thicknesses far below the natural spalling depth, where maintaining uniformity remains difficult despite recent progress. The interface-engineering strategies discussed in this review can help address this limitation by guiding crack propagation along engineered weak planes, but these benefits often come with trade-offs. In particular, interface modification may degrade the crystalline quality of subsequently grown epilayers, and such strategies are not universally applicable across different material systems.

Another near-term priority is post-release integration. In most practical cases, membrane release is not the final objective, but only the first step toward heterogeneous integration onto a foreign substrate. As a result, the success of lift-off technologies depends not only on whether membranes can be released, but also on whether they can be transferred and bonded with sufficient mechanical robustness and interfacial quality for subsequent fabrication and device operation. In practice, achieving such bonding often requires extremely smooth surfaces, stringent surface preparation, and sometimes elevated pressure or temperature, all of which can be difficult to implement reliably. The challenge is even greater when mechanically spalled membranes retain stressor layers, or when the receiving substrates are flexible, textured, or otherwise incompatible with conventional bonding schemes. Developing substrate- and material-specific integration routes is therefore an immediate requirement for translating lift-off-enabled membranes into practical device platforms.

In the long term, the field must move beyond successful membrane release and transfer demonstrations toward manufacturing-ready and operationally reliable integration workflows. In this context, throughput and process compatibility remain major barriers, particularly for applications in which lift-off is expected to provide economic benefit at scale. A representative example is substrate reuse, which has long been regarded as one of the most attractive opportunities for lift-off technologies, especially for costly III–V platforms. However, meaningful cost reduction will require far more than demonstrating that reuse is possible. Instead, it will depend on achieving many recycling cycles with minimal surface damage, tight thickness control, minimal refurbishment processing, and stable regrowth quality, such that the cumulative cost and yield penalties associated with repeated lift-off, surface recovery, and regrowth do not outweigh the anticipated savings.

Once membranes are integrated onto foreign substrates, additional challenges related to structural integrity, process compatibility, and operational stability must also be considered. Bonding-induced stress, residual stress from lift-off, and stress accumulated during later fabrication steps can all degrade membrane quality and device performance. In addition, thermal expansion mismatch between the membrane and the host substrate, together with heat dissipation constraints introduced by multilayer stacking, may lead to cracking, delamination, or performance drift under demanding operating conditions, particularly in harsh environments or high-power devices. These considerations highlight that the practical success of lift-off technologies depends not only on membrane release and transfer, but also on whether the integrated membrane platform can remain process-compatible, operationally stable, and scalable within a manufacturing environment.

Fully unlocking the potential of lift-off technologies will require end-to-end co-design and co-optimization across membrane release, integration, and downstream device fabrication. In this review, we discussed several emerging strategies that have already advanced lift-off technologies in the near term by improving the quality, precision, and yield of released membranes, particularly through interface engineering, stressor design and crack initiation. We also highlighted advances that may contribute to longer-term manufacturing goals, such as 2D-material-assisted lift-off to improve substrate reusability. At the same time, substantial progress is still needed in long-term integration directions, particularly in throughput, substrate refurbishment, and compatibility with downstream fabrication and integration. With such holistic development, lift-off technologies may progress from standalone membrane-release methods into a broadly applicable platform for heterogeneous integration across diverse material systems.

## Conflicts of interest

The authors declare no competing financial interest.

## Data availability

No primary research results, software or code have been included and no new data were generated or analysed as part of this review.

## Acknowledgements

This study was supported by the National Research Foundation of Korea (NRF) grant funded by the Korea government (MSIT, RS-2024-00445081), the National Science Foundation (ECCS-2328839), NSF-MRSEC (DMR-2309037), NSF IUCRC (EEC-2231625), and DARPA (HR0011-24-2-0376).

Open Access Article. Published on 11 maio 2026. Downloaded on 27/05/2026 13:44:17.
This article is licensed under a Creative Commons Attribution-NonCommercial 3.0 Unported Licence.

## References


1 F. C. Frank and J. H. Van Der Merwe, One-dimensional dislocations. II. Misfitting monolayers and oriented overgrowth, *Proc. R. Soc. London, Ser. A*, 1949, **198**, 216–225.

2 J. W. Matthews and A. E. Blakeslee, Defects in epitaxial multilayers: I. Misfit dislocations, *J. Cryst. Growth*, 1974, **27**, 118–125.

3 M. F. Doerner and W. D. Nix, Stresses and deformation processes in thin films on substrates, *Crit. Rev. Solid State Mater. Sci.*, 1988, **14**, 225–268.

4 U. Gösele, Q.-Y. Tong, A. Schumacher, G. Kräuter, M. Reiche, A. Plößl, P. Kopperschmidt, T.-H. Lee and W.-J. Kim, Wafer bonding for microsystems technologies, *Sens. Actuators, A*, 1999, **74**, 161–168.

5 E. Yablonovitch, T. Gmitter, J. P. Harbison and R. Bhat, Extreme selectivity in the lift-off of epitaxial GaAs films, *Appl. Phys. Lett.*, 1987, **51**, 2222–2224.

6 E. Yablonovitch, D. M. Hwang, T. J. Gmitter, L. T. Florez and J. P. Harbison, van der Waals bonding of GaAs epitaxial liftoff films onto arbitrary substrates, *Appl. Phys. Lett.*, 1990, **56**, 2419–2421.

7 D. J. Frank, R. H. Dennard, E. Nowak, P. M. Solomon, Y. Taur and H.-S. P. Wong, Device scaling limits of Si MOSFETs and their application dependencies, *Proc. IEEE*, 2001, **89**, 259–288.

8 W. Cao, H. Bu, M. Vinet, M. Cao, S. Takagi, S. Hwang, T. Ghani and K. Banerjee, The future transistors, *Nature*, 2023, **620**, 501–515.

9 T. Komljenovic, M. Davenport, J. Hulme, A. Y. Liu, C. T. Santis, A. Spott, S. Srinivasan, E. J. Stanton, C. Zhang and J. E. Bowers, Heterogeneous Silicon Photonic Integrated Circuits, *J. Lightwave Technol.*, 2016, **34**, 20–35.

10 Y. Ren, Z. Qiao and Q. Niu, Topological phases in two-dimensional materials: a review, *Rep. Prog. Phys.*, 2016, **79**, 066501.

11 C. Choi, H. Kim, J.-H. Kang, M.-K. Song, H. Yeon, C. S. Chang, J. M. Suh, J. Shin, K. Lu, B.-I. Park, Y. Kim, H. E. Lee, D. Lee, J. Lee, I. Jang, S. Pang, K. Ryu, S.-H. Bae, Y. Nie, H. S. Kum, M.-C. Park, S. Lee, H.-J. Kim, H. Wu, P. Lin and J. Kim, Reconfigurable heterogeneous integration using stackable chips with embedded artificial intelligence, *Nat. Electron.*, 2022, **5**, 386–393.

12 M. D. Thouless, A. G. Evans, M. F. Ashby and J. W. Hutchinson, The edge cracking and spalling of brittle plates, *Acta Metall.*, 1987, **35**, 1333–1341.

13 M. D. Drory, M. D. Thouless and A. G. Evans, On the decohesion of residually stressed thin films, *Acta Metall.*, 1988, **36**, 2019–2028.

14 Z. Suo and J. W. Hutchinson, Steady-state cracking in brittle substrates beneath adherent films, *Int. J. Solids Struct.*, 1989, **25**, 1337–1353.

15 H. Kim, S. Lee, J. Shin, M. Zhu, M. Akl, K. Lu, N. M. Han, Y. Baek, C. S. Chang, J. M. Suh, K. S. Kim, B.-I. Park, Y. Zhang, C. Choi, H. Shin, H. Yu, Y. Meng, S.-I. Kim, S. Seo, K. Lee, H. S. Kum, J.-H. Lee, J.-H. Ahn, S.-H. Bae, J. Hwang, Y. Shi and J. Kim, Graphene nanopattern as a universal epitaxy platform for single-crystal membrane production and defect reduction, *Nat. Nanotechnol.*, 2022, **17**, 1054–1059.

16 H.-S. Yang, J. Kim, S. Kim, N. S. A. Eom, S. Kang, C.-S. Han, S. H. Kim, D. Lim, J.-H. Lee, S. H. Park, J. W. Choi, C.-L. Lee, B. Yoo and J.-H. Lim, Kerf-Less Exfoliated Thin Silicon Wafer Prepared by Nickel Electrodeposition for Solar Cells, *Front. Chem.*, 2019, **6**, 600.

17 H. Park, C. Lim, Y. Noh, C.-J. Lee, H. Won, J. Jung, M. Choi, J.-J. Kim, H. Yoo and H. Park, Investigation of electrical characteristics of flexible CMOS devices fabricated with thickness-controlled spalling process, *Solid-State Electron.*, 2020, **173**, 107901.

18 Y. H. Lee, Y.-J. Kim, S. M. J. Han, H. Song and J. Oh, Sub-5 μm-thick spalled single crystal Si foils by decoupling crack initiation and propagation, *Appl. Phys. Lett.*, 2016, **109**, 132101.

19 S. W. Bedell, K. Fogel, P. Lauro, D. Shahrjerdi, J. A. Ott and D. Sadana, Layer transfer by controlled spalling, *J. Phys. D: Appl. Phys.*, 2013, **46**, 152002.

20 D. Crouse, J. Simon, K. L. Schulte, D. L. Young, A. J. Ptak and C. E. Packard, Increased fracture depth range in controlled spalling of (100)-oriented germanium via electroplating, *Thin Solid Films*, 2018, **649**, 154–159.

21 R. W. Margevicius and P. Gumbsch, Influence of crack propagation direction on {110} fracture toughness of gallium arsenide, *Philos. Mag.*, 1998, **78**, 567–581.

22 A. K. Braun, S. Theingi, W. E. McMahon, A. J. Ptak and C. E. Packard, Controlled spalling of (100)-oriented GaAs with a nanoimprint lithography interlayer for thin-film layer transfer without facet formation, *Thin Solid Films*, 2022, **742**, 139049.

23 J. Chen and C. E. Packard, Controlled spalling-based mechanical substrate exfoliation for III-V solar cells: A review, *Sol. Energy Mater. Sol. Cells*, 2021, **225**, 111018.

24 F. Dross, J. Robbelein, B. Vandevelde, E. Van Kerschaver, I. Gordon, G. Beaucarne and J. Poortmans, Stress-induced large-area lift-off of crystalline Si films, *Appl. Phys. A*, 2007, **89**, 149–152.

25 A. S. McKeown-Green, H. J. Zeng, A. P. Saunders, J. Li, J. Shi, Y. Shen, F. Pan, J. Hu, J. A. Dionne, T. F. Heinz, S. M. Wu, F. Zheng and F. Liu, Millimeter-Scale Exfoliation of hBN with Tunable Flake Thickness for Scalable Encapsulation, *ACS Appl. Nano Mater.*, 2024, **7**, 6574–6582.

26 T. An, M. Wen, C. Q. Hu, H. W. Tian and W. T. Zheng, Interfacial fracture for TiN/SiNx nano-multilayer coatings on Si(111) characterized by nanoindentation experiments, *Mater. Sci. Eng., A*, 2008, **494**, 324–328.

27 J. A. Thornton and D. W. Hoffman, Internal stresses in titanium, nickel, molybdenum, and tantalum films deposited by cylindrical magnetron sputtering, *J. Vac. Sci. Technol.*, 1977, **14**, 164–168.

28 J. K. Dennis and T. E. Such, *Nickel and Chromium Plating*, Elsevier, Amsterdam, Netherlands, 1993.


 This journal is © The Royal Society of Chemistry 2026

Open Access Article. Published on 11 maio 2026. Downloaded on 27/05/2026 13:44:17.
This article is licensed under a Creative Commons Attribution-NonCommercial 3.0 Unported Licence.

29 D. R. Crouse, *Controlled Spalling in (100)-Oriented Germanium by Electroplating*, M.S. thesis, Colorado School of Mines, 2017.

30 C. P. Horn, C. Wicker, A. Wellisz, C. Zeledon, P. V. K. Nittala, F. J. Heremans, D. D. Awschalom and S. Guha, Controlled Spalling of 4H Silicon Carbide with Investigated Spin Coherence for Quantum Engineering Integration, *ACS Nano*, 2024, **18**, 31381–31389.

31 H. Yang and S.-W. Kang, Improvement of thickness uniformity in nickel electroforming for the LIGA process, *Int. J. Mach. Tools Manuf.*, 2000, **40**, 1065–1072.

32 T. G. Kollie, Measurement of the thermal-expansion coefficient of nickel from 300 to 1000 K and determination of the power-law constants near the Curie temperature, *Phys. Rev. B*, 1977, **16**, 4872–4881.

33 H. Z. Yu and C. V. Thompson, Grain growth and complex stress evolution during Volmer–Weber growth of polycrystalline thin films, *Acta Mater.*, 2014, **67**, 189–198.

34 E. Chason, J. W. Shin, S. J. Hearne and L. B. Freund, Kinetic model for dependence of thin film stress on growth rate, temperature, and microstructure, *J. Appl. Phys.*, 2012, **111**, 083520.

35 J. S. Tello, A. F. Bower, E. Chason and B. W. Sheldon, Kinetic Model of Stress Evolution during Coalescence and Growth of Polycrystalline Thin Films, *Phys. Rev. Lett.*, 2007, **98**, 216104.

36 E. Chason, B. W. Sheldon, L. B. Freund, J. A. Floro and S. J. Hearne, Origin of Compressive Residual Stress in Polycrystalline Thin Films, *Phys. Rev. Lett.*, 2002, **88**, 156103.

37 M. Huff, Review Paper: Residual Stresses in Deposited Thin-Film Material Layers for Micro- and Nano-Systems Manufacturing, *Micromachines*, 2022, **13**, 2084.

38 L. B. Freund and S. Suresh, *Thin Film Materials: Stress, Defect Formation and Surface Evolution*, Cambridge University Press, Cambridge, UK, 2004.

39 M. J. Ward, *Wafer scale exfoliation of monocrystalline microscale silicon films*, PhD thesis, University of Texas at Austin, 2020.

40 I. Alhomoudi, S. W. Bedell, C.-W. Cheng, K. E. Fogel, D. K. Sadana, K. L. Saenger, N. E. Sosa and N. Li, Spalling with Laser-Defined Spall Edge Regions, *US Pat*, US9324564B2, 2016.

41 B. E. Ley, *Wafer-scale Controlled Spalling and Reuse of (100)-Oriented Germanium*, M.S. thesis, Colorado School of Mines, 2019.

42 M. Ward and M. Cullinan, A fracture model for exfoliation of thin silicon films, *Int. J. Fract.*, 2019, **216**, 161–171.

43 S. W. Bedell, D. Shahrjerdi, B. Hekmatshoar, K. Fogel, P. A. Lauro, J. A. Ott, N. Sosa and D. Sadana, Kerf-Less Removal of Si, Ge, and III–V Layers by Controlled Spalling to Enable Low-Cost PV Technologies, *IEEE J. Photovolt.*, 2012, **2**, 141–147.

44 J. S. Mangum, A. D. Rice, J. Chen, J. Chenenko, E. W. K. Wong, A. K. Braun, S. Johnston, H. Guthrey, J. F. Geisz, A. J. Ptak and C. E. Packard, High–Efficiency Solar Cells Grown on Spalled Germanium for Substrate Reuse without Polishing, *Adv. Energy Mater.*, 2022, **12**, 2201332.

45 G. Picun, E. Guiot, F. Allibert, J. Leib, T. Becker, O. Rusch, A. Drouin and W. Schwarzenbach, A 150 & 200 mm engineered substrate increasing SiC power device current density up to 30%, in *presented in part at PCIM Asia 2024; International Exhibition and Conference for Power Electronics, Intelligent Motion, Renewable Energy and Energy Management*, Shenzhen, China, August, 2024.

46 C. Maleville, T. Barge, B. Ghyselen, A. J. Auberton, H. Moriceau and A. M. Cartier, Multiple SOI layers by multiple Smart-Cut® transfers, in *presented in part at 2000 IEEE International SOI Conference*, Williamsburg, VA, USA, October, 2000.

47 V. V. Voronenkov, Y. S. Lelikov, A. S. Zubrilov, Y. G. Shreter and A. A. Leonidov, Thick GaN Film Stress-induced Self-separation, in *presented in part at 2019 IEEE Conference of Russian Young Researchers in Electrical and Electronic Engineering (EIConRus)*, Saint Petersburg and Moscow, Russia, January, 2019.

48 K. Fujito, S. Kubo, H. Nagaoka, T. Mochizuki, H. Namita and S. Nagao, Bulk GaN crystals grown by HVPE, *J. Cryst. Growth*, 2009, **311**, 3011–3014.

49 H. Park, H. Won, C. Lim, Y. Zhang, W. S. Han, S.-B. Bae, C.-J. Lee, Y. Noh, J. Lee, J. Lee, S. Jung, M. Choi, S. Lee and H. Park, Layer-resolved release of epitaxial layers in III-V heterostructure via a buffer-free mechanical separation technique, *Sci. Adv.*, 2022, **8**, eabl6406.

50 K. Tomita, T. Kachi, S. Nagai, A. Kojima, S. Yamasaki and M. Koike, Self-Separation of Freestanding GaN from Sapphire Substrates by Hydride Vapor Phase Epitaxy, *Phys. Status Solidi A*, 2002, **194**, 563–567.

51 Y. Lu, X. Zou, S. Krishna, X. Tang, Z. Liu, M. Nong, C.-H. Liao, S. Yuvaraja, M. Ben Hassine, H. Fariborzi and X. Li, Thermal mismatch engineering induced freestanding and ultrathin Ga2O3 membrane for vertical electronics, *Mater. Today Phys.*, 2023, **36**, 101181.

52 R. W. McClelland, C. O. Bozler and J. C. C. Fan, A technique for producing epitaxial films on reuseable substrates, *Appl. Phys. Lett.*, 1980, **37**, 560–562.

53 J. S. Mangum, S. Theingi, M. A. Steiner, W. E. McMahon and E. L. Warren, Development of High-Efficiency GaAs Solar Cells Grown on Nanopatterned GaAs Substrates, *Cryst. Growth Des.*, 2021, **21**, 5955–5960.

54 K. Hiramatsu, K. Nishiyama, M. Onishi, H. Mizutani, M. Narukawa, A. Motogaito, H. Miyake, Y. Iyechika and T. Maeda, Fabrication and characterization of low defect density GaN using facet-controlled epitaxial lateral overgrowth (FACELO), *J. Cryst. Growth*, 2000, **221**, 316–326.

55 N. Julian, P. Mages, C. Zhang, J. Zhang, S. Kraemer, S. Stemmer, S. Denbaars, L. Coldren, P. Petroff and J. Bowers, Coalescence of InP Epitaxial Lateral Overgrowth by MOVPE with V/III Ratio Variation, *J. Electron. Mater.*, 2012, **41**, 845–852.

Open Access Article. Published on 11 maio 2026. Downloaded on 27/05/2026 13:44:17.
This article is licensed under a Creative Commons Attribution-NonCommercial 3.0 Unported Licence.

56 C. S. Solanki, R. Bilyalov, J. Poortmans, J. Nijs and R. Mertens, Porous silicon layer transfer processes for solar cells, *Sol. Energy Mater. Sol. Cells*, 2004, **83**, 101–113.
57 H. S. Radhakrishnan, R. Martini, V. Depauw, K. Van Nieuwenhuysen, M. Debucquoy, J. Govaerts, I. Gordon, R. Mertens and J. Poortmans, Improving the quality of epitaxial foils produced using a porous silicon-based layer transfer process for high-efficiency thin-film crystalline silicon solar cells, *IEEE J. Photovolt.*, 2013, **4**, 70–77.
58 E. Rojas, B. Terheiden, H. Plagwitz, J. Hensen, C. Baur, G. Strobl and R. Brendel, Formation of mesoporous germanium double layers by electrochemical etching for layer transfer processes, *Electrochem. Commun.*, 2010, **12**, 231–233.
59 E. G. Rojas, J. Hensen, J. Carstensen, H. Föll and R. Brendel, Porous Germanium Layers by Electrochemical Etching for Layer Transfer Processes of High-Efficiency Multi-Junction Solar Cells, *ECS Trans.*, 2011, **33**, 95.
60 J.-H. Min, K. Lee, T.-H. Chung, J.-W. Min, K.-H. Li, C. H. Kang, H.-M. Kwak, T.-H. Kim, Y. Yuan, K.-K. Kim, D.-S. Lee, T. K. Ng and B. S. Ooi, Large-scale and high-quality III-nitride membranes through microcavity-assisted crack propagation by engineering tensile-stressed Ni layers, *Opto-Electron. Sci.*, 2022, **1**, 220016.
61 H. Zhang, J. Min, T. Chung, K. Lee, P. Gnanasekar, J. Min, T. Park, Y. Wang, T. K. Ng, U. Schwingenschlögl, Q. Gan and B. S. Ooi, Nanostructured Gallium Nitride Membrane at Wafer Scale for Photo(Electro)catalytic Polluted Water Remediation, *Adv. Sci.*, 2023, **10**, 2205612.
62 E. G. Rojas, C. Hampe, H. Plagwitz and R. Brendel, Formation of mesoporous gallium arsenide for lift-off processes by electrochemical etching, in *presented in part at 2009 34th IEEE Photovoltaic Specialists Conference (PVSC)*, Philadelphia, PA, USA, June, 2009.
63 M. B. Joshi and M. S. Goorsky, Transfer of InP thin films from engineered porous silicon substrates, *J. Appl. Phys.*, 2010, **107**, 024906.
64 D. Chen, X. Kou, S. Sareminaeini and M. S. Goorsky, Epitaxial Growth and Layer Transfer of InP through Electrochemically Etched and Annealed Porous Buried Layers, *ECS Trans.*, 2014, **64**, 49.
65 D. H. Kim, H. E. Lee, B. K. You, S. B. Cho, R. Mishra, I.-S. Kang and K. J. Lee, Flexible Crossbar-Structured Phase Change Memory Array via Mo-Based Interfacial Physical Lift-Off, *Adv. Funct. Mater.*, 2019, **29**, 1806338.
66 X. Zhang, O. Ericksen, S. Lee, M. Akl, M.-K. Song, H. Lan, P. Pal, J. M. Suh, S. Lindemann, J.-E. Ryu, Y. Shao, X. Zheng, N. M. Han, B. Bhatia, H. Kim, H. S. Kum, C. S. Chang, Y. Shi, C.-B. Eom and J. Kim, Atomic lift-off of epitaxial membranes for cooling-free infrared detection, *Nature*, 2025, **641**, 98–105.
67 K. Chung, C.-H. Lee and G.-C. Yi, Transferable GaN layers grown on ZnO-coated graphene layers for optoelectronic devices, *Science*, 2010, **330**, 655–657.
68 Y. Kim, S. S. Cruz, K. Lee, B. O. Alawode, C. Choi, Y. Song, J. M. Johnson, C. Heidelberger, W. Kong, S. Choi, K. Qiao, I. Almansouri, E. A. Fitzgerald, J. Kong, A. M. Kolpak, J. Hwang and J. Kim, Remote epitaxy through graphene enables two-dimensional material-based layer transfer, *Nature*, 2017, **544**, 340–343.
69 W. Kong, H. Li, K. Qiao, Y. Kim, K. Lee, Y. Nie, D. Lee, T. Osadchy, R. J. Molnar, D. K. Gaskill, R. L. Myers-Ward, K. M. Daniels, Y. Zhang, S. Sundram, Y. Yu, S. H. Bae, S. Rajan, Y. Shao-Horn, K. Cho, A. Ougazzaden, J. C. Grossman and J. Kim, Polarity governs atomic interaction through two-dimensional materials, *Nat. Mater.*, 2018, **17**, 999–1004.
70 F. Liu, T. Wang, X. Gao, H. Yang, Z. Zhang, Y. Guo, Y. Yuan, Z. Huang, J. Tang and B. Sheng, Determination of the preferred epitaxy for III-nitride semiconductors on wet-transferred graphene, *Sci. Adv.*, 2023, **9**, eadf8484.
71 Q. Chen, K. Yang, B. Shi, X. Yi, J. Wang, J. Li and Z. Liu, Principles for 2D-Material-Assisted Nitrides Epitaxial Growth, *Adv. Mater.*, 2023, **35**, e2211075.
72 L. Dai, J. Zhao, J. Li, B. Chen, S. Zhai, Z. Xue, Z. Di, B. Feng, Y. Sun, Y. Luo, M. Ma, J. Zhang, S. Ding, L. Zhao, Z. Jiang, W. Luo, Y. Quan, J. Schwarzkopf, T. Schroeder, Z.-G. Ye, Y.-H. Xie, W. Ren and G. Niu, Highly heterogeneous epitaxy of flexoelectric BaTiO3-$\delta$ membrane on Ge, *Nat. Commun.*, 2022, **13**, 2990.
73 J. Jeong, D. K. Jin, J. Cha, B. K. Kang, Q. Wang, J. Choi, S. W. Lee, V. Y. Mikhailovskii, V. Neplokh, N. Amador-Mendez, M. Tchernycheva, W. S. Yang, J. Yoo, M. J. Kim, S. Hong and Y. J. Hong, Selective-Area Remote Epitaxy of ZnO Microrods Using Multilayer–Monolayer-Patterned Graphene for Transferable and Flexible Device Fabrications, *ACS Appl. Nano Mater.*, 2020, **3**, 8920–8930.
74 Y. Jia, J. Ning, J. Zhang, C. Yan, B. Wang, Y. Zhang, J. Zhu, X. Shen, J. Dong, D. Wang and Y. Hao, Transferable GaN Enabled by Selective Nucleation of AlN on Graphene for High-Brightness Violet Light-Emitting Diodes, *Adv. Opt. Mater.*, 2020, **8**, 1901632.
75 H. Kim, K. Lu, Y. Liu, H. S. Kum, K. S. Kim, K. Qiao, S.-H. Bae, S. Lee, Y. J. Ji, K. H. Kim, H. Paik, S. Xie, H. Shin, C. Choi, J. H. Lee, C. Dong, J. A. Robinson, J.-H. Lee, J.-H. Ahn, G. Y. Yeom, D. G. Schlom and J. Kim, Impact of 2D–3D Heterointerface on Remote Epitaxial Interaction through Graphene, *ACS Nano*, 2021, **15**, 10587–10596.
76 M. J. Motala, E. W. Blanton, A. Hilton, E. Heller, C. Muratore, K. Burzynski, J. L. Brown, K. Chabak, M. Durstock, M. Snure and N. R. Glavin, Transferrable AlGaN/GaN High-Electron Mobility Transistors to Arbitrary Substrates via a Two-Dimensional Boron Nitride Release Layer, *ACS Appl. Mater. Interfaces*, 2020, **12**, 21837–21844.
77 J. Jeong, D. K. Jin, J. Choi, J. Jang, B. K. Kang, Q. Wang, W. I. Park, M. S. Jeong, B.-S. Bae, W. S. Yang, M. J. Kim and Y. J. Hong, Transferable, flexible white light-emitting diodes of GaN p–n junction microcrystals fabricated by remote epitaxy, *Nano Energy*, 2021, **86**, 106075.
78 Y. Yin, B. Liu, Q. Chen, Z. Chen, F. Ren, S. Zhang, Z. Liu, R. Wang, M. Liang, J. Yan, J. Sun, X. Yi, T. Wei, J. Wang,

 This journal is © The Royal Society of Chemistry 2026

Open Access Article. Published on 11 maio 2026. Downloaded on 27/05/2026 13:44:17.
This article is licensed under a Creative Commons Attribution-NonCommercial 3.0 Unported Licence.

J. Li, Z. Liu, P. Gao and Z. Liu, Continuous Single-Crystalline GaN Film Grown on WS2-Glass Wafer, *Small*, 2022, **18**, 2202529.

79 T. Ayari, S. Sundaram, X. Li, S. Alam, C. Bishop, W. El Huni, M. B. Jordan, Y. Halfaya, S. Gautier, P. L. Voss, J. P. Salvestrini and A. Ougazzaden, Heterogeneous Integration of Thin-Film InGaN-Based Solar Cells on Foreign Substrates with Enhanced Performance, *ACS Photonics*, 2018, **5**, 3003–3008.

80 L. Wang, S. Yang, F. Zhou, Y. Gao, Y. Duo, R. Chen, J. Yang, J. Yan, J. Wang, J. Li, Y. Zhang and T. Wei, Wafer-Scale Transferrable GaN Enabled by Hexagonal Boron Nitride for Flexible Light-Emitting Diode, *Small*, 2024, **20**, 2306132.

81 H. Kim, J. C. Kim, Y. Jeong, J. Yu, K. Lu, D. Lee, N. Kim, H. Y. Jeong, J. Kim and S. Kim, Role of transferred graphene on atomic interaction of GaAs for remote epitaxy, *J. Appl. Phys.*, 2021, **130**, 174901.

82 S. Lee, J. Kim, B.-I. Park, H. I. Kim, C. Lim, E. Lee, J. Y. Yang, J. Choi, Y. J. Hong, C. S. Chang, H. S. Kum, J. Kim, K. Lee, H. Kim and G.-C. Yi, GaN remote epitaxy on a pristine graphene buffer layer via controlled graphitization of SiC, *Appl. Phys. Lett.*, 2024, **125**, 252102.

83 M. Yuan, J. Feng, H. Li, H. Gao, Y. Qiu, L. Jiang and Y. Wu, Remote epitaxial crystalline perovskites for ultra-high-resolution micro-LED displays, *Nat. Nanotechnol.*, 2025, **20**, 381–387.

84 Y. Kobayashi, K. Kumakura, T. Akasaka and T. Makimoto, Layered boron nitride as a release layer for mechanical transfer of GaN-based devices, *Nature*, 2012, **484**, 223–227.

85 M. Snure, E. W. Blanton, V. Soukhoveev, T. Vogt, A. Osinsky, T. Prusnick, W. J. Kennedy and N. R. Glavin, Spalling induced van der Waals lift-off and transfer of 4-in. GaN epitaxial films, *J. Appl. Phys.*, 2023, **134**, 025307.

86 P. Vuong, T. Moudakir, R. Gujrati, A. Srivastava, V. Ottapilakkal, S. Gautier, P. Voss, S. Sundaram, J. Salvestrini and A. Ougazzaden, Scaling up of Growth, Fabrication, and Device Transfer Process for GaN-based LEDs on H-BN Templates to 6-inch Sapphire Substrates, *Adv. Mater. Technol.*, 2023, **8**, 2300600.

87 B. Liu, Q. Chen, Z. Chen, S. Yang, J. Shan, Z. Liu, Y. Yin, F. Ren, S. Zhang, R. Wang, M. Wu, R. Hou, T. Wei, J. Wang, J. Sun, J. Li, Z. Liu, Z. Liu and P. Gao, Atomic Mechanism of Strain Alleviation and Dislocation Reduction in Highly Mismatched Remote Heteroepitaxy Using a Graphene Interlayer, *Nano Lett.*, 2022, **22**, 3364–3371.

88 B. Shi, Z. Liu, Y. Li, Q. Chen, J. Liu, K. Yang, M. Liang, X. Yi, J. Wang, J. Li, J. Kang, P. Gao and Z. Liu, Atomic Evolution Mechanism and Suppression of Edge Threading Dislocations in Nitride Remote Heteroepitaxy, *Nano Lett.*, 2024, **24**, 7458–7466.

89 K. Qiao, Y. Liu, C. Kim, R. J. Molnar, T. Osadchy, W. Li, X. Sun, H. Li, R. L. Myers-Ward, D. Lee, S. Subramanian, H. Kim, K. Lu, J. A. Robinson, W. Kong and J. Kim, Graphene Buffer Layer on SiC as a Release Layer for High-Quality Freestanding Semiconductor Membranes, *Nano Lett.*, 2021, **21**, 4013–4020.

90 Y. Wen, J. Ning, H. Wu, H. Zhang, R. Cheng, L. Yin, H. Wang, X. Zhang, Y. Liu, D. Wang, Y. Hao, J. Zhang and J. He, van der Waals Integration of 4-Inch Single-Crystalline III-Nitride Semiconductors, *Adv. Mater.*, 2025, **37**, 2501916.

91 E. Blanton, M. Motala, T. Prusnick, A. Hilton, J. Brown, A. Bhattacharyya, S. Krishnamoorthy, K. Leedy, N. Glavin and M. Snure, Spalling-Induced Liftoff and Transfer of Electronic Films Using a van der Waals Release Layer, *Small*, 2021, **17**, 2102668.

92 S. Karrakchou, S. Sundaram, R. Gujrati, P. Vuong, A. Mballo, H. E. Adjmi, V. Ottapilakkal, W. El Huni, K. Bouzid, G. Patriarche, A. Ahaitouf, P. L. Voss, J. P. Salvestrini and A. Ougazzaden, Monolithic Free-Standing Large-Area Vertical III-N Light-Emitting Diode Arrays by One-Step h-BN-Based Thermomechanical Self-Lift-Off and Transfer, *ACS Appl. Electron. Mater.*, 2021, **3**, 2614–2621.

93 H. Kim, Y. Liu, K. Lu, C. S. Chang, D. Sung, M. Akl, K. Qiao, K. S. Kim, B.-I. Park, M. Zhu, J. M. Suh, J. Kim, J. Jeong, Y. Baek, Y. J. Ji, S. Kang, S. Lee, N. M. Han, C. Kim, C. Choi, X. Zhang, H.-K. Choi, Y. Zhang, H. Wang, L. Kong, N. N. Afeefah, M. N. M. Ansari, J. Park, K. Lee, G. Y. Yeom, S. Kim, J. Hwang, J. Kong, S.-H. Bae, Y. Shi, S. Hong, W. Kong and J. Kim, High-throughput manufacturing of epitaxial membranes from a single wafer by 2D materials-based layer transfer process, *Nat. Nanotechnol.*, 2023, **18**, 464–470.

94 H.-M. Kwak, J.-S. Lee, B.-I. Park, J. Baik, J. Kim, W.-L. Jeong, K.-P. Kim, S.-H. Mun, H. Kim, J. Kim and D.-S. Lee, Stability of Graphene and Influence of AlN Surface Pits on GaN Remote Heteroepitaxy for Exfoliation, *ACS Nano*, 2023, **17**, 11739–11748.

95 J. Choi, J. Jeong, X. Zhu, J. Kim, B. K. Kang, Q. Wang, B.-I. Park, S. Lee, J. Kim, H. Kim, J. Yoo, G.-C. Yi, D.-S. Lee, J. Kim, S. Hong, M. J. Kim and Y. J. Hong, Exceptional Thermochemical Stability of Graphene on N-Polar GaN for Remote Epitaxy, *ACS Nano*, 2023, **17**, 21678–21689.

96 B.-I. Park, J. Kim, K. Lu, X. Zhang, S. Lee, J. M. Suh, D.-H. Kim, H. Kim and J. Kim, Remote Epitaxy: Fundamentals, Challenges, and Opportunities, *Nano Lett.*, 2024, **24**, 2939–2952.

97 S. H. Choi, Y. Kim, I. Jeon and H. Kim, Heterogeneous Integration of Wide Bandgap Semiconductors and 2D Materials: Processes, Applications, and Perspectives, *Adv. Mater.*, 2025, **37**, 2411108.

98 J. Jing, F. Sun, Z. Wang, L. Ma, Y. Luo, Z. Du, T. Zhang, Y. Wang, F. Xu, T. Zhang, C. Chen, X. Ma, Y. He, Y. Zhu, H. Sun, X. Wang, Y. Zhou, J. K. H. Tsoi, J. Wrachtrup, N. Wong, C. Li, D.-K. Ki, Q. Wang, K. H. Li, Y. Lin and Z. Chu, Scalable production of ultraflat and ultraflexible diamond membrane, *Nature*, 2024, **636**, 627–634.

99 X. Li, H. L. Bristow, A. Said, F. Kamoliddinov, S. T. Thoroddsen, S. De Wolf and G. Lubineau, Stick-slips

Open Access Article. Published on 11 maio 2026. Downloaded on 27/05/2026 13:44:17.
This article is licensed under a Creative Commons Attribution-NonCommercial 3.0 Unported Licence.

of peeling adhesive tapes: not just high-speed, *SSRN*, 2025, 5118697.

100 M. Bertoni and P. G. Coll, Sound-Assisted Crack Propagation for Semiconductor Wafering, *US Pat*, US10828800B2, 2020.

101 E. Sacchitella, S. Polly, S. Hubbard, P. Coll and M. Bertoni, Demonstration of Substrate Reuse using Acoustic Spalling in GaAs based Photovoltaics, in *presented in part at 2024 IEEE 52nd Photovoltaic Specialist Conference (PVSC)*, Seattle, WA, USA, June, 2024.

102 P. G. Coll, T. Black, J. Abraham, S. Kamishetty, A. P. Merkle, L. Bathurst and M. Bertoni, Sonic Lift-off (SLO) to Enable Substrate Reuse of Bulk GaN and SiC Substrates, in *presented in part at CSMANTECH*, Tucson, Arizona, USA, June, 2024.

103 K. L. Schulte, S. W. Johnston, A. K. Braun, J. T. Boyer, A. N. Neumann, W. E. McMahon, M. Young, P. G. Coll, M. I. Bertoni, E. L. Warren and M. A. Steiner, GaAs solar cells grown on acoustically spalled GaAs substrates with 27% efficiency, *Joule*, 2023, **7**, 1529–1542.

104 H. Chen and J. Ravichandran, A System Built for Both Deterministic Transfer Processes and Contact Photolithography, *Adv. Eng. Mater.*, 2024, **26**, 2401228.

105 C. Camperi-Ginestet, M. Hargis, N. Jokerst and M. Allen, Alignable epitaxial liftoff of GaAs materials with selective deposition using polyimide diaphragms, *IEEE Photonics Technol. Lett.*, 1991, **3**, 1123–1126.

106 G. Roelkens, J. Brouckaert, D. Van Thourhout, R. Baets, R. Nötzel and M. Smit, Adhesive Bonding of InP/InGaAsP Dies to Processed Silicon-On-Insulator Wafers using DVS-bis-Benzocyclobutene, *J. Electrochem. Soc.*, 2006, **153**, G1015.

107 D. J. Monk, D. S. Soane and R. T. Howe, A review of the chemical reaction mechanism and kinetics for hydrofluoric acid etching of silicon dioxide for surface micromachining applications, *Thin Solid Films*, 1993, **232**, 1–12.

108 A. Tilke, M. Rotter, R. H. Blick, H. Lorenz and J. P. Kotthaus, Single-crystalline silicon lift-off films for metal–oxide–semiconductor devices on arbitrary substrates, *Appl. Phys. Lett.*, 2000, **77**, 558–560.

109 E. Menard, K. J. Lee, D.-Y. Khang, R. G. Nuzzo and J. A. Rogers, A printable form of silicon for high performance thin film transistors on plastic substrates, *Appl. Phys. Lett.*, 2004, **84**, 5398–5400.

110 H. S. Radhakrishnan, V. Depauw, K. V. Nieuwenhuysen, I. Gordon and J. Poortmans, Epitaxial Si lift-off technology: Current status and challenges, *Photovoltaics Int*, 2017, **38**, 44–56.

111 D. Van Der Woude, L. B. Rebouças, E. Vlieg, J. Smits and J. Schermer, A review on epitaxial lift-off for III-V solar cells, *Thin Solid Films*, 2024, **808**, 140570.

112 M. M. A. J. Voncken, J. J. Schermer, A. T. J. Van Niftrik, G. J. Bauhuis, P. Mulder, P. K. Larsen, T. P. J. Peters, B. De Bruin, A. Klaassen and J. J. Kelly, Etching AlAs with HF for Epitaxial Lift-Off Applications, *J. Electrochem. Soc.*, 2004, **151**, G347.

113 C.-W. Cheng, K.-T. Shiu, N. Li, S.-J. Han, L. Shi and D. K. Sadana, Epitaxial lift-off process for gallium arsenide substrate reuse and flexible electronics, *Nat. Commun.*, 2013, **4**, 1577.

114 K. Lee, J. D. Zimmerman, X. Xiao, K. Sun and S. R. Forrest, Reuse of GaAs substrates for epitaxial lift-off by employing protection layers, *J. Appl. Phys.*, 2012, **111**, 033527.

115 M. J. Cich, J. A. Johnson, G. M. Peake and O. B. Spahn, Crystallographic dependence of the lateral undercut wet etching rate of InGaP in HCl, *Appl. Phys. Lett.*, 2003, **82**, 651–653.

116 T. Ansbæk, E. S. Semenova, K. Yvind and O. Hansen, Crystallographic dependence of the lateral undercut wet etch rate of Al0.5In0.5P in diluted HCl for III–V sacrificial release, *J. Vac. Sci. Technol., B: Microelectron. Nanometer Struct.–Process., Meas., Phenom.*, 2012, **31**, 011209.

117 E. S. Hellman, The Polarity of GaN: a Critical Review, *MRS Internet J. Nitride Semicond. Res.*, 1998, **3**, e11.

118 C.-F. Lin, J.-J. Dai, M.-S. Lin, K.-T. Chen, W.-C. Huang, C.-M. Lin, R.-H. Jiang and Y.-C. Huang, An AlN Sacrificial Buffer Layer Inserted into the GaN/Patterned Sapphire Substrate for a Chemical Lift-Off Process, *Appl. Phys. Express*, 2010, **3**, 031001.

119 R.-H. Horng, H.-H. Hsueh, S.-L. Ou, C.-T. Tsai, T.-Y. Tsai and D.-S. Wuu, Chemical lift-off process for nitride LEDs from an Eco-GaN template using an AlN/strip-patterned-$SiO_2$ sacrificial layer, *Phys. Status Solidi A*, 2017, **214**, 1600657.

120 A. J. Fischer, B. Leung and G. T. Wang, *Photoelectrochemical Etching of GaN Quantum Wires*, Sandia National Laboratories, NM, United States, 2015, SAND2015–8086.

121 C. Youtsey, R. McCarthy, R. Reddy, A. Xie, E. Carlson and L. Guido, Epitaxial Lift-Off from Native GaN Substrates Using Photoenhanced Wet Etching, in *presented in part at 2017 International Conference on Compound Semiconductor Manufacturing Technology*, Indian Wells, CA, USA, May, 2017.

122 C. Youtsey, R. McCarthy, R. Reddy, K. Forghani, A. Xie, E. Beam, J. Wang, P. Fay, T. Ciarkowski, E. Carlson and L. Guido, Wafer-scale epitaxial lift-off of GaN using bandgap-selective photoenhanced wet etching, *Phys. Status Solidi B*, 2017, **254**, 1600774.

123 J. Wang, C. Youtsey, R. McCarthy, R. Reddy, N. Allen, L. Guido, J. Xie, E. Beam and P. Fay, Thin-film GaN Schottky diodes formed by epitaxial lift-off, *Appl. Phys. Lett.*, 2017, **110**, 173503.

124 J. Wang, R. McCarthy, C. Youtsey, R. Reddy, J. Xie, E. Beam, L. Guido, L. Cao and P. Fay, Ion-Implant Isolated Vertical GaN p-n Diodes Fabricated with Epitaxial Lift-Off From GaN Substrates, *Phys. Status Solidi A*, 2019, **216**, 1800652.

125 Y. Zhang, S.-W. Ryu, C. Yerino, B. Leung, Q. Sun, Q. Song, H. Cao and J. Han, A conductivity-based selective etching for next generation GaN devices, *Phys. Status Solidi B*, 2010, **247**, 1713–1716.

 This journal is © The Royal Society of Chemistry 2026

Open Access Article. Published on 11 maio 2026. Downloaded on 27/05/2026 13:44:17.
This article is licensed under a Creative Commons Attribution-NonCommercial 3.0 Unported Licence.

126 T.-H. Chang, K. Xiong, S. H. Park, G. Yuan, Z. Ma and J. Han, Strain Balanced AlGaN/GaN/AlGaN nanomembrane HEMTs, *Sci. Rep.*, 2017, **7**, 6360.
127 K.-P. Huang, K.-C. Wu, P.-F. Cheng, W.-P. Tseng, B.-C. Shieh, C.-F. Lin, B. Leung and J. Han, InGaN light-emitting diodes with band-pass-filter-like GaN : Si nanoporous structures, *J. Phys. D: Appl. Phys.*, 2014, **47**, 145101.
128 G. Li, Y. Li, J. Xie, C. Li, Q. Xin and W. Mu, Self-Supported Flexible α-$Ga_2O_3$ Thin Films Enabled by Nanopillar-Integrated Sacrificial Layers, *ACS Appl. Mater. Interfaces*, 2025, **17**, 20004–20012.
129 T. Haggren, J. Tournet, C. Jagadish, H. H. Tan and J. Oksanen, Strain-Engineered Multilayer Epitaxial Lift-Off for Cost-Efficient III–V Photovoltaics and Optoelectronics, *ACS Appl. Mater. Interfaces*, 2023, **15**, 1184–1191.
130 S. Sharma, C. A. Favela, B. Yu, E. Galstyan and V. Selvamanickam, Conversion efficiency improvement of ELO GaAs solar cell, deposited on water soluble sacrificial buffer, *Surf. Coat. Technol.*, 2023, **456**, 129282.
131 B. Keimer, S. A. Kivelson, M. R. Norman, S. Uchida and J. Zaanen, From quantum matter to high-temperature superconductivity in copper oxides, *Nature*, 2015, **518**, 179–186.
132 G. V. Tendeloo, O. I. Lebedev, M. Hervieu and B. Raveau, Structure and microstructure of colossal magnetoresistant materials, *Rep. Prog. Phys.*, 2004, **67**, 1315–1365.
133 S.-E. Park and T. R. Shrout, Ultrahigh strain and piezoelectric behavior in relaxor based ferroelectric single crystals, *J. Appl. Phys.*, 1997, **82**, 1804–1811.
134 I. Vrejoiu, G. Le Rhun, L. Pintilie, D. Hesse, M. Alexe and U. Gösele, Intrinsic Ferroelectric Properties of Strained Tetragonal $PbZr_{0.2}Ti_{0.8}O_3$ Obtained on Layer–by–Layer Grown, Defect–Free Single–Crystalline Films, *Adv. Mater.*, 2006, **18**, 1657–1661.
135 J. H. Lee, L. Fang, E. Vlahos, X. Ke, Y. W. Jung, L. F. Kourkoutis, J.-W. Kim, P. J. Ryan, T. Heeg, M. Roeckerath, V. Goian, M. Bernhagen, R. Uecker, P. C. Hammel, K. M. Rabe, S. Kamba, J. Schubert, J. W. Freeland, D. A. Muller, C. J. Fennie, P. Schiffer, V. Gopalan, E. Johnston-Halperin and D. G. Schlom, A strong ferroelectric ferromagnet created by means of spin–lattice coupling, *Nature*, 2010, **466**, 954–958.
136 D.-S. Park, A. D. Rata, I. V. Maznichenko, S. Ostanin, Y. L. Gan, S. Agrestini, G. J. Rees, M. Walker, J. Li, J. Herrero-Martin, G. Singh, Z. Luo, A. Bhatnagar, Y. Z. Chen, V. Tileli, P. Muralt, A. Kalaboukhov, I. Mertig, K. Dörr, A. Ernst and N. Pryds, The emergence of magnetic ordering at complex oxide interfaces tuned by defects, *Nat. Commun.*, 2020, **11**, 3650.
137 T. J. Park, S. Deng, S. Manna, A. N. M. N. Islam, H. Yu, Y. Yuan, D. D. Fong, A. A. Chubykin, A. Sengupta, S. K. R. S. Sankaranarayanan and S. Ramanathan, Complex Oxides for Brain–Inspired Computing: A Review, *Adv. Mater.*, 2023, **35**, 2203352.
138 Y. Z. Chen, N. Bovet, F. Trier, D. V. Christensen, F. M. Qu, N. H. Andersen, T. Kasama, W. Zhang, R. Giraud, J. Dufouleur, T. S. Jespersen, J. R. Sun, A. Smith, J. Nygård, L. Lu, B. Büchner, B. G. Shen, S. Linderoth and N. Pryds, A high-mobility two-dimensional electron gas at the spinel/perovskite interface of γ-$Al_2O_3$/$SrTiO_3$, *Nat. Commun.*, 2013, **4**, 1371.
139 Y. Kim, Y. Choi, S. A. Lee, W. S. Choi and K. T. Kang, Complex oxide thin films: A review on pulsed laser epitaxy growth, *Curr. Appl. Phys.*, 2024, **68**, 113–130.
140 P. Salles, P. Machado, P. Yu and M. Coll, Chemical synthesis of complex oxide thin films and freestanding membranes, *Chem. Commun.*, 2023, **59**, 13820–13830.
141 D. Ji, S. Cai, T. R. Paudel, H. Sun, C. Zhang, L. Han, Y. Wei, Y. Zang, M. Gu, Y. Zhang, W. Gao, H. Huyan, W. Guo, D. Wu, Z. Gu, E. Y. Tsymbal, P. Wang, Y. Nie and X. Pan, Freestanding crystalline oxide perovskites down to the monolayer limit, *Nature*, 2019, **570**, 87–90.
142 P. Salles, I. Caño, R. Guzman, C. Dore, A. Mihi, W. Zhou and M. Coll, Facile Chemical Route to Prepare Water Soluble Epitaxial $Sr_3$ $Al_2$ $O_6$ Sacrificial Layers for Free–Standing Oxides, *Adv. Mater. Interfaces*, 2021, **8**, 2001643.
143 P. Salles, R. Guzman, A. Barrera, M. Ramis, J. M. Caicedo, A. Palau, W. Zhou and M. Coll, On the Role of the $Sr_{3-x}Ca_xAl_2O_6$ Sacrificial Layer Composition in Epitaxial $La_{0.7}$ $Sr_{0.3}$ $MnO_3$ Membranes, *Adv. Funct. Mater.*, 2023, **33**, 2304059.
144 S. Yun, T. E. le Cozannet, C. H. Christoffersen, E. Brand, T. S. Jespersen and N. Pryds, Strain Engineering: Perfecting Freestanding Perovskite Oxide Fabrication, *Small*, 2024, **20**, 2310782.
145 P. Singh, A. Swartz, D. Lu, S. S. Hong, K. Lee, A. F. Marshall, K. Nishio, Y. Hikita and H. Y. Hwang, Large-Area Crystalline $BaSnO_3$ Membranes with High Electron Mobilities, *ACS Appl. Electron. Mater.*, 2019, **1**, 1269–1274.
146 S. Varshney, S. Choo, L. Thompson, Z. Yang, J. Shah, J. Wen, S. J. Koester, K. A. Mkhoyan, A. S. McLeod and B. Jalan, Hybrid Molecular Beam Epitaxy for Single-Crystalline Oxide Membranes with Binary Oxide Sacrificial Layers, *ACS Nano*, 2024, **18**, 6348–6358.
147 R. Takahashi and M. Lippmaa, Sacrificial Water-Soluble BaO Layer for Fabricating Free-Standing Piezoelectric Membranes, *ACS Appl. Mater. Interfaces*, 2020, **12**, 25042–25049.
148 H. Shang, T. Sheng, H. Dong, Y. Wu, Q. Ma, X. Zhang, L. Lv, H. Cao, F. Deng, X. Liang, S. Hu and S. Shen, Synthesizing ordered polar patterns in nonpolar $SrTiO_3$ nanofilms via wrinkle-induced flexoelectricity, *Proc. Natl. Acad. Sci. U. S. A.*, 2024, **121**, e2414500121.
149 S. Huang, S. Xu, C. Ma, P. Li, E. Guo, C. Ge, C. Wang, X. Xu, M. He, G. Yang and K. Jin, Ferroelectric Order Evolution in Freestanding $PbTiO_3$ Films Monitored by Optical Second Harmonic Generation, *Adv. Sci.*, 2024, **11**, 2307571.
150 J. Lin, H. Wang, Y. Zheng, Y. Kan, R. Chen, M. Long, Y. Chen, Z. Zhou, R. Qi, F. Yue, C. Duan, J. Chu and L. Sun, Enhanced Bulk Photovoltaic Effect of Single–

Open Access Article. Published on 11 maio 2026. Downloaded on 27/05/2026 13:44:17.
This article is licensed under a Creative Commons Attribution-NonCommercial 3.0 Unported Licence.

Domain Freestanding $BiFeO_3$ Membranes, *Adv. Mater.*, 2025, **37**, 2414113.

151 S. Caspi, M. Baskin, S. S. Shusterman, D. Zhang, A. Chen, D. Cohen-Elias, N. Sicron, M. Katz, E. Yalon, N. Pryds and L. Kornblum, The Role of Interface Band Alignment in Epitaxial $SrTiO_3$ /GaAs Heterojunctions, *ACS Appl. Electron. Mater.*, 2024, **6**, 7235–7243.

152 L. Han, G. Dong, M. Liu and Y. Nie, Freestanding Perovskite Oxide Membranes: A New Playground for Novel Ferroic Properties and Applications, *Adv. Funct. Mater.*, 2024, **34**, 2309543.

153 F. Wang, Q. Liu, J. Xia, M. Huang, X. Wang, W. Dai, G. Zhang, D. Yu, J. Li and R. Sun, Laser Lift-Off Technologies for Ultra-Thin Emerging Electronics: Mechanisms, Applications, and Progress, *Adv. Mater. Technol.*, 2023, **8**, 2201186.

154 J. Bian, L. Zhou, B. Yang, Z. Yin and Y. Huang, Theoretical and experimental studies of laser lift-off of nonwrinkled ultrathin polyimide film for flexible electronics, *Appl. Surf. Sci.*, 2020, **499**, 143910.

155 W. Sun, L. Ji, Z. Lin, J. Zheng, Z. Wang, L. Zhang and T. Yan, Low-Energy UV Ultrafast Laser Controlled Lift-Off for High-Quality Flexible GaN-Based Device, *Adv. Funct. Mater.*, 2022, **32**, 2111920.

156 S. Kang, J. Chang, J. Lim, D. J. Kim, T.-S. Kim, K. C. Choi, J. H. Lee and S. Kim, Graphene-enabled laser lift-off for ultrathin displays, *Nat. Commun.*, 2024, **15**, 8288.

157 M. K. Kelly, O. Ambacher, R. Dimitrov, R. Handschuh and M. Stutzmann, Optical Process for Liftoff of Group III-Nitride Films, *Phys. Status Solidi A*, 1997, **159**, R3–R4.

158 W. S. Wong, T. Sands and N. W. Cheung, Damage-free separation of GaN thin films from sapphire substrates, *Appl. Phys. Lett.*, 1998, **72**, 599–601.

159 T. Ueda, M. Ishida and M. Yuri, Separation of Thin GaN from Sapphire by Laser Lift-Off Technique, *Jpn. J. Appl. Phys.*, 2011, **50**, 041001.

160 Y. Zhang, F. Qin, J. Zhu, X. Chen, J. Li, D. Tang, Y. Yang, F.-F. Ren, C. Xu, S. Gu, R. Zhang, Y. Zheng and J. Ye, Low-threshold ultraviolet stimulated emissions from large-sized single crystalline ZnO transferable membranes, *Opt. Express*, 2018, **26**, 31965–31975.

161 K.-I. Park, J. H. Son, G.-T. Hwang, C. K. Jeong, J. Ryu, M. Koo, I. Choi, S. H. Lee, M. Byun, Z. L. Wang and K. J. Lee, Nanogenerators: Highly-Efficient, Flexible Piezoelectric PZT Thin Film Nanogenerator on Plastic Substrates, *Adv. Mater.*, 2014, **26**, 2450.

162 C. K. Jeong, S. B. Cho, J. H. Han, D. Y. Park, S. Yang, K.-I. Park, J. Ryu, H. Sohn, Y.-C. Chung and K. J. Lee, Flexible highly-effective energy harvester via crystallographic and computational control of nanointerfacial morphotropic piezoelectric thin film, *Nano Res.*, 2017, **10**, 437–455.

163 G. J. Hayes and B. M. Clemens, Laser liftoff of gallium arsenide thin films, *MRS Commun.*, 2015, **5**, 1–5.

164 H. E. Lee, S. Kim, J. Ko, H.-I. Yeom, C.-W. Byun, S. H. Lee, D. J. Joe, T.-H. Im, S.-H. K. Park and K. J. Lee, Skin-Like Oxide Thin-Film Transistors for Transparent Displays, *Adv. Funct. Mater.*, 2016, **26**, 6170–6178.

165 H. Mizuno, H. Ishii, H. Kato, T. Mori, H. Ishikawa, Y. Maruyama, K. Ohkita and K. Hasegawa, UV Laser Releasable Temporary Bonding Materials for FO-WLP, *Trans. Jpn. Inst. Electron. Packag.*, 2018, **11**, E18–004–1.

166 O. Haupt, OLED Display Manufacturing—A Task for UV Lasers, *Inf. Disp.*, 2024, **40**, 24–27.

167 D. Xu, H.-W. Wang, J. Patel, X. F. Brun, K. Hirota, E. Capsuto, H. Kato and M. Sugo, A Novel Design of Temporary Bond Debond Adhesive Technology for Wafer-Level Assembly, in *presented in part at 2020 IEEE 70th Electronic Components and Technology Conference (ECTC)*, June, 2020.

168 C. Ma, F. Wang, H. Liu, Q. Liu, W. Dai, M. Huang, G. Zhang and R. Sun, Controlled interfacial debonding based on laser induced deformation-impact coupling effect for advanced packaging, *Appl. Surf. Sci.*, 2026, **721**, 165350.

169 S.-W. Choi, J.-H. Park, J.-W. Seo, C. Mun, Y. Kim, P. Song, M. Shin and J.-D. Kwon, Flexible and transparent thin-film light-scattering photovoltaics about fabrication and optimization for bifacial operation, *npj Flexible Electron.*, 2023, **7**, 17.

170 C. Zhu, D. Guo, D. Ye, S. Jiang and Y. Huang, Flexible PZT-Integrated, Bilateral Sensors via Transfer-Free Laser Lift-Off for Multimodal Measurements, *ACS Appl. Mater. Interfaces*, 2020, **12**, 37354–37362.

171 H. Long, X. Feng, Y. Wei, T. Yu, S. Fan, L. Ying and B. Zhang, Carbon nanotube assisted Lift off of GaN layers on sapphire, *Appl. Surf. Sci.*, 2017, **394**, 598–603.

172 J. Bian, F. Chen, H. Ling, N. Sun, J. Hu and Y. Huang, Experimental and modeling study of controllable laser lift-off via low-fluence multiscanning of polyimide-substrate interface, *Int. J. Heat Mass Transfer*, 2022, **188**, 122609.

173 A. P. Kirk, D. W. Cardwell, J. D. Wood, A. Wibowo, K. Forghani, D. Rowell, N. Pan and M. Osowski, Recent Progress in Epitaxial Lift-Off Solar Cells, in *presented in part at 2018 IEEE 7th World Conference on Photovoltaic Energy Conversion (WCPEC) (A Joint Conference of 45th IEEE PVSC, 28th PVSEC & 34th EU PVSEC)*, June, 2018.

174 J. Adams, V. Elarde, A. Hains, C. Stender, F. Tuminello, C. Youtsey, A. Wibowo and M. Osowski, Demonstration of Multiple Substrate Reuses for Inverted Metamorphic Solar Cells, *IEEE J. Photovolt.*, 2013, **3**, 899–903.

175 A. Goodrich and M. Woodhouse, *A Manufacturing Cost Analysis Relevant to Single- and Dual-Junction Photovoltaic Cells Fabricated with III-Vs and III-Vs Grown on Czochralski Silicon*, National Renewable Energy Laboratory, Golden, CO, 2013, NREL/PR–6A20-60126.

176 J. S. Ward, T. Remo, K. Horowitz, M. Woodhouse, B. Sopori, K. VanSant and P. Basore, Techno-economic analysis of three different substrate removal and reuse strategies for III-V solar cells, *Prog. Photovolt. Res. Appl.*, 2016, **24**, 1284–1292.

 This journal is © The Royal Society of Chemistry 2026

177 R. Delmdahl, M. Fricke and B. Fechner, Laser lift-off systems for flexible-display production, *J. Inf. Disp.*, 2014, **15**, 1–4.
178 S. Li and O. Haupt, 46.4: Laser Processes for MicroLED Display Manufacturing, *SID Int. Symp. Dig. Tech. Pap.*, 2022, **53**, 465–466.
179 O. Haupt, J. Brune, M. Fatahilah and R. Delmdahl, MicroLEDs: high precision large scale UV laser lift-off and mass transfer processes, in presented in part at Laser-based Micro- and Nanoprocessing XVI, March, 2022.
180 R. Delmdahl, R. Pätzel and J. Brune, Large-Area Laser-Lift-Off Processing in Microelectronics, *Phys. Procedia*, 2013, **41**, 241–248.
181 J. Bian, L. Zhou, X. Wan, M. Liu, C. Zhu, Y. Huang and Z. Yin, Experimental study of laser lift-off of ultra-thin polyimide film for flexible electronics, *Sci. China: Technol. Sci.*, 2019, **62**, 233–242.
182 M. D. Alam, K. Hussain, S. Mollah, G. Simin, A. Khan and M. Chandrashekhar, Realization of flexible AlGaN/GaN HEMT by laser liftoff, *Appl. Phys. Express*, 2022, **15**, 071011.
183 H. Ji, J. Das, M. Germain and M. Kuball, Laser lift-off transfer of AlGaN/GaN HEMTs from sapphire onto Si: A thermal perspective, *Solid-State Electron.*, 2009, **53**, 526–529.
184 M.-S. Noh, S. Kim, D.-K. Hwang and C.-Y. Kang, Self-powered flexible touch sensors based on PZT thin films using laser lift-off, *Sens. Actuators, A*, 2017, **261**, 288–294.
185 Y. Zhai, L. Mathew, R. Rao, D. Xu and S. K. Banerjee, High-Performance Flexible Thin-Film Transistors Exfoliated from Bulk Wafer, *Nano Lett.*, 2012, **12**, 5609–5615.
186 D. Shahrjerdi and S. W. Bedell, Extremely Flexible Nanoscale Ultrathin Body Silicon Integrated Circuits on Plastic, *Nano Lett.*, 2013, **13**, 315–320.
187 J. Yoon, S. Jo, I. S. Chun, I. Jung, H.-S. Kim, M. Meitl, E. Menard, X. Li, J. J. Coleman, U. Paik and J. A. Rogers, GaAs photovoltaics and optoelectronics using releasable multilayer epitaxial assemblies, *Nature*, 2010, **465**, 329–333.
188 Y. Zhang, S. An, Y. Zheng, J. Lai, J. Seo, K. H. Lee and M. Kim, Releasable AlGaN/GaN 2D Electron Gas Heterostructure Membranes for Flexible Wide–Bandgap Electronics, *Adv. Electron. Mater.*, 2022, **8**, 2100652.
189 J. Jeong, Q. Wang, J. Cha, D. K. Jin, D. H. Shin, S. Kwon, B. K. Kang, J. H. Jang, W. S. Yang, Y. S. Choi, J. Yoo, J. K. Kim, C.-H. Lee, S. W. Lee, A. Zakhidov, S. Hong, M. J. Kim and Y. J. Hong, Remote heteroepitaxy of GaN microrod heterostructures for deformable light-emitting diodes and wafer recycle, *Sci. Adv.*, 2020, **6**, eaaz5180.
190 Y. Liu, Y. Xu, B. Cao, Z. Li, E. Zhao, S. Yang, C. Wang, J. Wang and K. Xu, Transferable GaN Films on Graphene/SiC by van der Waals Epitaxy for Flexible Devices, *Phys. Status Solidi A*, 2019, **216**, 1801027.
191 K. Lee, J. Park, Y. Tchoe, J. Yoon, K. Chung, H. Yoon, S. Lee, C. Yoon, B. H. Park and G.-C. Yi, Flexible resistive random access memory devices by using NiOx/GaN microdisk arrays fabricated on graphene films, *Nanotechnology*, 2017, **28**, 205202.
192 J. Park, N. Kim, Y. Kim, S. Lee and G. Yi, Metal catalyst-assisted growth of GaN nanowires on graphene films for flexible photocatalyst applications, *Curr. Appl. Phys.*, 2014, **14**, 1437–1442.
193 Y. Xu, B. Cao, Z. Li, D. Cai, Y. Zhang, G. Ren, J. Wang, L. Shi, C. Wang and K. Xu, Growth Model of van der Waals Epitaxy of Films: A Case of AlN Films on Multilayer Graphene/SiC, *ACS Appl. Mater. Interfaces*, 2017, **9**, 44001–44009.
194 M. Hiroki, K. Kumakura and H. Yamamoto, Enhancement of performance of AlGaN/GaN high-electron-mobility transistors by transfer from sapphire to a copper plate, *Jpn. J. Appl. Phys.*, 2016, **55**, 05FH07.
195 Y. Kim, J. M. Suh, J. Shin, Y. Liu, H. Yeon, K. Qiao, H. S. Kum, C. Kim, H. E. Lee, C. Choi, H. Kim, D. Lee, J. Lee, J.-H. Kang, B.-I. Park, S. Kang, J. Kim, S. Kim, J. A. Perozek, K. Wang, Y. Park, K. Kishen, L. Kong, T. Palacios, J. Park, M.-C. Park, H. Kim, Y. S. Lee, K. Lee, S.-H. Bae, W. Kong, J. Han and J. Kim, Chip-less wireless electronic skins by remote epitaxial freestanding compound semiconductors, *Science*, 2022, **377**, 859–864.
196 Y. H. Lee, J. Kim and J. Oh, Wafer-Scale Ultrathin, Single-Crystal Si and GaAs Photocathodes for Photoelectrochemical Hydrogen Production, *ACS Appl. Mater. Interfaces*, 2018, **10**, 33230–33237.
197 Y. Lee, B. Gupta, H. H. Tan, C. Jagadish, J. Oh and S. Karuturi, Thin silicon via crack-assisted layer exfoliation for photoelectrochemical water splitting, *iScience*, 2021, **24**, 102921.
198 D. Shahrjerdi, S. W. Bedell, C. Bayram, C. C. Lubguban, K. Fogel, P. Lauro, J. A. Ott, M. Hopstaken, M. Gayness and D. Sadana, Ultralight High–Efficiency Flexible InGaP/(In)GaAs Tandem Solar Cells on Plastic, *Adv. Energy Mater.*, 2013, **3**, 566–571.
199 S. W. Bedell, C. Bayram, K. Fogel, P. Lauro, J. Kiser, J. Ott, Y. Zhu and D. Sadana, Vertical Light-Emitting Diode Fabrication by Controlled Spalling, *Appl. Phys. Express*, 2013, **6**, 112301.
200 K. A. Horowitz, T. W. Remo, B. Smith and A. J. Ptak, *A Techno-Economic Analysis and Cost Reduction Roadmap for III-V Solar Cells*, National Renewable Energy Laboratory, Golden, CO, 2018, NREL/TP–6A20-72103.
201 Y. Lee, S. H. Choi, H. Kim and J. Yoo, Epitaxy of Emerging Materials and Advanced Heterostructures for Microelectronics and Quantum Sciences, *Small Methods*, 2025, **9**, 2401815.
202 P. Thureja, A. W. Nyholm, M. Thomaschewski, P. R. Jahelka, J. Belleville and H. A. Atwater, Spalled Barium Titanate Single Crystal Thin Films for Functional Device Applications, *Nano Lett.*, 2025, **25**, 11089–11096.
203 D.-M. Geum, M.-S. Park, J. Y. Lim, H.-D. Yang, J. D. Song, C. Z. Kim, E. Yoon, S. Kim and W. J. Choi, Ultra-high-

Open Access Article. Published on 11 maio 2026. Downloaded on 27/05/2026 13:44:17.
This article is licensed under a Creative Commons Attribution-NonCommercial 3.0 Unported Licence.

Open Access Article. Published on 11 maio 2026. Downloaded on 27/05/2026 13:44:17.
This article is licensed under a Creative Commons Attribution-NonCommercial 3.0 Unported Licence.

throughput Production of III-V/Si Wafer for Electronic and Photonic Applications, *Sci. Rep.*, 2016, **6**, 20610.

204 S. Lee, S. K. Kim, J.-H. Han, J. D. Song, D.-H. Jun and S.-H. Kim, Epitaxial Lift-Off Technology for Large Size III–V-on-Insulator Substrate, *IEEE Electron Device Lett.*, 2019, **40**, 1732–1735.

205 J. Shin, H. Kim, S. Sundaram, J. Jeong, B.-I. Park, C. S. Chang, J. Choi, T. Kim, M. Saravanapavanantham, K. Lu, S. Kim, J. M. Suh, K. S. Kim, M.-K. Song, Y. Liu, K. Qiao, J. H. Kim, Y. Kim, J.-H. Kang, J. Kim, D. Lee, J. Lee, J. S. Kim, H. E. Lee, H. Yeon, H. S. Kum, S.-H. Bae, V. Bulovic, K. J. Yu, K. Lee, K. Chung, Y. J. Hong, A. Ougazzaden and J. Kim, Vertical full-colour micro-LEDs via 2D materials-based layer transfer, *Nature*, 2023, **614**, 81–87.

206 F.-L. Wu, S.-L. Ou, Y.-C. Kao, C.-L. Chen, M.-C. Tseng, F.-C. Lu, M.-T. Lin and R.-H. Horng, Thin-film vertical-type AlGaInP LEDs fabricated by epitaxial lift-off process via the patterned design of Cu substrate, *Opt. Express*, 2015, **23**, 18156.

207 G. J. Bauhuis, P. Mulder, E. J. Haverkamp, J. C. C. M. Huijben and J. J. Schermer, 26.1% thin-film GaAs solar cell using epitaxial lift-off, *Sol. Energy Mater. Sol. Cells*, 2009, **93**, 1488–1491.

208 F. Chancerel, P. Regreny, J. L. Leclercq, S. Brottet, M. Volatier, A. Jaouad, M. Darnon, S. Fafard, N. P. Blanchard, M. Gendry and V. Aimez, Epitaxial lift-off of InGaAs solar cells from InP substrate using a strained AlAs/InAlAs superlattice as a novel sacrificial layer, *Sol. Energy Mater. Sol. Cells*, 2019, **195**, 204–212.

209 K. M. Burzynski, N. R. Glavin, M. Snure, M. J. Motala, J. Ferguson, E. Blanton, E. Heckman and C. Muratore, Graphite Nanocomposite Substrates for Improved Performance of Flexible, High-Power AlGaN/GaN Electronic Devices, *ACS Appl. Electron. Mater.*, 2021, **3**, 1228–1235.

210 J. Jing, Y. Luo, Y. Wang, Z. Wang, Q. Wang, K. H. Li and Z. Chu, Strain-Enhanced Responsivity of Scalable and Flexible Diamond UV Detector, *IEEE Electron Device Lett.*, 2025, **46**, 541–544.